CHARACTERIZATION OF TWO NEW TYPES OF FIN LINE DISCONTINUITIES

A Thesis Submitted

in Partial Fulfillment of the Requirements

for the Degree of

Master of Technology

by

Alok Kumar Gupta

to the

DEPARTMENT OF ELECTRICAL ENGINEERING

INDIAN INSTITUTE OF TECHNOLOGY, KANPUR

November 1993

Certificate

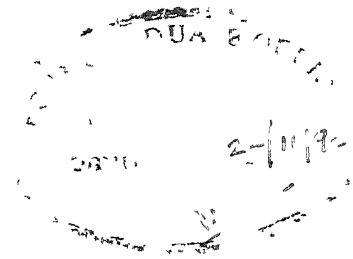

It is certified that work contained in the thesis entitled **CHARACTERIZATION OF TWO NEW TYPES OF FIN LINE DISCONTINUITIES**, by Alok Kumar Gupta , has been carried out under my supervision and that this work has not been submitted elsewhere for a degree

22 November 1993

(Dr Animesh Biswas)

Asstt Professor

Department of Electrical Engineering

I I T Kanpur

EE-1993-M-GUP-CHA

ABSTRACT

Two new types of fin line discontinuities (one each in unilateral and insulated fin lines) have been proposed and characterized in this thesis The discontinuity proposed in unilateral fin line is a rectangular conducting strip, placed in the air dielectric interface of the substrate which otherwise does not have any metalization For insulated fin line, the discontinuity consists of two rectangular conducting strips, placed closed enough but again on two different 'otherwise metalization free' air dielectric interfaces Eigenvalue matrix formulation for finding out the resonant length of the fin line cavity containing the discontinuity, has been done using modal analysis approach in case of unilateral fin line and spectral domain immittance approach in case of insulated fin line The transverse resonance technique has been applied then to extract the equivalent circuit parameters of the discontinuity in both the cases Appropriate basis functions for field in the slot and the current on the strip have been chosen, which satisfy the edge conditions Measurements of transmission coefficient of a sample discontinuity in unilateral fin line have been done and compared with the theoretical results The two results have been shown matching well, which proves the validity of the choice of basis functions A low pass filter in unilateral fin line has also been realized by cascading three conducting strips with different widths separated by uniform fin line sections of different lengths. Theoretical results of insertion loss of the filter have been calculated and compared with the measured results

To

my Parents

Acknowledgement

First of all I would like to thank to my Supreme Guide for imparting me enough patience, timely wisdom and sequencing the events for my better

After Him I would like to thank my guide Dr Animesh Biswas for suggesting the problem and guiding so actively and enthusiastically all the time, I could hardly feel stuck at any stage of my thesis Working under him was a nice experience for me as he not only guided me in the thesis but also helped me when I felt emotionally disturbed It feels really nice to be his first M Tech student

I really have a great respect for Dr M Sachchidananda and Dr N C Mathur for their ever readiness to help during the course work and providing a clear understanding of the concepts of electromagnetics I would also like to thank to Dr C Das Gupta for covering Fin Lines sufficiently enough in his course so that I could start working on my problem

One resonant fin line cavity full of thanks to Rupendra Kumar and Akhilesh Jain who added to the appearance of my thesis

Thanks to Apu who helped me in solving the problem of discontinuity in Insulated fin line and to Srikant who was ever ready when it came to measurements

Last but not the least I would like to thank to all my friends, who made my stay at I I T K live

CONTENTS

LIST OF FIGURES

CHAPTER 1

INTRODUCTION

The congestion of microwave spectrum in recent years has brought about an increasing demand for the use of millimeter wave frequencies [1-4] Unlike microwave band at its lower end and optical region at its upper end, techniques and technologies are not well developed in millimeter band Because of the smaller wavelengths (1-10mm) millimeter waves offer some distinct advantages [3] over microwaves along with a few disadvantages which can be overcome Due to the increasing demand and the advantages offered by millimeter waves a lot of research has been done in last couple of years in an attempt to develop systems at these frequencies

Development of systems requires suitable transmission line as a transmission medium, distributed or lumped circuit elements, microwave solid state devices and suitable technology for circuit integration The work presented in this thesis is devoted to characterization of discontinuities which find their application in realizing one of the distributed circuit elements i e a low pass filter which is extensively used in converters, multipliers and multiplexers Amongst the various transmission structures suitable for millimeter wave applications, fin line has been considered for realization of filter because of its specific advantages in 30-100 GHz frequency band They are described in following sections

1.1 FIN LINE:A VIABLE TRANSMISSION LINE FOR MILLIMETER WAVE FREQUENCIES

In the frequency range 3-30 GHz, microstrip is the most extensively used

planar transmission line Although its use can be extended to millimeter band, it starts facing various problems [5] [6] in this band These problems include radiation loss, spurious coupling, dispersion and higher order mode propagation Also as the frequency increases,dimensional tolerances become more critical due to very small dimensions at higher frequencies, reproducibility decreases hence the cost increases As the operating frequency is raised and the microstrip dimensions are decreased, a limit will be reached where the strip width is no longer compatible with chip and beam lead devices [8] Though some other variations of microstrip which are less lossy and have guide wavelengths much greater than that in microstrip can be used at millimeter wave frequencies, there is yet another transmission structure known as FIN LINE [7-10] which has special advantages in millimeter wave frequencies

FIN LINE was proposed by P J Meier [8] in 1972 It can be viewed as slotline inserted in the E-plane of a rectangular wave guide (WG) or a ridged WG with thin ridges backed by a dielectric substrate or as dielectric slab loaded WG with fins Fin line differs from slotline in that the former has a lower cut off frequency, but does not require high permittivity substrate to avoid radiations [9] Since fin line resembles the ridged WG, it's single mode bandwidth is relatively wide The structure is considered quasi planar in the sense that entire circuit pattern including the active devices, is incorporated on the planar surface of a dielectric substrate, while the design takes into account the effect of the WG housing The mode of propagation is hybrid mode consisting of a combination of TE and TM modes Fig 1 1 shows cross sectional views of four basic types of fin lines used in practice (a) Unilateral, (b) Bilateral, (c) Insulated, (d) Antipodal In these structures suspended fins concentrate the field energy in the fin gap region as depicted in Fig 1 2, which causes the capacitive loading of dominant HE mode of propagation in the

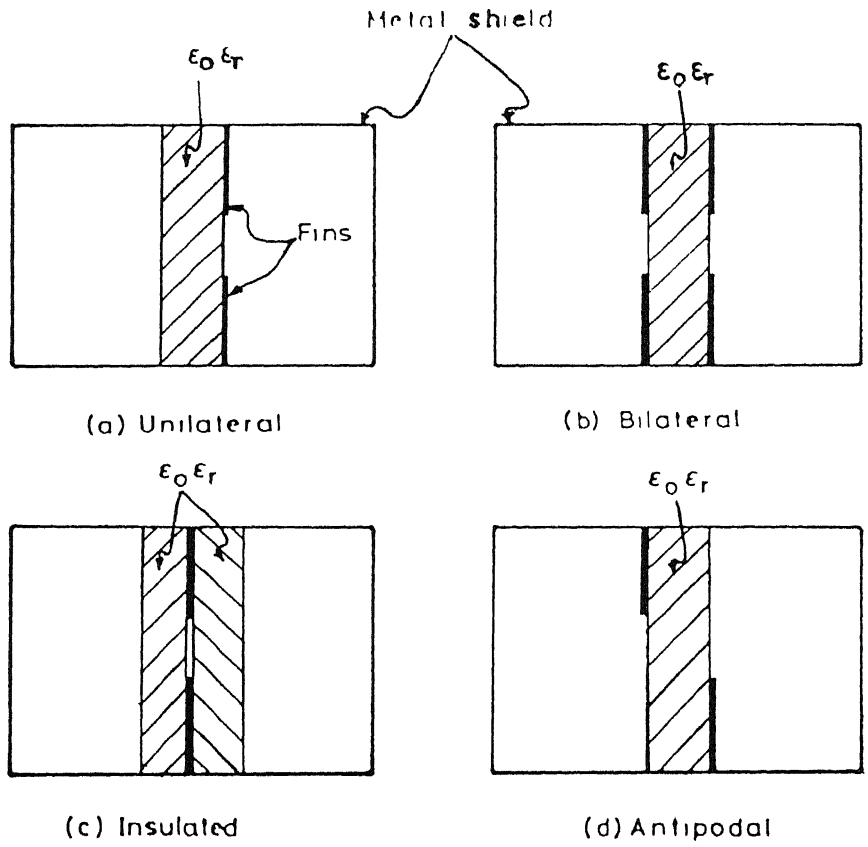

Fig 1 1 Basis fin Line Structures [1]

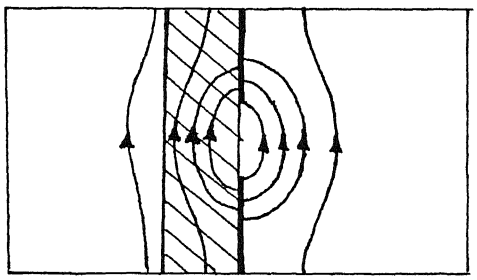

(a) Unilateral

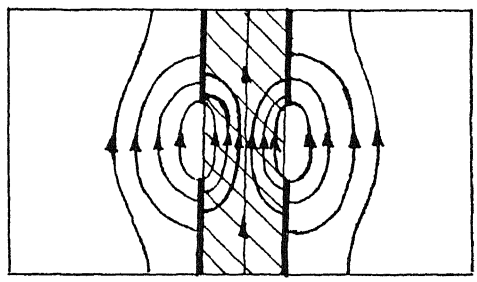

(b) Bilateral

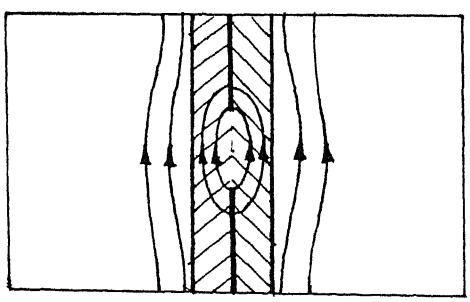

(c) Insulated

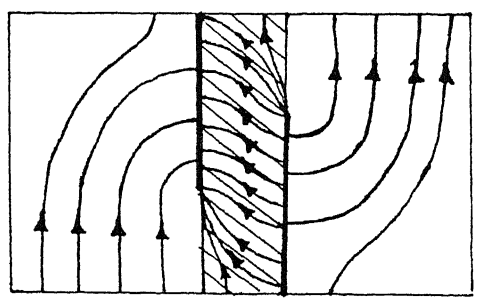

(d) Antipodal

Fig 1 2 Field configurations in fin lines

slab loaded WG This has the effect of lowering the frequency of the fundamental mode to a considerable degree and that of the next higher mode to a very small degree,resulting in large bandwidth for fundamental mode operation Besides the large bandwidth that is available, any devices that are connected to the fins for integrated circuit fabrication will be subjected to large power densities, resulting in better matching However the field concentration results in larger conductor and dielectric losses The attenuation in fin line is typically of the order of 0 1dB/λ_g, where λ_g is the guide wavelength Therefore fin line is not suited for long distance transmission [11]

Amongst the configurations shown in Fig 1 1 the unilateral fin line is the simplest and the best suited for the fabrication of fin line components In bilateral fin line Fig 1 1(b) since the fins are directly grounded to metallic WG walls, this configuration is applicable only to passive devices Insulated fin line facilitates dc bias to be applied to active components Antipodal fin line is used for realizing lower impedance values For frequencies in the range of 30 to 100 GHz, the fin line offers a versatile transmission medium It overcomes the disadvantages of having to maintain tight dimensional tolerances as in the WG and incorporates the advantageous features of planar technology Thus the major advantages [1] of fin lines can be summarized as (1) the dimensions of the circuits in 30-100GHz frequency band are compatible with beam lead and chip devices, thus offering the potential for constructing passive and integrated circuits (2) guide wavelength is longer than in microstrip, thus permitting less stringent dimensional tolerances (3) it permits easy transition to a standard WG and (4) low loss propagation

1.2 FIN LINE DISCONTINUITIES A LITERATURE SURVEY

Fin line discontinuities are used in almost all of the fin line circuits

Some of the commonly encountered discontinuities and their equivalent circuits are shown in Fig 1 3

Of the various discontinuities shown step discontinuity, capacitive strips and notches are used for performing impedance transformation Low pass filters are often realized by cascading capacitive strips and inductive notches A capacitive strip in an asymmetric fin-line is useful for mounting beam lead semiconductor devices A narrow inductive strip bridging the slot Fig 1 3(d) serves as a coupling element to the transmission types of resonators Fig 1 3(e) shows a narrow slit in metalization which can be used as dc separation in complex circuits Amongst all the discontinuities discussed above, the inductive strips and impedance step have received the most wide spread attention, and have been analyzed using different approaches The properties of an E-plane inductive strip as an element in printed E-plane were first investigated by Meier [8] He used an empirical approach to characterize an inductive strip printed on a dielectric substrate Konishi and Uenakada [21] treated the same structure with no dielectric backing by using the Releigh Ritz variational technique The main difference between a discontinuity in pure metal insert E-plane circuit and a fin line circuit is that the higher order mode effect is relatively small in the former Conversely in a fin line circuit, due to the presence of dielectric, the field becomes concetrated in the slot region, thus causing a stronger excitation of higher order mode

An analysis of inductive strip discontinuity in unilateral and bilateral fin lines that takes into account the higher order modes has been presented by Saad and Schunemann [22] This method makes use of fin line line modeling by a set of rectangular WG with homogeneous dielectric An experimental approach for characterizing fin line discontinuities has been reported by Pic and Hoefer They have obtained equivalent circuit parameters

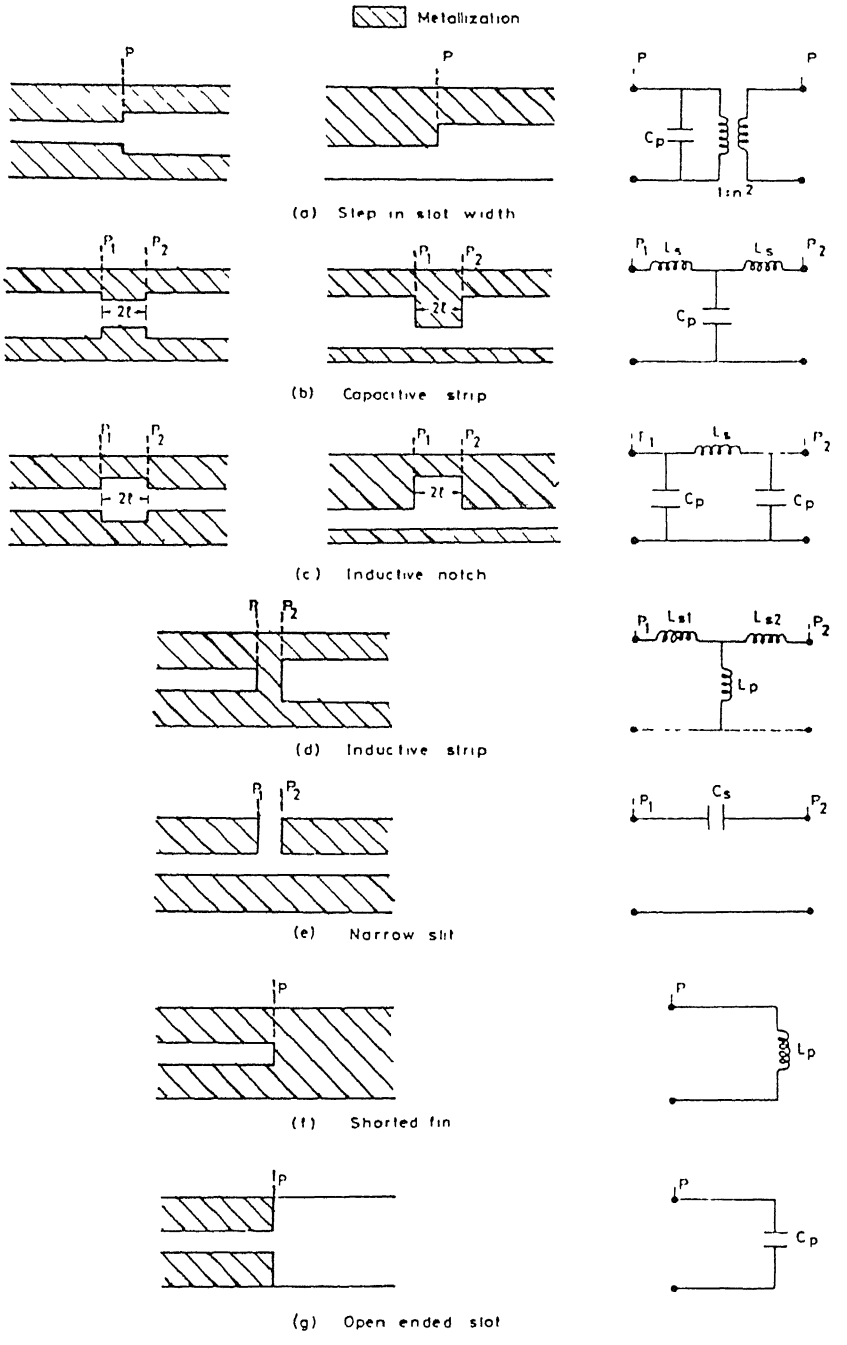

Fig 1 3 Various fin line discontinuities and their equivalent circuits [1]

of inductive strips and impedance step in unilateral fin line from the measured resonant frequencies of a rectangular cavity containing the discontinuity elements By using rigorous hybrid mode spectral domain approach [17], Koster and Jansen [23] have analyzed the equivalent circuit parameters of symmetric and asymmetric inductive strip discontinuity in unilateral fin line The effects of finite metalization thickness and thickness of mount slits on the calculation of step discontinuities have been reported by Bayer

A general modal analysis technique described by Wexler [24]for solving WG discontinuity has been applied to fin line discontinuities by Hennaway and schunemann [25] In this method the fields on either sides of the junction are calculated in terms of suitable set of fin line modes then matched at the junction Another equally important analytical tool is the transverse resonance technique developed by Sorrentino and Itoh [26] This is reported to offer considerable saving in computer time as compared with direct modal analysis method [24] A technique that combines the spectral domain approach with direct modal analysis for calculating the scattering matrix elements of a fin line discontinuity has been reported by Helard et al [27] J B Knorr and J C Deal [28] have reported the scattering coefficient of an inductive strip using spectral domain approach With accurate choice of basis functions for slot field, A Biswas and B Bhat [29] have used transverse resonance technique to accurately characterize the inductive strip discontinuity The accurate choice of basis functions is reported to result in large saving in computer time Giovani,Piero and Sorrentino [30] have considered generalized case of coupled fin line discontinuities and treated inductive strip discontinuity as a special case of this generalization Again, they also used the transverse resonance technique for characterization The paper has considered only the dominant mode for characterization

1.3 MOTIVATION FOR THE THESIS

Of the many fin line discontinuities reported so far inductive strip discontinuity has been analyzed by many authors using different approaches, but the problem of a rectangular strip in the dielectric air interface which does not contain slot, has not been attempted by anyone so far Before attempting the problem we had one of its possible application in mind that is, the strip can be used for biasing the transistor mounted across the slot Another of it's use we thought (and confirmed experimentally in the thesis) is in realization of some kind of filter based on its characteristics by cascading similar strips Since the discontinuity analyzed in this work exists in a plane which does not contain slot , it has been referred as off-slot discontinuity here after Fig 1 4 depicts some of the possible future applications of the off-slot discontinuity

1.4 ORGANIZATION OF THE REPORT

The problem of off -slot discontinuity has been considered in two fin line structures namely unilateral fin line and insulated fin line The problem has been formulated using hybrid mode analysis which uses LSE and LSM modes for the expansion of fields in case of unilateral fin line and spectral domain immitance approach in case of insulated fin line Transverse resonance technique [26] is then applied to extract the equivalent circuit parameters of the discontinuity Use of transverse resonance condition requires the information about propagation characteristics of fin line Chapter(2) describes the spectral domain immitance approach with Galerkin's procedure to determine propagation constants of unilateral and insulated fin lines Beginning with a brief description of transverse resonance technique

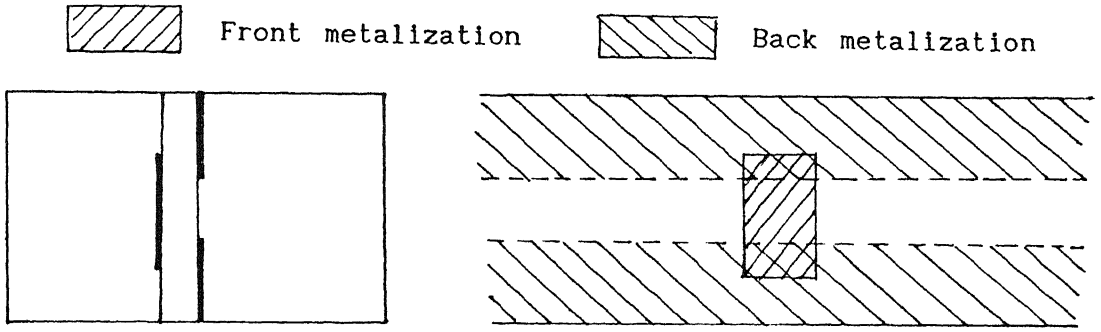

(a) Discontinuity proposed in unilateral fin line

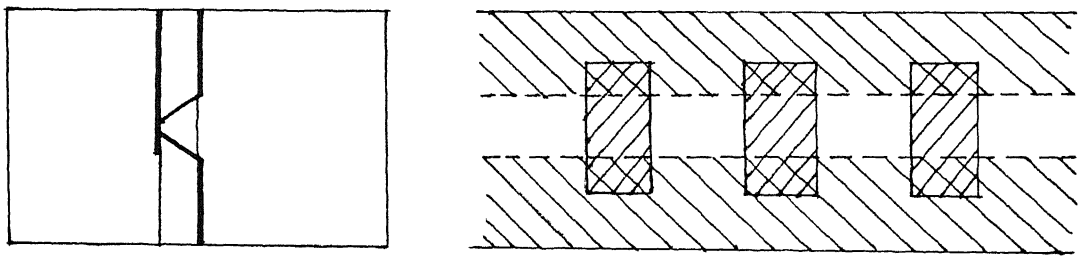

(i) (ii)

(b) Application (i) In biasing a transistor (ii) In realizing a filter

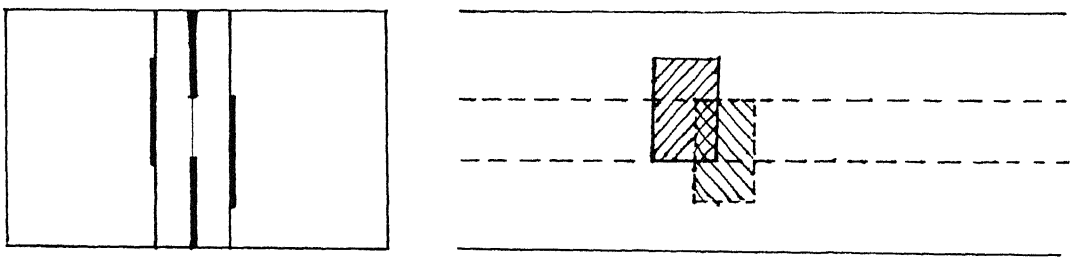

(c) Discontinuity proposed in insulated fin line

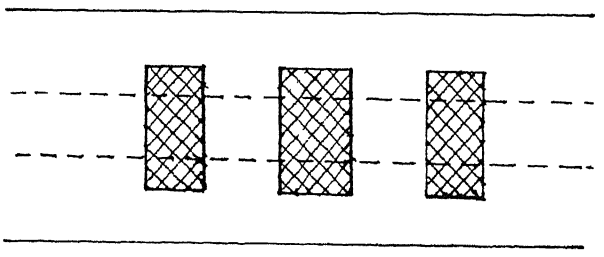

(d) Application in realizing a filter

Fig 1 4 Proposed discontinuities and their possible applications

chapter (3) presents detailed analysis of the discontinuity in unilateral fin line and chapter(4) presents the analysis of discontinuity in insulated fin line structure Chapter(5) deals with the Scattering matrix formulation of T-equivalent circuit of the discontinuities and also of the cascade of three similar discontinuities It also discusses some of the design aspects of the fin line fixture Chapter(6) contains the theoretical results for the discontinuities in unilateral and insulated fin line both and experimental results for unilateral fin line case alone Next few pages contain the conclusions and Discussion A list of references and appendix follow the conclusions

CHAPTER 2

PROPAGATION CHARACTERISTICS OF FIN LINES

2.1 INTRODUCTION

Since the day the fin line has been introduced, many researchers have analysed it using rigorous as well as approximate methods References [12-16] covers the analysis' presented by some of them What we are concerned about in this chapter is the propagation constants of two of the fin lines For their other characteristics, the literature available in the above references should be looked into The information about the propagation constant is necessary while using the *Transverse Resonance Technique* (to be introduced later) to extract the equivalent circuit parameters of the disconinuity The chapter presents the analysis of unilateral and insulated fin line using the *spectral domain immittance approach* [19] for determining their propagation constants

The *immittance approach* is the simplified form of the conventional *spectral domain technique* introduced by R Mittra and T Itoh [17] In this approach we don't have to go through the lengthy derivational process at the formulation stage as it is required in the conventional spectral domain technique The approach is based on the transverse equivalent circuit concept as applied in the spectral domain in conjunction with simple co-ordinate transformation rule It has been used in this chapter to find out the propagation constant of unilateral and insulated fin lines Numerical results of dominant mode propagation constants of the two fin lines have been computed and presented in this chapter

2.2 ANALYSIS OF FIN LINES USING SPECTRAL DOMAIN IMMITTANCE APPROACH

2.2.1 *Derivation of dydic Green's functions*

In a source free, homogeneous, and isotropic region Maxwell's equations take the following form

$$\nabla \times \vec{H} = \partial \vec{D}/\partial t \qquad (2\ 1a)$$

$$\nabla \times \vec{E} = -\partial \vec{B}/\partial t \qquad (2\ 1b)$$

$$\nabla \cdot \vec{B} = 0 \qquad (2\ 1c)$$

$$\nabla \cdot \vec{D} = 0 \qquad (2\ 1d)$$

The above equations can be solved to give following solution for the fields

$$\vec{E}^e = \nabla (\nabla \cdot \vec{\Pi}^e) + k^2 \vec{\Pi}^e \qquad (2\ 2a)$$

$$\vec{H}^e = j \omega \varepsilon \nabla \times \vec{\Pi}^e \qquad (2\ 2b)$$

$$\vec{E}^h = -j \omega \mu \nabla \times \vec{\Pi}^h \qquad (2\ 2c)$$

$$\vec{H}^h = \nabla (\nabla \cdot \vec{\Pi}^h) + k^2 \vec{\Pi}^h \qquad (2\ 2d)$$

Where $\vec{\Pi}^e$ and $\vec{\Pi}^h$ in the above equations are electric and magnetic Hertzian potentials, respectively and they are the solutions of wave equations

$$\nabla^2 \vec{\Pi}^e + k^2 \vec{\Pi}^e = 0 \qquad (2\ 3a)$$

$$\nabla^2 \vec{\Pi}^h + k^2 \vec{\Pi}^h = 0 \qquad (2\ 3b)$$

Also we have assumed $e^{j\omega t}$ as the time dependence in solving equations (2 1)

Superscript 'e' and 'h' in the above equations corresponds to TM and TE modes respectively

Since the electromagnetic fields in general can be expressed as the superposition of TE and TM fields, we can therefore write the total $\vec{E}$ and $\vec{H}$ fields as follows

$$\vec{E} = \vec{E}^e + \vec{E}^h \qquad (2\ 4a)$$

$$\vec{H} = \vec{H}^e + \vec{H}^h \qquad (2\ 4b)$$

Now if we choose $\vec{\Pi}^e$ and $\vec{\Pi}^h$ such that

$$\vec{\Pi}^e = \hat{y}\,\hat{\phi}^e\,(x, y, z)$$

and

$$\vec{\Pi}^h = \hat{y}\,\hat{\phi}^e\,(x, y, z)$$

instead of

$$\vec{\Pi}^e = \hat{z}\,\hat{\phi}^e\,(x, y, z)$$

and

$$\vec{\Pi}^h = \hat{z}\,\hat{\phi}^e\,(x, y, z)$$

Or in other words, if we express all the field components in different regions of fin lines shown in Fig 2 1 and 2 2, in terms of E_y and H_y in place of E_z and H_z (as we do in conventional spectral domain analysis) we can considerably simplify the formulations and also we can use the equivalent transmission line concept This is also because in the absence of metalization on the interface, the modal spectrum consists of TM-to-y and TE-to-y modes only The fields in the fin line can therefore be expressed in terms of these modal fields

Assume the field propagates in the z-direction, according to $\exp(-j\beta z)$ The Fourier transform of the components along the y-direction is given by

$$\hat{E}_y\,(\alpha_n, y) = \int_0^{2b} E_y\,(x, y)\,e^{j\,\alpha_n\,x}\,dx \qquad (2\ 5a)$$

where

$$\alpha_n = \frac{n\,\pi}{b}\,, \qquad n = 0, \pm1, \pm2, \qquad (2.6a)$$

for arbitrarily located slot

$$= \frac{2\,n\,\pi}{b}\,, \quad n = 0, \pm1, \pm2, \qquad (2\ 6b)$$

for centrally located slot

and similarly for $\hat{H}_y(\alpha_n, y)$ From the inverse Fourier transform we have

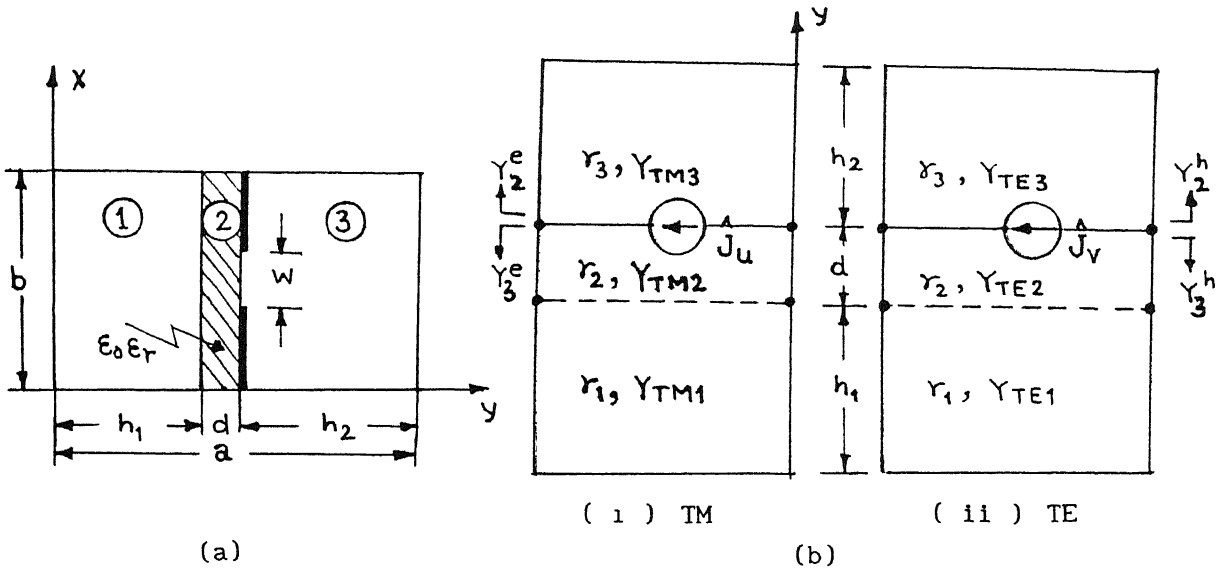

Fig 2 1 Unilateral fin line and it's equivalent transmission line representation

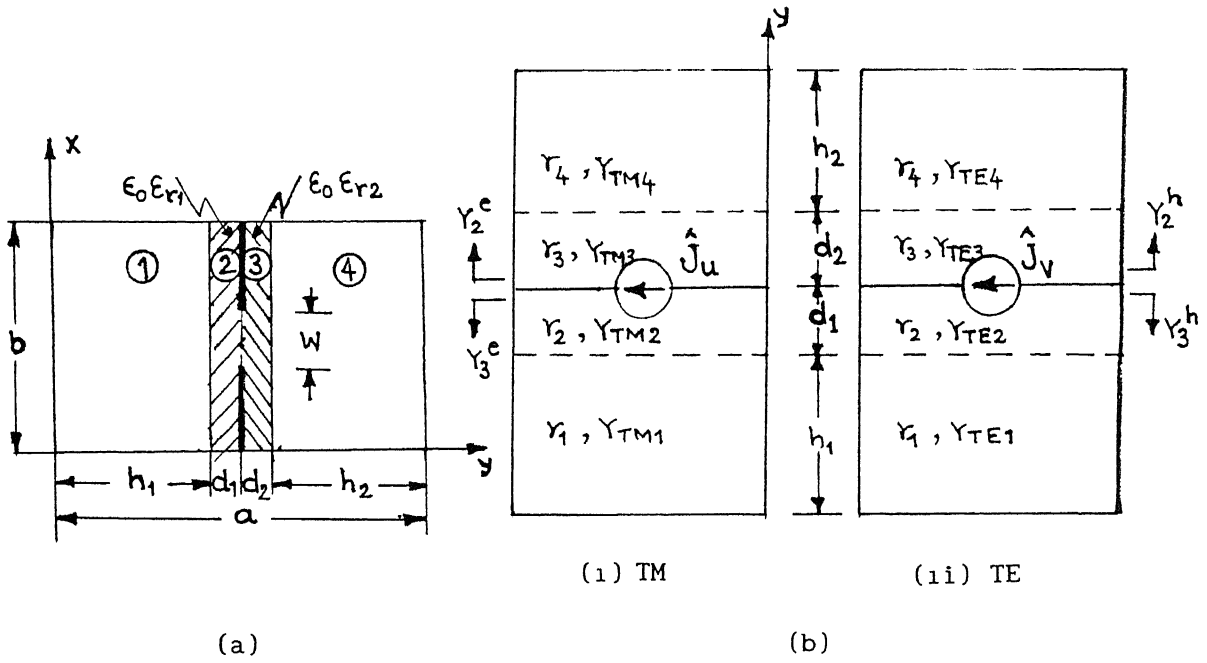

Fig 2 2 Insulated fin line and it's equivalent transmission line representation

$$E_y(x, y)\, e^{j\beta z} = \frac{1}{2b} \sum_{n=-\infty}^{\infty} \hat{E}_y(\alpha_n, y)\, e^{-j(\alpha_n x + \beta z)} \qquad (2\ 5b)$$

From this equation, we can see that the field components are the superposition of inhomogeneous plane waves propagating in θ direction with respect to z-axis, where $\theta = \cos^{-1}(\beta/\sqrt{\alpha_n^2 + \beta^2})$ By taking this into account, we transform the (x,z) coordinate into a (u,v) coordinate system, u being taken along the propagation direction and v being transverse to u and y (see Fig 2 3) This transformation has the form

$$\begin{bmatrix} u \\ v \end{bmatrix} = \begin{bmatrix} \sin\theta & \cos\theta \\ -\cos\theta & \sin\theta \end{bmatrix} \begin{bmatrix} x \\ z \end{bmatrix} \qquad (2\ 7)$$

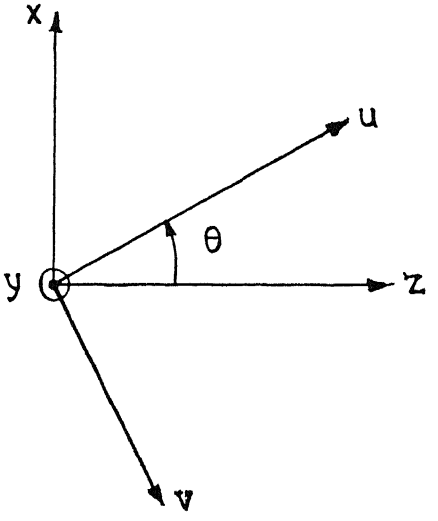

Fig 2 3 Coordinate transformation from (u,v) coordinate system to (x,y) coordinate system

The plane waves in the u- direction are now decomposed into TE-to-y ($\hat{H}_y$, $\hat{E}_v$, $\hat{H}_u$) and TM-to-y ($\hat{E}_y$, $\hat{E}_u$, $\hat{H}_v$) The metalizations at $y = d + h_1$ in Fig 2 1 and at $y = d_1 + h_1$ in Fig 2 2 are taken into account by introducing current densities $\hat{J}_u$ and $\hat{J}_v$, the first generating only TM fields and the second

generating only the TE fields

We can now draw equivalent circuits for each spectral component of TM and TE waves as shown in Fig 2 1 and Fig 2 2 The wave admittances for TM and TE waves are defined as

$$Y_{TMi} = \frac{\hat{H}_v}{\hat{E}_u} = \frac{j \omega \varepsilon_0 \varepsilon_{ri}}{\gamma_i} \qquad (2\ 8a)$$

$$Y_{TEi} = \frac{\hat{H}_u}{\hat{E}_v} = \frac{\gamma_i}{j \omega \mu_0}, \qquad (2\ 8b)$$

i=1, 2, 3 for unilateral finline

i=1, 2, 3, 4 for insulated fin line

where $\gamma_i = \sqrt{\alpha_n^2 + \beta^2 - \varepsilon_{ri} k_0^2}$ is the propagation constant

in y-direction in ith region All the boundary conditions for TM and TE waves are incorporated in the equivalent circuits

By using the transmission line theory

$$\hat{J}_u (\alpha_n, y_0) = Y_{11}^e \hat{E}_u (\alpha_n, y_0) \qquad (2\ 9a)$$

$$\hat{J}_v (\alpha_n, y_0) = Y_{11}^h \hat{E}_v (\alpha_n, y_0) \qquad (2\ 9b)$$

where

$y_0 = d + h_1$ for unilateral fin line

$y_0 = d_1 + h_1$ for insulated fin line

Y_{11}^e and Y_{11}^h are the driving point admittances at $y = d + h_1$ for unilateral fin line and $y = d_1 + h_1$ for insulated fin line, for TE and TM modes, respectively

Equations (2 9)can be written in matrix form as follows

$$\begin{bmatrix} \hat{J}_u(\alpha_n, y_0) \\ \hat{J}_v(\alpha_n, y_0) \end{bmatrix} = \begin{bmatrix} \mathbf{Y}^e_{11} & 0 \\ 0 & \mathbf{Y}^h_{11} \end{bmatrix} \begin{bmatrix} \hat{E}_u(\alpha_n, y_0) \\ \hat{E}_v(\alpha_n, y_0) \end{bmatrix} \qquad (2\ 10)$$

$\mathbf{Y}^e_{11}$ and $\mathbf{Y}^h_{11}$ for both the fin lines are derived as below

2 2.1 1 *Derivation of* $\mathbf{Y}^e_{11}$ *and* $\mathbf{Y}^h_{11}$ *for unilateral fin line*

From Fig 2 1(b) ,we have

$$\mathbf{Y}^e_{11} = Y^e_2 + Y^e_3 \qquad (2\ 11a)$$

where

$$Y^e_2 = \frac{Y_{TM2}\,[\,Y_{TM2} + Y^e_1 \coth(\gamma_2 d)]}{[\,Y^e_1 + Y_{TM2} \coth(\gamma_2 d)\,]} \qquad (2\ 11b)$$

$$Y^e_1 = Y_{TM1} \coth(\gamma_1 h_1) \qquad (2\ 11c)$$

$$Y^e_3 = Y_{TM3} \coth(\gamma_3 h_2) \qquad (2\ 11d)$$

similar expressions can be derived for $\mathbf{Y}^h_{11}$ also, From the equivalent circuit shown in Fig 2 1(b), we have

$$\mathbf{Y}^h_{11} = Y^h_2 + Y^h_3 \qquad (2\ 12a)$$

where

$$Y^h_2 = \frac{Y_{TE2}\,[\,Y_{TE2} + Y^h_1 \coth(\gamma_2 d)]}{[\,Y^h_1 + Y_{TE2} \coth(\gamma_2 d)\,]} \qquad (2\ 12b)$$

$$Y^h_1 = Y_{TE1} \coth(\gamma_1 h_1) \qquad (2\ 12c)$$

$$Y^h_3 = Y_{TE3} \coth(\gamma_3 h_2) \qquad (2\ 12d)$$

2 2 1 2 *Derivation of* $\mathbf{Y}^e_{11}$ *and* $\mathbf{Y}^h_{11}$ *for insulated fin line*

From Fig 2 2(b) ,we have

$$Y_{11}^{e} = Y_{2}^{e} + Y_{3}^{e} \qquad (2\ 13a)$$

where

$$Y_{2}^{e} = \frac{Y_{TM2}\ [\ Y_{TM2} + Y_{1}^{e} \coth(\gamma_{2} d_{1})]}{[\ Y_{1}^{e} + Y_{TM2} \coth(\gamma_{2} d_{1})\ ]} \qquad (2\ 13b)$$

$$Y_{1}^{e} = Y_{TM1} \coth(\gamma_{1} h_{1}) \qquad (2\ 13c)$$

$$Y_{3}^{e} = \frac{Y_{TM3}\ [\ Y_{TM3} + Y_{4}^{e} \coth(\gamma_{3} d_{2})]}{[\ Y_{4}^{e} + Y_{TM3} \coth(\gamma_{3} d_{2})\ ]} \qquad (2\ 13d)$$

$$Y_{4}^{e} = Y_{TM4} \coth(\gamma_{4} h_{2}) \qquad (2\ 13e)$$

similarly from the equivalent circuit shown in Fig 2 2(b), we have

$$Y_{11}^{h} = Y_{2}^{h} + Y_{3}^{h} \qquad (2\ 14a)$$

where

$$Y_{2}^{h} = \frac{Y_{TE2}\ [\ Y_{TE2} + Y_{1}^{h} \coth(\gamma_{2} d_{1})]}{[\ Y_{1}^{h} + Y_{TE2} \coth(\gamma_{2} d_{1})\ ]} \qquad (2\ 14b)$$

$$Y_{1}^{h} = Y_{TE1} \coth(\gamma_{1} h_{1}) \qquad (2\ 14c)$$

$$Y_{3}^{h} = \frac{Y_{TE3}\ [\ Y_{TE3} + Y_{4}^{h} \coth(\gamma_{3} d_{2})]}{[\ Y_{4}^{h} + Y_{TE3} \coth(\gamma_{3} d_{2})\ ]} \qquad (2\ 14d)$$

$$Y_{4}^{h} = Y_{TE4} \coth(\gamma_{4} h_{2}) \qquad (2\ 12e)$$

As we can see the regions '1' and '3' in unliteral fin line and regions '1' and '4' in insulted fin line have air as dielectric, we have

$$\gamma_1 = \gamma_3 = \sqrt{\alpha^2 + \beta_0^2 - k^2} \qquad \text{for unilateral fin line}$$

and

$$\gamma_1 = \gamma_4 = \sqrt{\alpha^2 + \beta^2 - k^2} \qquad \text{for insulated fin line}$$

By using coordinate transformation(2 7), we can rewrite(2 10) in term of (x, z) coordinate system as

$$\begin{bmatrix} \hat{J}_x(\alpha_n, y_0) \\ \hat{J}_z(\alpha_n, y_0) \end{bmatrix} = \begin{bmatrix} \hat{G}_{11} & \hat{G}_{12} \\ \hat{G}_{21} & \hat{G}_{22} \end{bmatrix} \begin{bmatrix} \hat{E}_z(\alpha_n, y_0) \\ \hat{E}_x(\alpha_n, y_0) \end{bmatrix} \qquad (2\ 15)$$

where

$$\hat{G}_{11}(\alpha_n, \beta) = (Y_{11}^e - Y_{11}^h) \sin\theta \cos\theta \qquad (2\ 16a)$$

$$\hat{G}_{12}(\alpha_n, \beta) = Y_{11}^e \sin^2\theta + Y_{11}^h \cos^2\theta \qquad (2\ 16b)$$

$$\hat{G}_{21}(\alpha_n, \beta) = Y_{11}^h \sin^2\theta + Y_{11}^e \cos^2\theta \qquad (2\ 16c)$$

$$\hat{G}_{22}(\alpha_n, \beta) = G_{11}(\alpha_n, \beta) \qquad (2\ 16d)$$

2 2 2 *Characteristic Equation*

In equation (2 15) $\hat{E}_x(\alpha_n, y_0)$, $\hat{E}_z(\alpha_n, y_0)$ and $\hat{J}_x(\alpha_n, y_0)$, $\hat{J}_z(\alpha_n, y_0)$ are the electric fields and currents at the interface in which slot and fins exist Since they are nonzero in the complementary regions it is possible to eliminate $\hat{J}_x$ and $\hat{J}_z$ by using *Galerkin's method* and *Parseval's theorem* and solve for $\hat{E}_x(\alpha_n)$ and $\hat{E}_z(\alpha_n)$

If we define inner product of the two functions as

$$< \hat{\psi}_1(\alpha_n), \hat{\psi}_2^*(\alpha_n) > = \sum^{\infty} \hat{\psi}_1(\alpha_n) \hat{\psi}_2^*(\alpha_n) \qquad (2\ 17)$$

According to Parseval's theorem, we have

$$\int_{-b/2}^{b/2} \hat{\psi}_1(x) \hat{\psi}_2(x) dx = \frac{1}{b} \sum_{n=-\infty}^{\infty} \hat{\psi}_1(\alpha_n) \hat{\psi}_2^*(\alpha_n) \qquad (2\ 18)$$

Expanding the slot fields $\hat{E}_x(\alpha n)$ and $\hat{E}_z(\alpha n)$ in terms of known basis functions

$\hat{f}_{xm}$ and $\hat{g}_{zm}$ respectively

$$\hat{E}_x(\alpha_n) = \sum_{m=1}^{M} C_m \hat{f}_{xm}(\alpha_n) \qquad (2\ 19a)$$

$$\hat{E}_z(\alpha_n) = \sum_{m=1}^{N} D_m \hat{g}_{zm}(\alpha_n) \qquad (2\ 19b)$$

where C_m and D_m are the coefficients of expansion Substituting (2 19) in (2 15) we get

$$\hat{G}_{11}(\alpha_n, \beta) \sum_{m=1}^{N} D_m \hat{g}_{zm}(\alpha_n) + \hat{G}_{12}(\alpha_n, \beta) \sum_{m=1}^{M} C_m \hat{f}_{xm}(\alpha_n) = \hat{J}_x(\alpha_n) \qquad (2\ 20a)$$

$$\hat{G}_{21}(\alpha_n, \beta) \sum_{m=1}^{N} D_m \hat{g}_{zm}(\alpha_n) + \hat{G}_{22}(\alpha_n, \beta) \sum_{m=1}^{M} C_m \hat{f}_{xm}(\alpha_n) = \hat{J}_z(\alpha_n) \qquad (2\ 20b)$$

taking the inner product of equation (2 20a) with f^*_{xl} and that of equation (2 20b) with g^*_{zl}, and using (2 17) and (2 18), along with the information that fields and currents at $y = y_0$ are nonzero in the complementary regions, we get the following set of homogeneous equations

$$\sum_{m=1}^{N} P_{lm} D_m + \sum_{m=1}^{M} Q_{lm} C_m = 0 \qquad l=1, 2, \quad M \qquad (2\ 21a)$$

$$\sum_{m=1}^{N} R_{lm} D_m + \sum_{m=1}^{M} S_{lm} C_m = 0 \qquad l=1, 2, \quad N \qquad (2\ 21b)$$

where

$$P_{lm} = \sum_{n=-\infty}^{\infty} \hat{f}^*_{xl}(\alpha_n) \hat{G}_{11}(\alpha_n, \beta) \hat{g}_{zm}(\alpha_n), \quad l=1, 2, \quad M \qquad (2\ 22a)$$

$$Q_{lm} = \sum_{n=-\infty}^{\infty} \hat{f}^*_{xi}(\alpha_n) \hat{G}_{12}(\alpha_n, \beta) \hat{f}_{xm}(\alpha_n), \quad l=1, 2, \quad M \qquad (2\ 22b)$$

$$R_{im} = \sum_{n=-\infty}^{\infty} \hat{g}^{*}_{zi}(\alpha_n)\, \hat{G}_{21}(\alpha_n, \beta)\, \hat{g}_{zm}(\alpha_n), \quad i=1, 2, \quad N \qquad (2\ 22c)$$

$$S_{im} = \sum_{n=-\infty}^{\infty} \hat{g}^{*}_{zi}(\alpha_n)\, \hat{G}_{22}(\alpha_n, \beta)\, \hat{f}_{xm}(\alpha_n), \quad i=1, 2, \quad N \qquad (2\ 22a)$$

The characteristic equation for determining the propagation constant of the dominant and higher order modes is obtained by setting the determinant of the coefficient matrix in (2 21) equal to zero Here the coefficients do not refer to the coefficients of expansions (C_m and D_m in (2 19)), rather they are P_{im}, Q_{im}, R_{im} and S_{im} as given in (2 22)

2 2 3 *Choice of Basis Functions*

The numerical solution of (2 21) is obtained by introducing a known set of basis functions The accuracy of the final solution depends on the accuracy with which the basis functions represents the true electric field distribution in the aperture Following basis functions for slot field which include the edge conditions [42] have been chosen for finding out the propagation constants of both the fin lines

$$f_{xm}(x) = \cos\ [\ (m-1)\pi\ (2x/w + 1)]\quad [1- (2x/w)^2\ ]^{-1/2} \qquad (2\ 23a)$$

$$g_{zm}(x) = \sin\ [\ (m-1)\pi\ (2x/w + 1)]\quad [1- (2x/w)^2\ ]^{-1/2} \qquad (2\ 23a)$$

Using the definition given in (2 5), equations (2 23) are transformed into the spectral domain and we get

$$\hat{f}_{xm}(\alpha_n) = (-1)^{m-1}\ \pi\ w/4\ [J_0(\alpha_n w/2 + (m-1)\pi\ ) + J_0(\alpha_n w/2 - (m-1)\pi)] \qquad (2\ 24a)$$

$$\hat{g}_{zm}(\alpha_n) = (-1)^{m-1}\ j\pi\ w/4\ [J_0(\alpha_n w/2 - (m-1)\pi\ ) - J_0(\alpha_n w/2 + (m-1)\pi)] \qquad (2\ 24b)$$

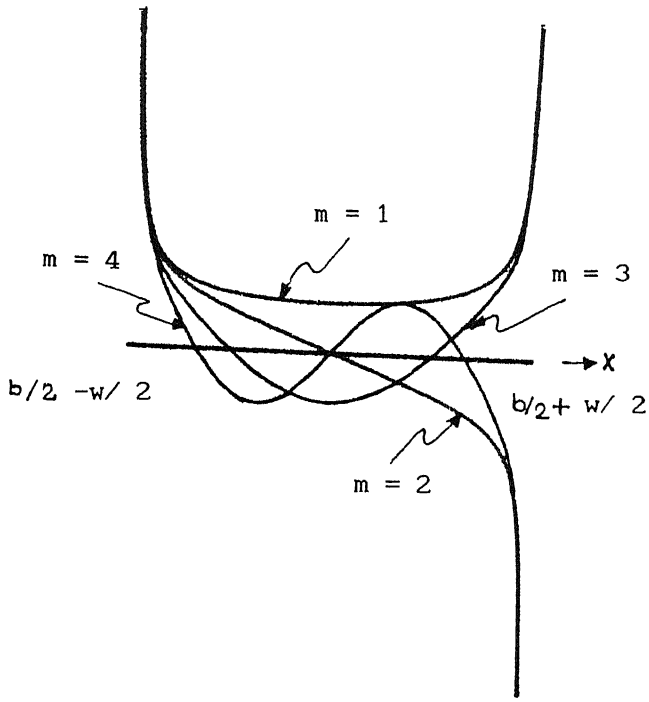

(a) $f_{xm}(x)$

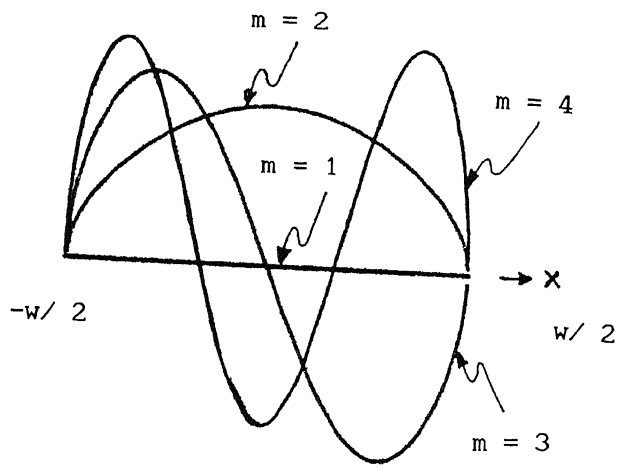

(b) $g_{zm}(x)$

Fig 2 4 Basis functions for slot field

Fig 2 4 shows their behaviour in the slot region in the transverse direction

2 2 4 *Numerical Results*

A FORTRAN program FINBETA is written to compute the propagation constant of unilateral fin line using equations (2 21) (2 22) and (2 23) which subsequently use the other expressions derived for unilateral fin line The same program with necessary modifications is later used for finding out propagation constant of insulated fin line With M = N = 3 in (2 19) and n = -150 to 150 gives an accuracy up to third decimal place Fig 2 5 and Fig 2 6 show the variation of propagation constant with frequency for unilateral and insulated fin line respectively These results are used in the subsequent chapters for characterization of discontinuities in these fin lines

The Dimensions of Unilateral and insulated fin lines for theoretical and experimetal purposes, in X-band and Ka-band, have been taken as follows

Unilateral fin line

(i) X-band: a = 22 86mm, b = 10 16mm, h_1= 10 636mm, h_2= 11 43mm, d = 794mm, ε_r= 2 22, W/b = 0 2

(ii) Ka-band: a = 7 112mm, b = 3 556mm, h_1= 3 302mm, h_2= 3 556mm, d = 0 254mm, ε_r= 2 22, W/b = 0 2

Insulated fin line

(i) X-band: a = 22 86mm, b = 10 16mm, h_1= 11 033mm, h_2= 11 033mm, d_1= 397mm, d_2 = 397mm, ε_r = 2 22, W/b = 0 2

(i) Ka-band: a = 7 112mm, b = 3 556mm, h_1= 3 429mm, h_2= 3 429mm, d_1= 127mm, d_2 = 127mm, ε_r = 2 22, W/b = 0 2

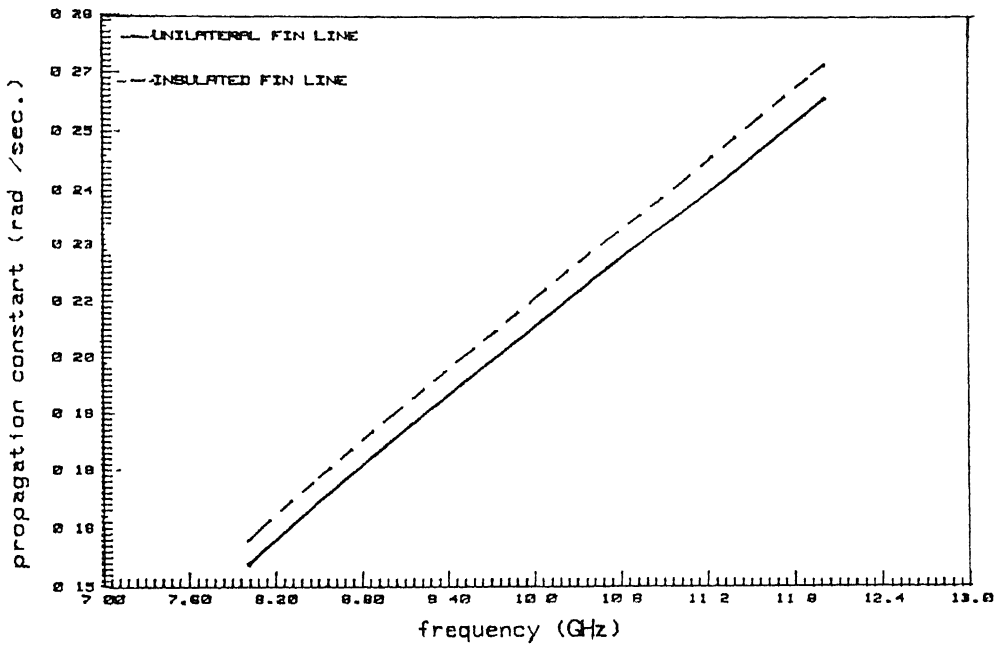

Fig 2 5 Propagation constant of unilateral and insulated fin line as a function of frequency in X-band

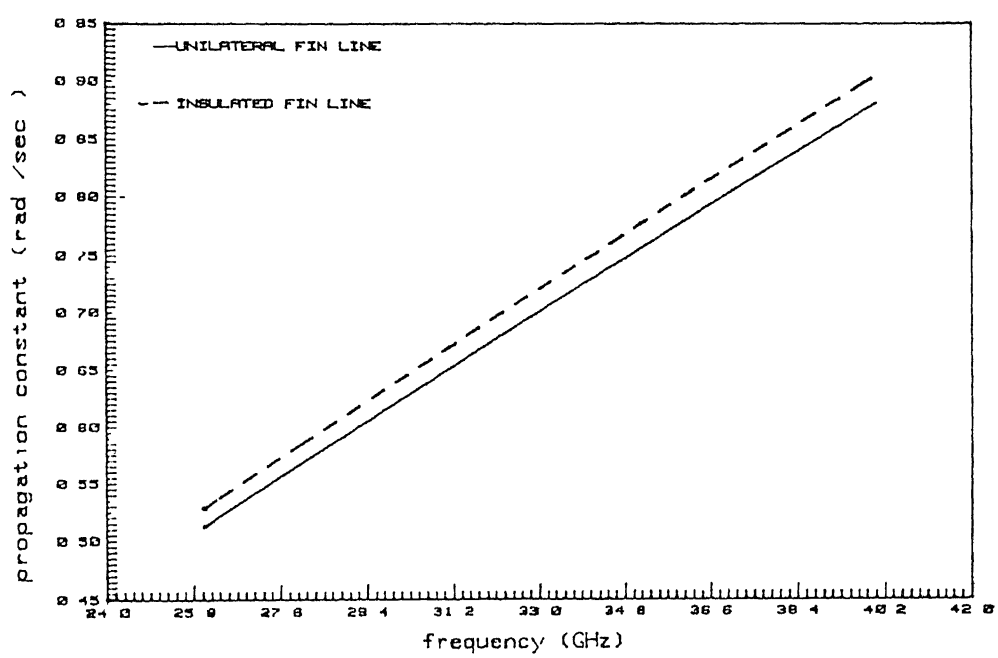

Fig 2 6 Propagation constant of unilateral and insulated fin line as a function of frequency in Ka-band

CHAPTER 3

CHARACTERIZATION OF OFF-SLOT DISCONTINUITY IN UNILATERAL FIN LINE

3 1 INTRODUCTION

The characterization of fin line discontinuity has been a subject of considerable research interest in past few years This is because, an accurate knowledge of the discontinuity parameters enables more accurate design of practical fin line circuits Of the various types of discontinuities encountered in fin lines, inductive strip has been analyzed by many researchers using various techniques We are going to present in this chapter a new type of discontinuity in unilateral fin line structure The discontinuity consists of a rectangular conducting strip placed symmetrically across the slot in the air-dielectric interface, which does not contain any metalization otherwise In the subsequent chapter it has been experimentally shown that the discontinuity is useful in realization of low pass filter

This chapter gives the general analysis of fin line discontinuity using transverse resonance technique proposed by Sorretino and Itoh [26] This technique makes use of a model of fin line cavity housing the discontinuity Before applying resonance condition, it is necessary to analyze the fin line cavity in the presence of discontinuity and obtain the resonant length We begin the analysis by expanding the fields in various regions of cavity in terms of hybrid modes whereas slot aperture fields and strip currents are expressed in terms of accurate basis functions Imposing the boundary conditions and then making use of *Galerkin's method*, we obtain a set of homogeneous equations in terms of unknown coefficients These are the coefficients used to expand the slot aperture fields and strip currents in terms of suitable sets of basis functions For a specified frequency, the

resonant length is calculated by setting the determinant of the coefficient matrix, obtained from the homogeneous equations, equal to Zero

3.2 TRANSVERSE RESONANCE TECHNIQUE

The application of the concept of transverse resonance involves setting the total reactance at any plane in the cavity equal to zero This concept can be utilized for evaluating the impedance parameters of any discontinuity in the cavity It is assumed that higher order modes generated by the discontinuity will not reach the cavity walls Fig 3 1 shows the cross sectional and longitudinal views of fin line cavity with an arbitrary discontinuity Fig 3 2 shows its equivalent circuit representation The resonance condition in terms of impedance parameters of the discontinuity is given by [26]

$$(Z_{11} + Z_1)(Z_{22} + Z_2) - Z_{12}^2 = 0 \qquad (3\ 1a)$$

where

$$Z_i = jZ_{0i}\tan(\beta_i \ell_i), \quad i = 1,2 \qquad (3\ 1b)$$

Z_{11}, Z_{12} $(= Z_{21})$ and Z_{22} are the Z-parameters of the discontinuity Z_{0i} and β_i with $i = 1, 2$, are the characteristic impedance and propagation constant of the two fin line sections as shown in Fig 3 2

In case of discontinuity with longitudinal symmetry, the resonance condition in terms of T-equivalent circuit parameters are given by

$$\bar{X}_{se} + j \tan(\beta \ell_e) = 0 \qquad (3\ 2a)$$

$$\bar{X}_{se} + 2\bar{X}_{sh} + j \tan(\beta \ell_m) = 0 \qquad (3\ 2b)$$

where $\bar{X}_{se}$ and $\bar{X}_{sh}$ are the normalized (with respect to characteristic impedance of the fin line) series and shunt impedance parameters of the T-equivalent network, ℓ_e and ℓ_m are the resonant lengths of the fin line for odd and even mode respectively and β is the dominant mode propagation constant of the fin line

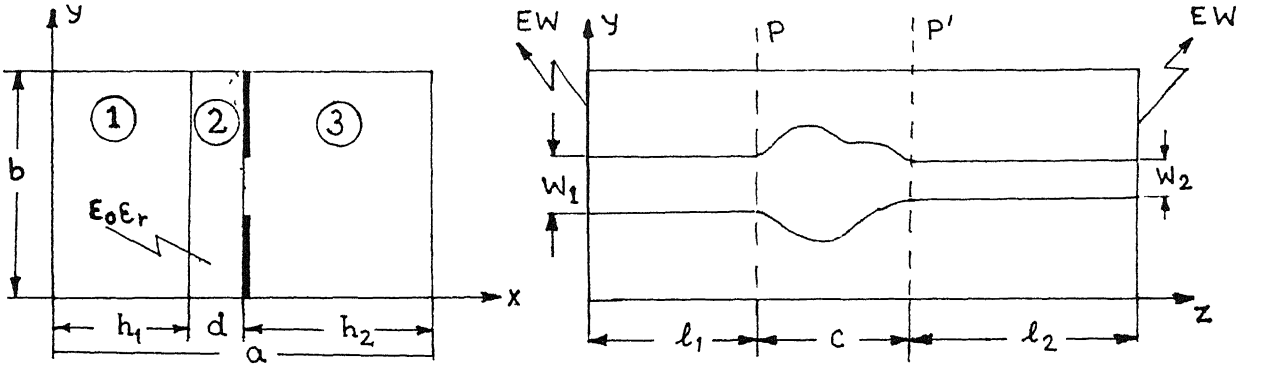

(a) Cross section (b) Longitudinal section

Fig 3 1 Cross sectional and longitudinal views of a unilateral fin line cavity containing an arbitrary discontinuity

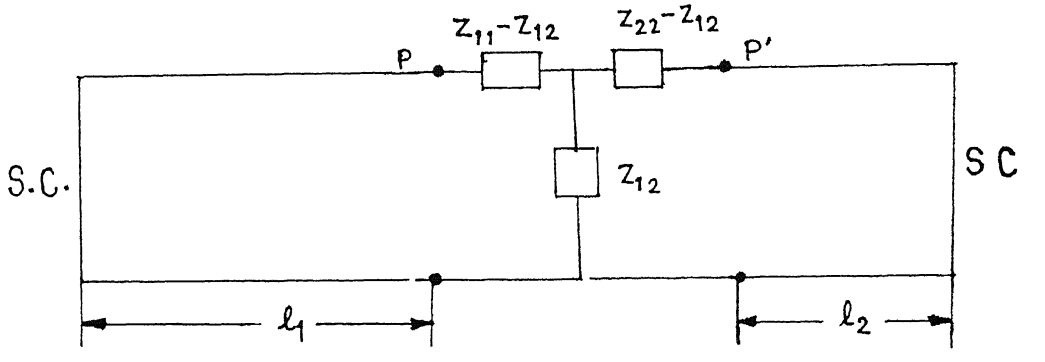

Fig 3 2 Equivalent circuit representation of the fin line cavity containing the discontinuity

3.3 ANALYSIS OF A DISCONTINUITY IN UNILATERAL FIN LINE USING MODAL ANALYSIS APPROACH

3 3 1 *Basic formulation*

Let the field inside the fin line cavity (Fig 3 3) housing the discontinuity with electric walls at $z = 0$ and $z = \ell$, has x, y, z and time dependence as $e^{-jkx\,x}$, $e^{-jky\,y}$, $e^{-jkz\,z}$ and $e^{j\omega t}$ respectively

In a source free region Maxwell's equations have the following form

$$\nabla \times \vec{H} = j\omega\,\varepsilon_0\varepsilon_r\,\vec{E} \qquad (3\ 3a)$$

$$\nabla \times \vec{E} = -j\omega\,\mu_0\,\vec{H} \qquad (3\ 3b)$$

where ε_r is the dielectric constant of the medium Equations (3 3) can be solved to give

$$\begin{bmatrix} \vec{E} \\ \vec{H} \end{bmatrix} = \frac{1}{(k^2 - k_x^2)} \begin{bmatrix} \partial/\partial x & j\,\omega_0\mu\,\hat{x} \\ -j\omega\,\varepsilon_0\varepsilon_r\,\hat{x} & \partial/\partial x \end{bmatrix} \begin{bmatrix} \nabla t\ Ex \\ \nabla t\ Hx \end{bmatrix} \qquad (3\ 4)$$

where

$$\vec{E}t = \hat{y}\,Ey + \hat{z}\,Ez \qquad (3\ 5a)$$

$$\vec{H}t = \hat{y}\,Hy + \hat{z}\,Hz \qquad (3\ 5b)$$

$$\nabla t = \partial/\partial y\ \hat{y} + \partial/\partial z\ \hat{z} \qquad (3\ 5c)$$

and

Ex and Hx satisfy Helmholtz's equation i e

$$[\ \nabla^2 + k^2\ ] \begin{bmatrix} Ex \\ Hx \end{bmatrix} = 0 \qquad (3.6a)$$

$$\text{where } k^2 = \omega^2\,\mu_0\varepsilon_0\varepsilon_r = k_0^2\,\varepsilon_r \qquad (3.6b)$$

From (3 6a) we can write

$$k_x^2 + k_y^2 + k_z^2 - k^2 = 0 \qquad (3.6c)$$

Solution of (3 6a) in regions 1, 2 and 3 ,as shown in Fig 3 1 are given below

$$Ex^{(1)} = \sum_{m=1}^{\infty} \sum_{n=1}^{\infty} A_{mn1} \cos[\gamma_{mn1}\,(x - h2)]\ \sin(\alpha_n y)\ \sin(\beta_m z) \qquad (3\ 7a)$$

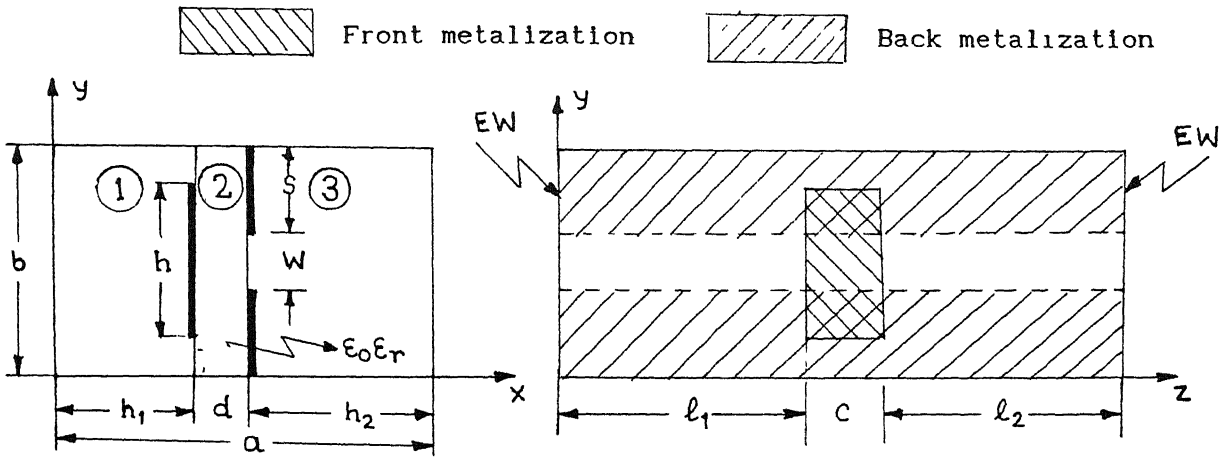

Fig 3 3 Cross sectional and longitudinal views of the symmetric off slot discontinuity in unilateral fin line

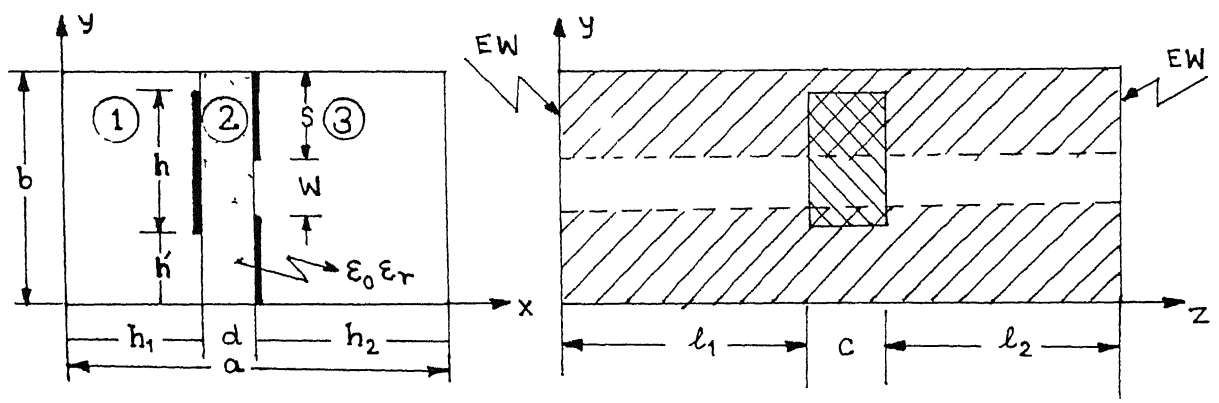

Fig 3 4 Cross sectional and longitudinal views of the asymmetric off slot discontinuity in unilateral fin line

$$H_x^{(1)} = \sum_{m=0}^{\infty} \sum_{n=0}^{\infty} B_{mn1} \sin[\gamma_{mn1} (x - h_2)] \cos(\alpha_n y) \cos(\beta_m z) \quad (3\ 7b)$$

$$E_x^{(2)} = \sum_{m=0}^{\infty} \sum_{n=0}^{\infty} [A_{mn2} \sin(\gamma_{mn2} x) + A'_{mn2} \cos(\gamma_{mn2} x)] \sin(\alpha_n y) \sin(\beta_m z) \quad (3\ 7c)$$

$$H_x^{(2)} = \sum_{m=0}^{\infty} \sum_{n=0}^{\infty} [B_{mn2} \cos(\gamma_{mn2} x) + B'_{mn2} \sin(\gamma_{mn2} x)] \cos(\alpha_n y) \cos(\beta_m z) \quad (3\ 7d)$$

$$E_x^{(3)} = \sum_{m=1}^{\infty} \sum_{n=1}^{\infty} A_{mn3} \cos[\gamma_{mn1}(x + d + h_1)] \sin(\alpha_n y) \sin(\beta_m z) \quad (3\ 7e)$$

$$H_x^{(3)} = \sum_{m=0}^{\infty} \sum_{n=0}^{\infty} B_{mn3} \sin[\gamma_{mn1}(x + d + h_1)] \cos(\alpha_n y) \cos(\beta_m z) \quad (3\ 7f)$$

Substituting (3 7) in (3 4) we get

$$E_y^{(1)} = \sum_{m=1}^{\infty} \sum_{n=0}^{\infty} S_{mn1} \sin[\gamma_{mn1} (x - h_2)] \cos(\alpha_n y) \sin(\beta_m z) \quad (3\ 8a)$$

$$H_y^{(1)} = \sum_{m=0}^{\infty} \sum_{n=1}^{\infty} M_{mn1} \cos[\gamma_{mn1} (x - h_2)] \sin(\alpha_n y) \cos(\beta_m z) \quad (3\ 8b)$$

$$E_y^{(2)} = \sum_{m=1}^{\infty} \sum_{n=0}^{\infty} [S_{mn2} \cos(\gamma_{mn2} x) + S'_{mn2} \sin(\gamma_{mn2} x)] \cos(\alpha_n y) \sin(\beta_m z) \quad (3\ 8c)$$

$$H_y^{(2)} = \sum_{m=0}^{\infty} \sum_{n=1}^{\infty} [M_{mn2} \sin(\gamma_{mn2} x) + M'_{mn2} \cos(\gamma_{mn2} x)] \sin(\alpha_n y) \cos(\beta_m z) \quad (3\ 8d)$$

$$E_y^{(3)} = \sum_{m=1}^{\infty} \sum_{n=0}^{\infty} S_{mn3} \sin[\gamma_{mn1}(x + d + h_1)] \cos(\alpha_n y) \sin(\beta_m z) \quad (3\ 8e)$$

$$H_y^{(3)} = \sum_{m=0}^{\infty} \sum_{n=1}^{\infty} M_{mn3} \cos[\gamma_{mn1}(x + d + h_1)] \sin(\alpha_n y) \cos(\beta_m z) \quad (3\ 8f)$$

where

$$S_{mn1} = (-A_{mn1} \alpha_n \gamma_{mn1} + j \omega \mu_0 \beta_m B_{mn1}) / (\alpha_n^2 + \beta_m^2) \quad (3\ 9a)$$

$$S_{mn2} = (A_{mn2} \alpha_n \gamma_{mn2} + j \omega \mu_0 \beta_m B_{mn2}) / (\alpha_n^2 + \beta_m^2) \quad (3\ 9b)$$

$$S'_{mn2} = (-A'_{mn2} \alpha_n \gamma_{mn2} + j \omega \mu_0 \beta_m B'_{mn2}) / (\alpha_n^2 + \beta_m^2) \quad (3\ 9c)$$

$$S_{mn3} = (-A_{mn3}\ \alpha_n\ \gamma_{mn1} + j\ \omega\ \mu_0\ \beta_m\ B_{mn3})/\ (\alpha_n^2 + \beta_m^2) \quad (3\ 9d)$$

$$M_{mn1} = (-B_{mn1}\ \alpha_n\ \gamma_{mn1} + j\ \omega\ \varepsilon_0\ \beta_m\ A_{mn1})/\ (\alpha_n^2 + \beta_m^2) \quad (3\ 9e)$$

$$M_{mn2} = (\ B_{mn2}\ \alpha_n\ \gamma_{mn2} + j\ \omega\ \varepsilon_0\ \varepsilon_r\ \beta_m\ A_{mn2})/\ (\alpha_n^2 + \beta_m^2) \quad (3\ 9f)$$

$$M'_{mn2} = (-B'_{mn2}\ \alpha_n\ \gamma_{mn2} + j\ \omega\ \varepsilon_0\ \varepsilon_r\ \beta_m\ A'_{mn2})/\ (\alpha_n^2 + \beta_m^2) \quad (3\ 9g)$$

$$M_{mn3} = (-B_{mn3}\ \alpha_n\ \gamma_{mn1} + j\ \omega\ \varepsilon_0\ \beta_m\ A_{mn3})/\ (\alpha_n^2 + \beta_m^2) \quad (3\ 9h)$$

and

$$Ez^{(1)} = \sum_{m=0}^{\infty}\ \sum_{n=1}^{\infty} C_{mn1}\ \sin[\gamma_{mn1}\ (x-h2)]\ \sin(\alpha_n y)\ \cos(\beta_m z) \quad (3\ 10a)$$

$$Hz^{(1)} = \sum_{m=1}^{\infty}\ \sum_{n=0}^{\infty} D_{mn1}\ \cos[\gamma_{mn1}\ (x-h2)]\ \cos(\alpha_n y)\ \sin(\beta_m z) \quad (3\ 10b)$$

$$Ez^{(2)} = \sum_{m=0}^{\infty}\ \sum_{n=1}^{\infty} [C_{mn2}\ \cos(\gamma_{mn2}\ x) + C'_{mn2}\ \sin(\gamma_{mn2}\ x)]\ \sin(\alpha_n y)\ \cos(\beta_m z) \quad (3\ 10c)$$

$$Hz^{(2)} = \sum_{m=1}^{\infty}\ \sum_{n=0}^{\infty} [D_{mn2}\ \sin(\gamma_{mn2}\ x) + D'_{mn2}\ \cos(\gamma_{mn2}\ x)]\ \cos(\alpha_n y)\ \sin(\beta_m z) \quad (3\ 10d)$$

$$Ez^{(3)} = \sum_{m=0}^{\infty}\ \sum_{n=1}^{\infty} C_{mn3}\ \sin[\gamma_{mn1}(x + d + h1)]\ \sin(\alpha_n y)\ \cos(\beta_m z) \quad (3\ 10e)$$

$$Hz^{(3)} = \sum_{m=1}^{\infty}\ \sum_{n=0}^{\infty} D_{mn3}\ \cos[\gamma_{mn1}(x + d + h1)]\ \cos(\alpha_n y)\ \sin(\beta_m z) \quad (3.10f)$$

where

$$C_{mn1} = (-A_{mn1}\ \beta_m\ \gamma_{mn1} - j\ \omega\ \mu_0\ \alpha_n\ B_{mn1})/\ (\alpha_n^2 + \beta_m^2) \quad (3\ 11a)$$

$$C_{mn2} = (\ A_{mn2}\ \beta_m\ \gamma_{mn2} - j\ \omega\ \mu_0\ \alpha_n\ B_{mn2})/\ (\alpha_n^2 + \beta_m^2) \quad (3\ 11b)$$

$$C'_{mn2} = (-A'_{mn2}\ \beta_m\ \gamma_{mn2} - j\ \omega\ \mu_0\ \alpha_n\ B'_{mn2})/\ (\alpha_n^2 + \beta_m^2) \quad (3\ 11c)$$

$$C_{mn3} = (-A_{mn3}\ \beta_m\ \gamma_{mn1} - j\ \omega\ \mu_0\ \alpha_n\ B_{mn3})/\ (\alpha_n^2 + \beta_m^2) \quad (3\ 11d)$$

$$D_{mn1} = (-B_{mn1}\ \beta_m\ \gamma_{mn1} - j\ \omega\ \varepsilon_0\ \alpha_n\ A_{mn1})/\ (\alpha_n^2 + \beta_m^2) \quad (3\ 11e)$$

$$D_{mn2} = (\ B_{mn2}\ \beta_m\ \gamma_{mn2} - j\ \omega\ \varepsilon_0\varepsilon_r\ \alpha_n\ A_{mn2})/\ (\alpha_n^2 + \beta_m^2) \quad (3\ 11f)$$

$$D'_{mn2} = (-B'_{mn2}\ \beta_m\ \gamma_{mn2} - j\ \omega\ \varepsilon_0\varepsilon_r\ \alpha_n\ A'_{mn2})/\ (\alpha_n^2 + \beta_m^2) \quad (3\ 11g)$$

$$D_{mn3} = (-B_{mn3}\ \beta_m\ \gamma_{mn1} - j\ \omega\ \varepsilon_0\ \alpha_n\ A_{mn3})/\ (\alpha_n^2 + \beta_m^2) \quad (3\ 11h)$$

where

$$kx1 = kx3 = \gamma_{mn1} = \sqrt{k_0^2 - \alpha_n^2 - \beta_m^2} = \gamma_{mn3} \qquad (3\ 12a)$$

$$kx2 = \gamma_{mn2} = \sqrt{k_0^2\varepsilon_r - \alpha_n^2 - \beta_m^2} \qquad (3\ 12b)$$

$$ky1 = ky2 = ky3 = \alpha_n = \begin{cases} n\pi/b, & b \neq 2s + W \text{ or } b \neq 2h' + h \\ 2n\pi/b, & b = 2s + W \text{ and } b = 2h' + h \end{cases} \qquad (3\ 12c)$$

$$kz1 = kz2 = kz3 = \beta_m = m\pi/\ell \qquad (3\ 12d)$$

Now applying boundary conditions at $x = 0$ and $x = -d$

at $x = 0$ we have

$$H_x^{(1)} = H_x^{(2)} \qquad (3\ 13a)$$

$$E_y^{(1)} = E_y^{(2)} \qquad (3\ 13b)$$

using (3 7) and (3 8) in (3 13), we have

$$A_{mn2} = A_{mn1}(\gamma_{mn1}/\gamma_{mn2})\sin(\gamma_{mn1} h_2) \qquad (3\ 13c)$$

$$B_{mn2} = -B_{mn1}\sin(\gamma_{mn1} h_2) \qquad (3\ 13d)$$

at $x = -d$, we have

$$E_y^{(2)} = E_y^{(3)} \qquad (3\ 14a)$$

$$E_z^{(2)} = E_z^{(3)} \qquad (3\ 14b)$$

using (3 8) and (3 10) in (3 14) we get

$$A_{mn3} = \left(\frac{-\gamma_{mn2}}{\gamma_{mn1}\sin(\gamma_{mn1} h_1)}\right)[A_{mn2}\cos(\gamma_{mn2} d) + A'_{mn2}\sin(\gamma_{mn2} d)] \qquad (3\ 15a)$$

$$B_{mn3} = \frac{1}{\sin(\gamma_{mn1} h_1)}[B_{mn2}\cos(\gamma_{mn2} d) - B'_{mn2}\sin(\gamma_{mn2} d)] \qquad (3\ 15a)$$

Substituting $x = 0$ in (3 8a) and (3 10a), we have

$$E_y^{(1)}\Big|_{x=0} = \sum_{m=1}^{\infty}\sum_{n=0}^{\infty} - S_{mn1}\sin(\gamma_{mn1} h_2)\cos(\alpha_n y)\sin(\beta_m z) \qquad (3\ 16a)$$

$$E_z^{(1)}\Big|_{x=0} = \sum_{m=0}^{\infty} \sum_{n=1}^{\infty} - C_{mn1} \sin(\gamma_{mn1} h_2) \sin(\alpha_n y) \cos(\beta_m z) \tag{3.16b}$$

Multiplying both sides of (3 16a) with $\cos(\alpha_n y)\ \sin(\beta_m z)$ and (3 16b) with $\sin(\alpha_n y)\ \cos(\beta_m z)$, integrating within limits, $y = 0$ to b and $z = 0$ to ℓ and using the orthogonality property , we have

$$\delta_{mn}\, L_{1emn} = -(\ell b/4)\ C_{mn1} \sin(\gamma_{mn1} h_2) \tag{3 17a}$$

$$\delta'_{mn}\, L_{2emn} = -(\ell b/4)\ S_{mn1} \sin(\gamma_{mn1} h_2) \tag{3 17b}$$

where we have defined

$$L_{1emn} = \int_{y=0}^{b}\int_{z=0}^{\ell} E_z^{(1)}\Big|_{x=0} \sin(\alpha_n y)\ \cos(\beta_m z)\ dydz \tag{3 18a}$$

$$L_{2emn} = \int_{y=0}^{b}\int_{z=0}^{\ell} E_y^{(1)}\Big|_{x=0} \cos(\alpha_n y)\ \sin(\beta_m z)\ dydz \tag{3 18b}$$

and

$$\delta_{mn} = \begin{cases} 0\ , & n = 0 \\ 1/2, & m=0,\ n\neq 0 \\ 1\ , & m\neq 0,\ n\neq 0 \end{cases} \tag{3 19a}$$

$$\delta'_{mn} = \begin{cases} 0\ , & m = 0 \\ 1/2, & n=0,\ m\neq 0 \\ 1\ , & m\neq 0,\ n\neq 0 \end{cases} \tag{3 19b}$$

Substituting (3 11a) in (3 17a) and (3 9a) in (3 17a) , we have

$$A_{mn1} = \frac{4\ [\ L_{1emn}\ \delta_{mn}\ \beta_m + L_{2emn}\ \delta'_{mn}\ \alpha_n\ ]}{\ell b\ \gamma_{mn1} \sin(\gamma_{mn1} h_2)} \tag{3 20a}$$

$$B_{mn1} = \frac{4\ [\ L_{1emn}\ \delta_{mn}\ \alpha_n - L_{2emn}\ \delta'_{mn}\ \beta_m\ ]}{j\ \omega\ \mu_0\ \ell b \sin(\gamma_{mn1} h_2)} \tag{3 20b}$$

Now at $x = -d$, we have following boundary conditions to be satisfied

$$H_y^{(2)} - H_y^{(3)} = I_{z2}\ (y, z) \tag{3 21a}$$

$$H_z^{(3)} - H_z^{(2)} = I_{y2}\ (y, z) \tag{3 21b}$$

making use of (3 8) and (3.10)in (3 21), using orthogonality property, subsequently using equations (3 9) and (3 11) and finally solving the resulting

two equations, we obtain

$$A_{mn3} = \frac{-1}{\cos(\gamma_{mn1} h_1)} \left[\varepsilon_r [A_{mn2} \sin(\gamma_{mn2} d) - A'_{mn2} \cos(\gamma_{mn2} d)] + \frac{4}{j\omega \varepsilon_0 \ell b} [L_{1Imn} \delta_{mn} \beta_m + L_{2Imn} \delta'_{mn} \alpha_n] \right] \quad (3\ 22a)$$

$$B_{mn3} = \frac{1}{\gamma_{mn1} \cos(\gamma_{mn1} h_1)} \left[\gamma_{mn2} [B_{mn2} \sin(\gamma_{mn2} d) + B'_{mn2} \cos(\gamma_{mn2} d)] + \frac{4}{\ell b} [L_{1Imn} \delta_{mn} \alpha_n - L_{2Imn} \delta'_{mn} \beta_m] \right] \quad (3\ 22b)$$

where, we have defined L1Imn and L2Imn as

$$L_{1Imn} = \int_{y=0}^{b} \int_{z=0}^{\ell} Iz2 \Big|_{X=-d} \sin(\alpha_n y) \cos(\beta_m z)\, dydz \quad (3\ 18c)$$

$$L_{2Imn} = \int_{y=0}^{b} \int_{z=0}^{\ell} Iy2 \Big|_{X=-d} \cos(\alpha_n y) \sin(\beta_m z)\, dydz \quad (3\ 18d)$$

Solving (3 15a) with (3 22a), we get

$$A'_{mn2} = P_1 - F_{mn1} A_{mn2} \quad (3\ 23a)$$

where

$$P_1 = \frac{4 \gamma_{mn1} \tan (\gamma_{mn1} h_1) [L_{1Imn} \delta_{mn} \beta_m + L_{2Imn} \delta'_{mn} \alpha_n]}{j\omega \varepsilon_0 \ell b \cos(\gamma_{mn2} d) [\gamma_{mn2} \tan(\gamma_{mn2} d) + \varepsilon_r \gamma_{mn1} \tan(\gamma_{mn1} h_1)]} \quad (3\ 23b)$$

and

$$F_{mn1} = \frac{[\gamma_{mn2} \cot(\gamma_{mn1} h_1) \cot (\gamma_{mn2} d) - \varepsilon_r \gamma_{mn1}]}{[\gamma_{mn2} \cot(\gamma_{mn1} h_1) + \varepsilon_r \gamma_{mn1} \cot(\gamma_{mn2} d)]} \quad (3\ 23c)$$

similarly, solving (3 15b) with (3 22b) we have

$$B'_{mn2} = F_{mn2} B_{mn2} - P_2 \quad (3\ 24a)$$

where

$$P_2 = \frac{4 \tan(\gamma_{mn1} h_1) [L_{1Imn} \delta_{mn} \alpha_n - L_{2Imn} \delta'_{mn} \beta_m]}{\ell b \cos(\gamma_{mn2} d) [\gamma_{mn1} \tan(\gamma_{mn2} d) + \gamma_{mn2} \tan(\gamma_{mn1} h_1)]} \quad (3\ 24b)$$

and

$$F_{mn2} = \frac{[\gamma_{mn1} \cot(\gamma_{mn1} h_1) \cot(\gamma_{mn2} d) - \gamma_{mn2}]}{[\gamma_{mn1} \cot(\gamma_{mn1} h_1) + \gamma_{mn2} \cot(\gamma_{mn2} d)]} \quad (3\ 24c)$$

Now at $x = 0$ also, we have two more boundary conditions to be satisfied

$$- H_z^{(1)} + H_z^{(2)} = I_{y1}(y, z) \quad (3\ 25a)$$

$$H_y^{(1)} - H_y^{(2)} = I_{z1}(y, z) \quad (3\ 25b)$$

using all the previous equations and definitions (3 25a) and (3 25b) can be expressed as

$$\sum_{m=1}^{\infty} \sum_{n=0}^{\infty} (G_{11} L_{1emn} + G_{12} L_{2emn} + G_{13} L_{1Imn} + G_{14} L_{2Imn}) \cos(\alpha_n y) \sin(\beta_m z) = I_{y1} \quad (3\ 26a)$$

$$\sum_{m=0}^{\infty} \sum_{n=1}^{\infty} (G_{21} L_{1emn} + G_{22} L_{2emn} + G_{23} L_{1Imn} + G_{24} L_{2Imn}) \sin(\alpha_n y) \cos(\beta_m z) = I_{z1} \quad (3\ 26b)$$

Also at $x = - d$, (3 8c) and (3 10c) can be written as

$$\sum_{m=1}^{\infty} \sum_{n=0}^{\infty} S_{mn3} \sin(\gamma_{mn1} h_1) \cos(\alpha_n y) \sin(\beta_m z) = E_{y3}(y, z) \quad (3.27a)$$

$$\sum_{m=0}^{\infty} \sum_{n=1}^{\infty} C_{mn3} \sin(\gamma_{mn1} h_1) \sin(\alpha_n y) \cos(\beta_m z) = E_{z3}(y, z) \quad (3.27b)$$

Substituting S_{mn3} and C_{mn3} in terms of L_{1emn}, L_{2emn}, L_{1Imn} and L_{2Imn}, we can express (3 27) as follows

$$\sum_{m=1}^{\infty} \sum_{n=0}^{\infty} (G_{31} L_{1emn} + G_{32} L_{2emn} + G_{33} L_{1Imn} + G_{34} L_{2Imn}) \cos(\alpha_n y) \sin(\beta_m z) = E_{y3} \quad (3\ 26c)$$

$$\sum_{m=0}^{\infty} \sum_{n=1}^{\infty} (G_{41} L_{1emn} + G_{42} L_{2emn} + G_{43} L_{1Imn} + G_{44} L_{2Imn}) \sin(\alpha_n y) \cos(\beta_m z) = E_{z3} \quad (3\ 26d)$$

In equation (3 26) above, I_{y1} and I_{z1} are the components of current at $x = 0$ and, E_{y3} and E_{z3} are the field components at $x = - d$ The expressions for

G_{11}, G_{12} G_{44} are given in Appendix A.

3 3 2 *Characteristic equation*

Applying *Galerkin's procedure* in equations (3 26) i e taking the inner product of (3 26a), (3 26b), (3 26c) and (3 26d) with $E_{y1}^{(i,j)}$, $E_{z1}^{(i',j')}$, $I_{y3}^{(k,l)}$ and $I_{z3}^{(k',l')}$, respectively and noting that the electric field components and currents at $x = 0$ and $x = -d$, are zero in the complementary regions, we get the following set of homogeneous equations

$$\sum_{p'=1}^{P'}\sum_{q'=1}^{Q'} C_{Ep'q'} \sum_{m=1}^{\infty}\sum_{n=0}^{\infty} G_{11}(\alpha_n, \beta_m) L_{1emn}^{(p',q')} L_{2emn}^{(i,j)}$$

$$+ \sum_{p=1}^{P}\sum_{q=1}^{Q} D_{Epq} \sum_{m=1}^{\infty}\sum_{n=0}^{\infty} G_{12}(\alpha_n, \beta_m) L_{2emn}^{(p,q)} L_{2emn}^{(i,j)}$$

$$+ \sum_{r'=1}^{R'}\sum_{s'=1}^{S'} C_{Ir's'} \sum_{m=1}^{\infty}\sum_{n=0}^{\infty} G_{13}(\alpha_n, \beta_m) L_{1Imn}^{(r',s')} L_{2emn}^{(i,j)}$$

$$+ \sum_{r=1}^{R}\sum_{s=1}^{S} D_{Irs} \sum_{m=1}^{\infty}\sum_{n=0}^{\infty} G_{14}(\alpha_n, \beta_m) L_{2Imn}^{(r,s)} L_{2emn}^{(i,j)}$$

$$= 0 \qquad i = 1,2 \quad P, \; j = 1,2 \quad Q \qquad (3\ 28a)$$

$$\sum_{p'=1}^{P'}\sum_{q'=1}^{Q'} C_{Ep'q'} \sum_{m=0}^{\infty}\sum_{n=1}^{\infty} G_{21}(\alpha_n, \beta_m) L_{1emn}^{(p',q')} L_{1emn}^{(i',j')}$$

$$+ \sum_{p=1}^{P}\sum_{q=1}^{Q} D_{Epq} \sum_{m=0}^{\infty}\sum_{n=1}^{\infty} G_{22}(\alpha_n, \beta_m) L_{2emn}^{(p,q)} L_{1emn}^{(i',j')}$$

$$+ \sum_{r'=1}^{R'}\sum_{s'=1}^{S'} C_{Ir's'} \sum_{m=0}^{\infty}\sum_{n=1}^{\infty} G_{23}(\alpha_n, \beta_m) L_{1Imn}^{(r',s')} L_{1emn}^{(i',j')}$$

$$+ \sum_{r=1}^{R}\sum_{s=1}^{S} D_{Irs} \sum_{m=0}^{\infty}\sum_{n=1}^{\infty} G_{24}(\alpha_n, \beta_m) L_{2Imn}^{(r,s)} L_{1emn}^{(i',j')}$$

$$= 0 \qquad i' = 1,2 \qquad P',\ j' = 1,2 \qquad Q' \tag{3 28b}$$

$$\sum_{p'=1}^{P'} \sum_{q'=1}^{Q'} C_{Ep'q'} \sum_{m=1}^{\infty} \sum_{n=0}^{\infty} G_{31}(\alpha_n, \beta_m)\, L_{1emn}^{(p',q')}\, L_{2Imn}^{(k,l)}$$

$$+ \sum_{p=1}^{P} \sum_{q=1}^{Q} D_{Epq} \sum_{m=1}^{\infty} \sum_{n=0}^{\infty} G_{32}(\alpha_n, \beta_m)\, L_{2emn}^{(p,q)}\, L_{2Imn}^{(k,l)}$$

$$+ \sum_{r'=1}^{R'} \sum_{s'=1}^{S'} C_{Ir's'} \sum_{m=1}^{\infty} \sum_{n=0}^{\infty} G_{33}(\alpha_n, \beta_m)\, L_{1Imn}^{(r',s')}\, L_{2Imn}^{(k,l)}$$

$$+ \sum_{r=1}^{R} \sum_{s=1}^{S} D_{Irs} \sum_{m=1}^{\infty} \sum_{n=0}^{\infty} G_{34}(\alpha_n, \beta_m)\, L_{2Imn}^{(r,s)}\, L_{2Imn}^{(k,l)}$$

$$= 0 \qquad k = 1,2 \qquad R,\ l = 1,2 \qquad S \tag{3 28c}$$

$$\sum_{p'=1}^{P'} \sum_{q'=1}^{Q'} C_{Ep'q'} \sum_{m=1}^{\infty} \sum_{n=0}^{\infty} G_{41}(\alpha_n, \beta_m)\, L_{1emn}^{(p',q')}\, L_{1Imn}^{(k',l')}$$

$$+ \sum_{p=1}^{P} \sum_{q=1}^{Q} D_{Epq} \sum_{m=1}^{\infty} \sum_{n=0}^{\infty} G_{42}(\alpha_n, \beta_m)\, L_{2emn}^{(p,q)}\, L_{1Imn}^{(k',l')}$$

$$+ \sum_{r'=1}^{R'} \sum_{s'=1}^{S'} C_{Ir's'} \sum_{m=1}^{\infty} \sum_{n=0}^{\infty} G_{43}(\alpha_n, \beta_m)\, L_{1Imn}^{(r',s')}\, L_{1Imn}^{(k',l')}$$

$$+ \sum_{r=1}^{R} \sum_{s=1}^{S} D_{Irs} \sum_{m=1}^{\infty} \sum_{n=0}^{\infty} G_{44}(\alpha_n, \beta_m)\, L_{2Imn}^{(r,s)}\, L_{1Imn}^{(k',l')}$$

$$= 0 \qquad k' = 1,2 \qquad R',\ l' = 1,2 \qquad S' \tag{3.28d}$$

where we have expanded slot field and strip current components in terms of known basis functions

$$E_{y1}(y, z) = \sum_{p=1}^{P} \sum_{q=1}^{Q} C_{Epq}\, f_y^{(p,q)}(y, z) = \sum_{p=1}^{P} \sum_{q=1}^{Q} C_{Epq}\, f_{yy}^{(p)}(y)\, f_{yz}^{(q)}(z) \tag{3 29a}$$

$$E_{z1}(y,\ z) = \sum_{p'=1}^{P'} \sum_{q'=1}^{Q'} D_{Ep'q'} f_z^{(p',q')}(y,\ z) = \sum_{p'=1}^{P} \sum_{q'=1}^{Q} D_{Ep'q'}\ f_{zy}^{(p')}(y)\ f_{zz}^{(q')}(z) \qquad (3\ 29b)$$

$$I_{y3}(y,\ z) = \sum_{r=1}^{R} \sum_{s=1}^{S} C_{Irs}\ g_y^{(r,s)}(y,\ z) = \sum_{r=1}^{R} \sum_{s=1}^{S} C_{Irs}\ g_{yy}^{(r)}(y)\ g_{yz}^{(s)}(z) \qquad (3\ 29c)$$

$$I_{z3}(y,\ z) = \sum_{r'=1}^{R'} \sum_{s'=1}^{S'} D_{Ir's'} g_z^{(r',s')}(y,\ z) = \sum_{r'=1}^{R} \sum_{s'=1}^{S} D_{Ir's'}\ g_{zy}^{(r')}(y)\ g_{zz}^{(s')}(z) \qquad (3\ 29d)$$

superscripts, in the above expressions, decides the order of the basis functions and subscript tells about the component of the field or current under consideration C_{Epq}, $D_{Ep'q'}$, C_{Irs} and $D_{Ir's'}$ are the coefficients of expansion, f_y and f_z are the basis functions for slot field and, g_y and g_z are the basis function for strip current

The characteristic equation for finding out the resonant length of the fin line cavity containing the discontinuity is obtained by setting the determinant of the coefficient matrix in (3 28), equal to zero

3 3 3 *Choice of the basis functions* [1]

The numerical solution of (3 28) is obtained by introducing a known set of basis function The accuracy of final solution depends on the accuracy with which the basis functions represent the true electric field distribution in the slot More accuracy with less no of basis functions can be achieved by incorporating the edge condition [42] into the basis functions Also for the case of symmetric discontinuity, we can incorporate the electric and magnetic wall condition in the choice of basis functions and thus, we can reduce the number of basis functions which will accurately represent the slot field or the strip current distribution

Following basis functions which incorporate the edge conditions have been chosen for the electric field in the slot and current on the strip

Case(i) Strip located symmetrically across the slot in the transverse direction (Fig 3 3)

$$f_y^{(p,q)}(y, z) = (y - b/2)^{(2p-2)}[(w/2)^2 - (y - b/2)^2]^{-1/2}\sin(q\pi z/\ell)$$
$$= f_{yy}^{(p)}(y)\, f_{yz}^{(q)}(z), \qquad p = 1, 2 \quad P \qquad q = 1, 2, \quad Q \qquad (3\ 30a)$$

$$f_z^{(p',q')}(y, z) = (y - b/2)^{(2p'-1)}[(w/2)^2 - (y - b/2)^2]^{1/2}\cos(q'\pi z/\ell)$$
$$= f_{zy}^{(p')}(y)\, f_{zz}^{(q')}(z), \qquad p' = 1, 2 \quad P' \qquad q' = 1, 2, \quad Q' \qquad (3\ 30b)$$

$$g_y^{(r,s)}(y, z) = \frac{\sin[(2r - 1)\pi/2\ (2y'/h + 1)]}{[1 - (2y'/h)^2]^{1/2}}\ (z')^{s-1}\ [(c/2)^2 - z'^2]^{-1/2}$$
$$= g_{yy}^{(r)}(y)\, g_{yz}^{(s)}(z), \qquad r = 1,2 \quad R \qquad s = 1,2 \quad S \qquad (3\ 30c)$$

$$g_z^{(r',s')}(y, z) = \frac{\cos[(2r' - 1)\pi/2\ (2y'/h + 1)]}{[1 - (2y'/h)^2]^{1/2}}\ (z')^{s'-1}\ [(c/2)^2 - z'^2]^{1/2}$$
$$= g_{zy}^{(r')}(y)\, g_{zz}^{(s')}(z), \qquad r' = 1,2 \quad R' \qquad s' = 1,2 \quad S' \qquad (3\ 30c)$$

where

$$y' = y - b/2 \text{ and } z' = z - (\ell_1 + c/2)$$

Now the definition given in (3 18) can be used to transform the above basis functions

$$L_{iemn}^{(p',q')} = \int_{y=0}^{b}\int_{z=0}^{\ell} f_{zy}^{(p')}\, f_{zz}^{(q')}\, \sin(\alpha_n y)\cos(\beta_m z)\, dydz$$
$$= \tilde{f}_{zy}^{(p')}(\alpha_n)\, \tilde{f}_{zz}^{(q')}(\beta_m) \qquad (3\ 31a)$$

where we have made following substitutions

$$\tilde{f}_{zy}^{(p')}(\alpha_n) = \int_{y=0}^{b} f_{zy}^{(p')}(y)\, \sin(\alpha_n y)\, dy \qquad (3\ 31b)$$

and

$$\tilde{f}_{zz}^{(q')}(\beta_m) = \int_{z=0}^{\ell} f_{zz}^{(q')}(z)\cos(\beta_m z)\,dz \qquad (3\ 31c)$$

similarly

$$L_{2emn}^{(p,q)} = \tilde{f}_{yy}^{(p)}(\alpha_n)\,\tilde{f}_{yz}^{(q)}(\beta_m) \qquad (3\ 32a)$$

$$L_{1Imn}^{(r',s')} = \tilde{g}_{yy}^{(r')}(\alpha_n)\,\tilde{g}_{yz}^{(s')}(\beta_m) \qquad (3\ 32b)$$

$$L_{2Imn}^{(r,s)} = \tilde{g}_{yy}^{(r)}(\alpha_n)\,\tilde{g}_{yz}^{(s)}(\beta_m) \qquad (3\ 32c)$$

where $\tilde{f}_{yy}$, $\tilde{f}_{yz}$, $\tilde{g}_{yy}$, $\tilde{g}_{yz}$, $\tilde{g}_{zy}$ and $\tilde{g}_{zz}$ can be defined in a similar way as we have defined $\tilde{f}_{zy}$ and $\tilde{f}_{zz}$ in equations (3 31a) and (3 31b)

Transforms of basis functions in equations (3 30) found using above equations are given in Appendix B

Case(ii) Strip located asymmetrically across the slot in the transverse direction (Fig 3 4)

In case of asymmetrically located strip y-dependent basis functions for both slot field and strip current will take the following form

$$f_{yy}^{(p)} = \frac{\cos[\,p\pi\,(\frac{y'}{W} + \frac{1}{2})]}{\sqrt{1 - (\frac{2y'}{W})^2}} \qquad (3\ 33a)$$

$$f_{zy}^{(p')} = \frac{\sin[\,p'\pi\,(\frac{y'}{W} + \frac{1}{2})]}{\sqrt{1 - (\frac{2y'}{W})^2}} \qquad (3\ 33b)$$

$$g_{yy}^{(r)} = \frac{\sin\left[\frac{r\pi(y - h')}{h}\right]}{\sqrt{1 - [\frac{2(y - h')}{h} - 1]^2}} \qquad (3\ 33c)$$

$$g_{zy}^{(r')} = \frac{\cos\left[\frac{r'\pi(y - h')}{h}\right]}{\sqrt{1 - \left[\frac{2\,(y - h')}{h} - 1\right]^2}} \qquad (3.33d)$$

z-dependent basis functions for the current and the field will remain the same Expressions for the transforms of above basis functions are also given in Appendix B

For the present problem, we have taken R = S = R' = S' = 2, P = P' = 1 and Q = Q' = 12 which gives an accuracy up to third decimal place in the results m =n = 100 has been taken in the summation The results of equivalent circuit parameters of the discontinuity for the two cases described above are presented in sec 6 2 of chapter 6.

CHAPTER 4

CHARACTERIZATION OF OFF SLOT DISCONTINUITY IN INSULATED FIN LINE

4.1 INTRODUCTION

The discontinuity in insulated fin line consists of two off slot discontinuities placed on two separate dielectric air interfaces as shown in the Fig 4 1 Due to the complexity of the structure, we have used *Spectral Domain immittance approach* proposed by T Itoh [26] to formulate the eigen value problem for determining the resonant length of the cavity housing the discontinuity The method saves quite a lot of analytical labor *Transverse resonance condition* is then applied to get the equivalent circuit parameters of the discontinuity Even and odd mode analysis as applied to a longitudinally symmetric discontinuity is also presented in this chapter We have also included the elaborate procedure for extraction of equivalent circuit parameters of the discontinuity in this chapter

4.2 ANALYSIS OF DISCONTINUITY IN INSULATED FIN LINE USING SPECTRAL DOMAIN IMMITTANCE APPROACH

4 2 2 *Basic Formulations*

We have used *Spectral Domain Immittance Approach* for formulating the 'G', functions matrix Fig 4 1 shows the cross sectional and longitudinal views of off slot discontinuity in an insulated fin line cavity Since all the preliminary formulations have already been done in chapter 2, we will begin with the equivalent transmission line model of the fin line cavity housing the discontinuity as shown in Fig 4 2

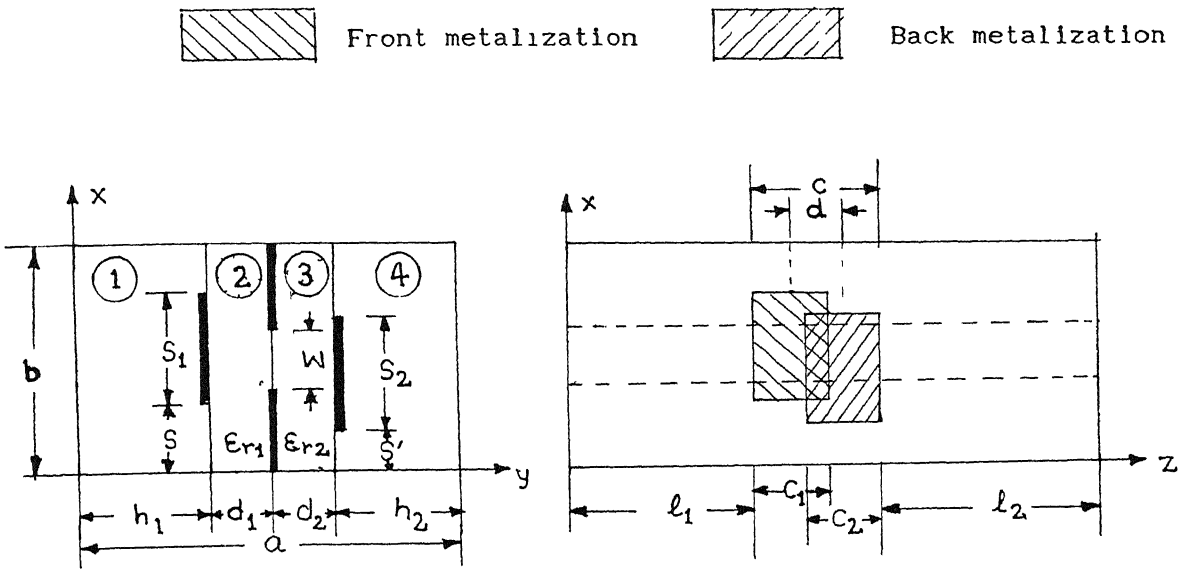

(a) Cross section

(b) Side view

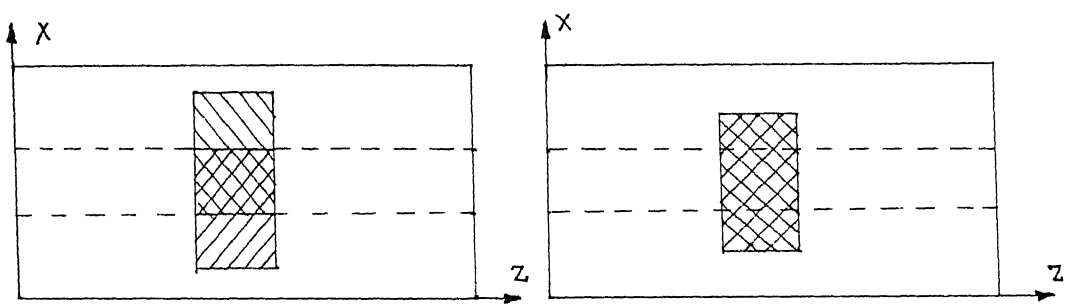

(c) logitudinally symmetric Strips

(d) Strips completely overlapping each other

Fig 4 1 Cross sectional and longitudinal views of the off slot discontinuity in insulated fin line general form and variations

Using the transmission line theory we can relate currents and fields at y = h_1, y = $h_1 + d_1$ and y = $h_1 + d_1 + d_2$ by following equations

$$\hat{E}u(\alpha_n, h_1+d_1+d_2) = Z^e_{11}\, \hat{J}u(\alpha_n, h_1+d_1+d_2) + FR^e_{12}\, \hat{E}u(\alpha_n, h_1+d_1) + Z^e_{13}\, \hat{J}u(\alpha_n, h_1) \quad (4\ 1a)$$

$$\hat{E}v(\alpha_n, h_1+d_1+d_2) = Z^h_{11}\, \hat{J}v(\alpha_n, h_1+d_1+d_2) + FR^h_{12}\, \hat{E}v(\alpha_n, h_1+d_1) + Z^h_{13}\, \hat{J}v(\alpha_n, h_1) \quad (4\ 1b)$$

$$\hat{J}u(\alpha_n, h_1+d_1) = CR^e_{21}\, \hat{J}u(\alpha_n, h_1+d_1+d_2) + Y^e_{22}\, \hat{E}u(\alpha_n, h_1+d_1) + CR^e_{23}\, \hat{J}u(\alpha_n, h_1) \quad (4\ 1c)$$

$$\hat{J}v(\alpha_n, h_1+d_1) = CR^h_{21}\, \hat{J}v(\alpha_n, h_1+d_1+d_2) + Y^h_{22}\, \hat{E}v(\alpha_n, h_1+d_1) + CR^e_{23}\, \hat{J}v(\alpha_n, h_1) \quad (4\ 1d)$$

$$\hat{E}u(\alpha_n, h_1) = Z^e_{31}\, \hat{J}u(\alpha_n, h_1+d_1+d_2) + FR^e_{32}\, \hat{E}u(\alpha_n, h_1+d_1) + Z^e_{33}\, \hat{E}u(\alpha_n, h_1) \quad (4\ 1e)$$

$$\hat{E}v(\alpha_n, h_1) = Z^h_{31}\, \hat{J}v(\alpha_n, h_1+d_1+d_2) + FR^h_{32}\, \hat{E}v(\alpha_n, h_1+d_1) + Z^h_{33}\, \hat{E}v(\alpha_n, h_1) \quad (4\ 1f)$$

where superscript 'e' corresponds to TM mode and 'h' corresponds to TE mode

By applying transmission line theory to TM wave equivalent circuit (Fig 4 2(a)) we obtain

$$Z^e_{11} = \frac{Z^e_4 Z^e_{3R}}{Z^e_4 + Z^e_{3R}} \quad (4\ 2a)$$

where $Z^e_4 = Z_{TM4} \tanh(\gamma_4 h_2)$ (4 2b)

$Z^e_{3R} = Z_{TM3} \tanh(\gamma_3 d_2)$ (4 2c)

$$FR^e_{12} = \frac{Z^e_4}{[\, Z^e_4 \cosh(\gamma_3 d_2) + Z_{TM3} \sinh(\gamma_3 d_2)\,]} \quad (4\ 3)$$

$$Z^e_{13} = 0 \quad (4\ 4)$$

$$CR^e_{21} = -FR^e_{12} \quad (4\ 5)$$

$$Y^e_{22} = Y^e_{3L} + Y^e_{2R} \quad (4\ 6a)$$

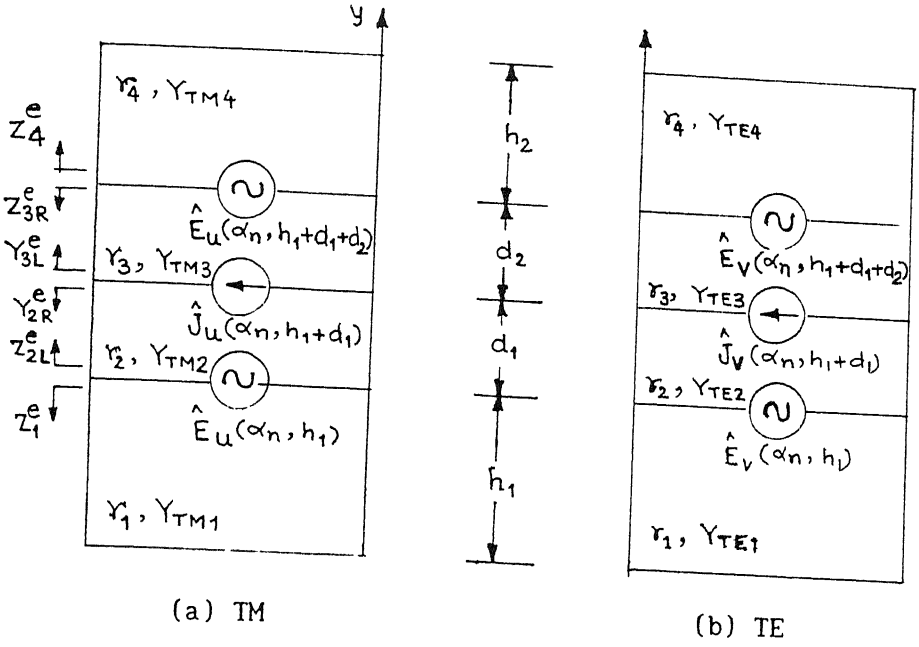

(a) TM (b) TE

Fig 4 2 Equivalent transmission line model of the insulated fin line cavity containing the discontinuity

where

$$Y^e_{3L} = \frac{Y_{TM3}\,[\,Y_{TM3} + Y^e_4 \coth(\gamma_3 d_2)\,]}{[\,Y^e_4 + Y_{TM3}\coth(\gamma_3 d_2)\,]} \qquad (4\ 6b)$$

$$Y^e_{2R} = \frac{Y_{TM2}\,[\,Y_{TM2} + Y^e_1 \coth(\gamma_2 d_1)\,]}{[\,Y^e_1 + Y_{TM2}\coth(\gamma_2 d_1)\,]} \qquad (4\ 6c)$$

$$CR^e_{23} = \frac{-Z^e_1}{[\,Z^e_1 \cosh(\gamma_2 d_1) + Z_{TM2}\sinh(\gamma_2 d_1)\,]} \qquad (4\ 7a)$$

$$\text{where } Z^e_1 = Z_{TM1}\tanh(\gamma_1 h_1) \qquad (4\ 7b)$$

$$Z^e_{31} = 0 \qquad (4\ 8)$$

$$FR^e_{32} = -CR^e_{23} \qquad (4\ 9)$$

$$Z^e_{33} = \frac{Z^e_1 Z^e_{2L}}{Z^e_1 + Z^e_{2L}} \qquad (4\ 10a)$$

$$\text{where } Z^e_{2L} = Z_{TM2}\tanh(\gamma_2 d_1) \qquad (4\ 10b)$$

Similarly for TE case also we can write down the expressions for Z^h_{11}, Z^h_{13}, Z^h_{31}, Z^h_{33}, Y^h_{22}, FR^h_{12}, FR^h_{32}, CR^h_{21} and CR^h_{23} by replacing the superscript 'e' by 'h', Y_{TMi} by Y_{TEi} and Z_{TMi} by Z_{TEi} for i = 1, 4 in equations (4 2) to (4 10) Y_{TMi}, Y_{TEi} and γ_i have already been defined in chapter 2

Now writing equations (4 1) in matrix form we have

$$[\,EJE\,]_{uv} = [\,G'\,]_{uv}\,[\,JEJ\,]_{uv} \qquad (4\ 11a)$$

The above equations can be transformed in (x, z) coordinate system using the transformation (2 7a), as follows

$$[\,EJE\,]_{xz} = [\,L\,]^{-1}\,[\,G'\,]_{uv}\,[\,L\,]\,[\,JEJ\,]_{xz} \qquad (4\ 11b)$$

where the different matrices in (4 11) are given in Appendix C

Equation (4 11b) can also be written as

$$[\ EJE\ ]_{xz} = [\ G\ ]_{xz}\ [\ JEJ\ ]_{xz} \qquad (4\ 11c)$$

where

$$[\ G\ ]_{xz} = [\ L\ ]^{-1}\ [\ G'\ ]_{uv}\ [\ L\ ] \qquad (4\ 11d)$$

After a little matrix manipulation and with the help of expressions given in Appendix C, we can write down the expressions for the elements of [G] matrix

$$G_{11} = Z^e_{11} \sin^2\theta + Z^h_{11} \cos^2\theta, \qquad G_{12} = (\ Z^e_{11} - Z^h_{11}) \sin\theta \cos\theta$$
$$G_{13} = FR^e_{12} \sin^2\theta + FR^h_{12} \cos^2\theta, \quad G_{14} = (\ FR^e_{12} - FR^h_{12}) \sin\theta \cos\theta$$
$$G_{15} = Z^e_{13} \sin^2\theta + Z^h_{13} \cos^2\theta, \qquad G_{16} = (\ Z^e_{13} - Z^h_{13}) \sin\theta \cos\theta$$
$$G_{22} = Z^e_{11} \cos^2\theta + Z^h_{11} \sin^2\theta, \qquad G_{21} = G_{12}$$
$$G_{24} = Z^e_{11} \cos^2\theta + Z^h_{11} \sin^2\theta, \qquad G_{23} = G_{24}$$
$$G_{26} = Z^e_{11} \cos^2\theta + Z^h_{11} \sin^2\theta, \qquad G_{25} = G_{26} \qquad (4\ 12)$$

and so on

4 2 2 *Characteristic Equation*

We use *Galerkin's method* and *parseval's theorem* in equation (3 39) to get a set of homogeneous equations , in terms of coefficients of expansion, we use in expanding the fields in the in the slot and currents on the strips The procedure is exactly the same as we have followed in chapter (2) to find the propagation constants of two fin line structures In this case the characteristic equation obtained by setting the determinant of coefficient matrix equal to zero gives the resonant length of the fin line cavity containing the discontinuity

4 2 3 *Choice of Basis Functions*

We have chosen most general type of basis function which are valid for arbitrarily located slot and arbitrarily located strips The basis functions include the edge conditions and can be modified for special cases , such as centrally located slot and strips with strips exactly overlapping each other

(Fig 4 1). The basis functions given below, if plotted, will look exactly like those given in Fig 2 4

The general expressions for basis functions are given below

$$f^{(k)}(\xi,\ h',\ h) = \cos[k\pi(\xi - h')/h] \Big/ \sqrt{1 - [\,2\,(\xi - h')/h - 1]^2} \qquad (4\ 13a)$$

$$g^{(k)}(\xi,\ h',\ h) = \sin[k\pi(\xi - h')/h] \Big/ \sqrt{1 - [\,2\,(\xi - h')/h - 1]^2} \qquad (4\ 13b)$$

Fourier transform for above functions is defined by

$$\hat{\psi}^{(k)}(\phi,\ h',\ h) = \int_{\psi=-\infty}^{\infty} \psi^{(k)}(\xi,h',h)\ e^{(j\ \phi\ \xi)}d\xi \qquad (4\ 14)$$

Taking the fourier transform of (4 13) according to (4 14) we obtain

$$\hat{f}^{(k)}(\phi,\ h',h) = \frac{\pi\ h}{4}\ e^{(j\phi(h' + h/2)}\{e^{(jk\pi/2)}J_0[\tfrac{1}{2}\ (\phi\ h + k\ \pi)] + e^{(-jk\pi/2)}J_0[\tfrac{1}{2}\ (\phi\ h - k\ \pi)]\} \qquad (4\ 15a)$$

$$\hat{g}^{(k)}(\phi,\ h',h) = -j\ \frac{\pi\ h}{4}\ e^{(j\phi(h' + h/2)}\{e^{(jk\pi/2)}J_0[\tfrac{1}{2}\ (\phi\ h + k\ \pi)] + e^{(-jk\pi/2)}J_0[\tfrac{1}{2}\ (\phi\ h - k\ \pi)]\} \qquad (4\ 15b)$$

Now basis functions for slot fields and strip currents can be written as

$$\begin{aligned}
&\mathcal{E}_{xx}^{(k)}(x) = f^{(k)}(x,s,w) \quad , \quad \mathcal{E}_{xz}^{(k)}(z) = \sin k\pi z/\ell \\
&\mathcal{E}_{zx}^{(k)}(x) = g^{(k)}(x,s,w) \quad , \quad \mathcal{E}_{zz}^{(k)}(z) = \cos k\pi z/\ell \\
&J_{1xx}^{(k)}(x) = g^{(k)}(x,s_1',s_1) \quad , \quad J_{1xz}^{(k)}(z) = f^{(k)}(z\ ,\ell_1,c_1) \\
&J_{1zx}^{(k)}(x) = f^{(k)}(x,s_1',s_1) \quad , \quad J_{1zz}^{(k)}(z) = g^{(k)}(z\ ,\ell_1,c_1) \\
&J_{2xx}^{(k)}(x) = g^{(k)}(x,s_2',s_2) \quad , \quad J_{2xz}^{(k)}(z) = f^{(k)}(z\ ,\ell_2,c_2) \\
&J_{2zx}^{(k)}(x) = f^{(k)}(x,s_2',s_2) \quad , \quad J_{2zz}^{(k)}(z) = g^{(k)}(z\ ,\ell_2,c_2)
\end{aligned} \qquad (4\ 16)$$

and their corresponding transforms [1] are written as

$$\hat{\mathcal{E}}_{xx}^{(k)}(\alpha_n) = \mathrm{Re}\ [\ \hat{f}^{(k)}(\alpha_n,\ s,\ w)\ ], \qquad \hat{\mathcal{E}}_{xz}^{(k)}(\beta_m) = J\ \ell/2,\ m = k \\ = 0\ \text{otherwise}$$

$$\hat{\mathcal{E}}_{zx}^{(k)}(\alpha_n) = \mathrm{Im}\ [\ \hat{g}^{(k)}(\alpha_n,\ s,\ w)\ ], \qquad \hat{\mathcal{E}}_{zz}^{(k)}(\beta_m) = \ell/2,\ m = k \\ = 0\ \text{otherwise}$$

$$\hat{J}^{(k)}_{1xx}(\alpha_n) = \mathrm{Re}[\,\hat{g}^{(k)}(\alpha_n, s'_1, s_1)],\ \hat{J}^{(k)}_{1xz}(\beta_m) = \mathrm{Im}[\,\hat{f}^{(k)}(\beta_m, \ell_1, c_1)]$$

$$\hat{J}^{(k)}_{1zx}(\alpha_n) = \mathrm{Im}[\,\hat{f}^{(k)}(\alpha_n, s'_1, s_1)],\ \hat{J}^{(k)}_{1zz}(\beta_m) = \mathrm{Re}[\,\hat{g}^{(k)}(\beta_m, \ell_1, c_1)]$$

(4 17)

Transforms of J_{2xx} J_{2zz} can be obtained, if we replace the subscript '1' by '2' in the transforms of J_{1xx} J_{1zz} in the above equation

Here, if we consider the most general case of arbitrarily located located slot and arbitrarily located strips, we will take k = 0, 1, 2 and define $\alpha_n = n\pi/b$ On the other hand for centrally located slot and strips with strips exactly overlapping each other, we take k = 0, 2, 4 and define $\alpha_n = 2n\pi/b$ so that the basis functions satisfy electric wall condition at x = b/2 (see Fig 4 1)

4 3 *Extraction of Discontinuity Equivalent Circuit Parameters*

For characterization of the discontinuity we model the discontinuity as a T or a Π equivalent circuit Now to find out equivalent circuit parameters, we first replace the cavity containing the discontinuity by its equivalent circuit as shown in Fig 4 1 Then we apply transverse resonance condition as given in equation (3 1)

As we can see, this equation contains three unknowns, we should have three equations to find them We can get these equations by substituting three different pairs of ℓ_1 and ℓ_2 These pairs are obtained by choosing three different values of ℓ_1 close to $\lambda_g/2$ [30] and solving (3 28) for getting the corresponding values of ℓ_2 while keeping the frequency fixed Solving these three equations resulted from substitution, we can evaluate the Z-parameters of the discontinuity and therefore T-equivalent circuit parameters

One important point to mention here is that, while finding out z_{12} using equation (3 1) , we will have

$$Z_{12} = \pm \sqrt{(Z_1 + Z_{11})\,(Z_2 + Z_{22})} \qquad (4\ 14)$$

the choice of '+' or '−' sign for z_{12} depends on the type of discontinuity being analyzed For the off slot discontinuities analyzed in this thesis we assumed the sign to be -ve, considering the position of the strip In chapter 6 sec 6 2 we have supported the assumption with the help of experimental results

4 4 Symmetric Off Slot Discontinuity

If the discontinuity element is placed symmetrically ($\ell_1 = \ell_2 = \ell_e$ or ℓ_m) in the fin line cavity, then it is sufficient to analyze one half of structure by putting an electric wall (odd - mode) and magnetic wall (even - mode) at the plane of symmetry AA' separately (Fig 4 3) The corresponding values of q = 2, 4, 6 12, q'= 2, 4, 6, 12 , s =1 and s' =2 for odd mode and q = 1, 3, 11, q' = 1, 3, 11, s =2 and s'=1 for even mode in equations (3 30) for unilateral fin line discontinuity, also we have to redefine

$$\beta_m = 2m\pi/\ell,\ \ell = 2\ell_e + c \qquad \text{for odd mode}$$

$$= (2m + 1)\pi/\ell,\ \ell = 2\ell_m + c \qquad \text{for even mode}$$

$$m = 0, 1, 2 \quad \infty$$

$$\alpha_n = 2n\pi/\ b, \quad n = 0, 1, 2, \quad \infty \qquad (4\ 16)$$

Similarly for insulated fin line discontinuity, we can incorporate the electric and magnetic wall condition for odd and even mode case respectively at $z = \ell/2$

Now solving the characteristic equation for even and odd mode case separately, we can find out even mode and odd mode resonant lengths of fin line cavity containing the discontinuity

Again we apply the transverse resonance condition for both the cases separately By making use of (3 2) we can get the equivalent circuit parameters

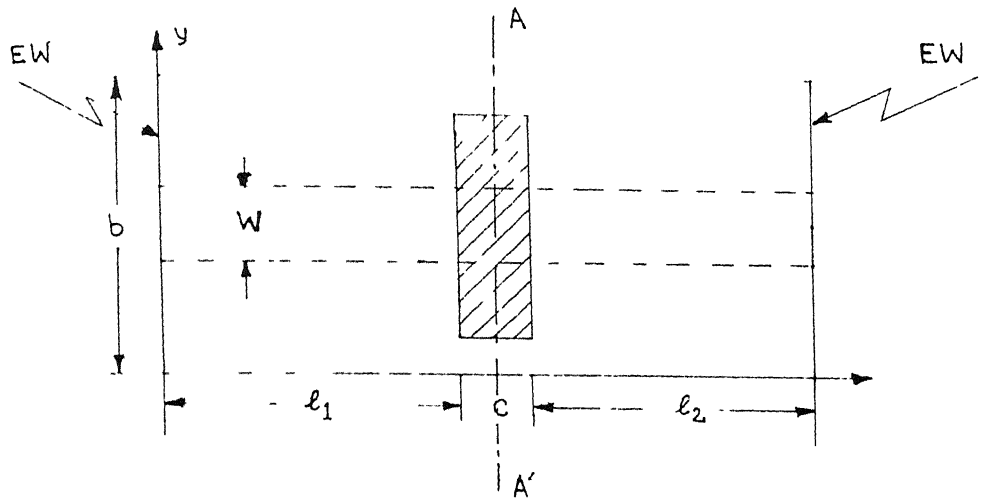

(a) Symmetric off slot discontinuity in unilateral fin line

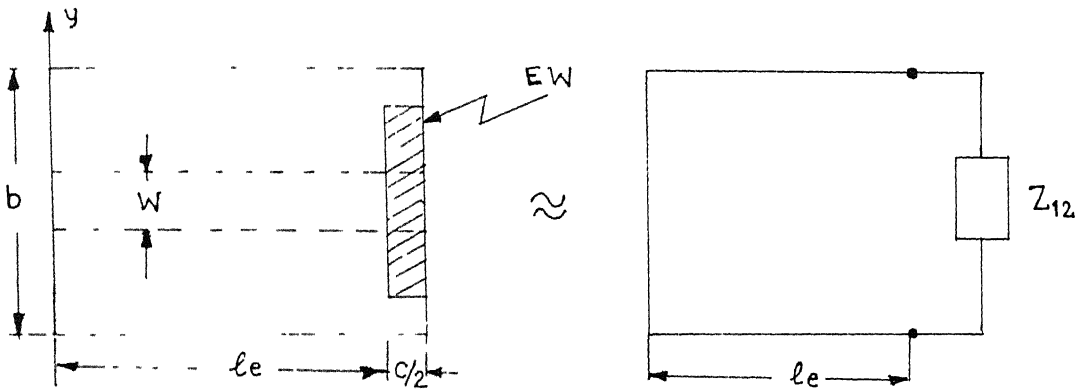

(b) Symmetric half of (a) for odd mode excitation and it's equivalent circuit

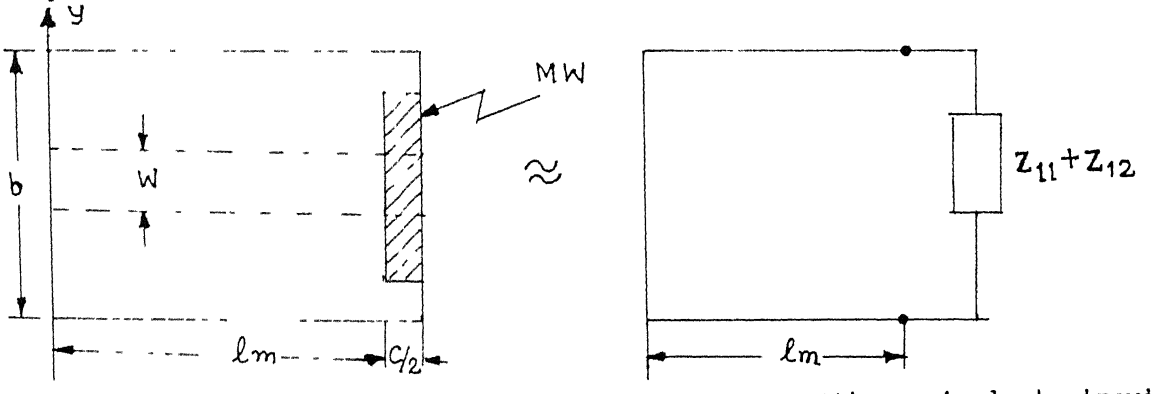

(c) Symmetric half of (a) for even mode excitation and it's equivalent circuit

Fig 4 3 Even and odd mode equivalent circuits of the symmetric off slot discontinuity

CHAPTER 5

SCATTERING MATRIX FORMULATION FOR SINGLE AND CASCADED DISCONTINUITIES AND REALIZATION OF LOW PASS FILTER

5 1 INTRODUCTION

The objective of this chapter is to verify the application of off slot discontinuity in realization of a low pass filter We have considered cascaded arrangement of three off slot discontinuities with varying strip width for this purpose A low pass filter cascading inductive and capacitive strips has been reported by C Nguyen [32] prior to this Scattering matrices for single and cascaded discontinuities have been formulated using the most simplified approach i e we have not taken evanescent mode interaction between the strips into account Though, this simplification leads to considerable amount of error between theory and experiment, it nevertheless demonstrates the application of the discontinuity in unilateral fin line as a low pass filter Since the characterization of discontinuities has been given more emphasis in this thesis, we could not use more accurate analysis for the design of low pass filter To achieve better results one should use modal analysis [24] For transmission and scattering matrix formulations of cascaded discontinuities method suggested in [34] and [35] could be used These methods take into account the effect of higher order modes and result in better accuracy

For measurement purpose , it is necessary to design a suitable transition from fin line to rectangular wave guide Later part of this chapter deals with the transition design and other design aspects of a fin line test fixture

5 2 SCATTERING MATRIX FORMULATION

5 2 1 *Single discontinuity*

5 2 1 1 Theoretical formulation

If we consider only dominant mode to be propagating and other scattered mode to be confined near the vicinity of the discontinuity, we can model the fin line cavity containing the discontinuity as two dispersion less transmission line sections, both shorted at one of their ends and in between the the discontinuity replaced by its equivalent circuit (see Fig 3 1)

ABCD parameters of the T-equivalent [38] are given by

$$A = 1 + Z_1/Z_3,\ B = D_s/Z_3,\ C = 1/Z_3,\ D = 1 + Z_2/Z_3 \qquad (5\ 1a)$$

where

$$D_s = Z_1Z_2 + Z_2Z_3 + Z_3Z_1 \qquad (5\ 1b)$$

if Z_{11}, Z_{22} and Z_{12} (= Z_{21} due to reciprocity being applicable to passive circuit) are the Z-parameters of the discontinuity, we can write

$$Z_1 = Z_{11} - Z_{12},\ Z_2 = Z_{22} - Z_{12},\ Z_3 = Z_{12} \qquad (5\ 1c)$$

if the discontinuity is symmetric in longitudinal direction, we have

$$Z_{11} = Z_{22},\ \text{therefore } Z_1 = Z_2 \qquad (5.1d)$$

For a symmetric network we can express S-parameters in terms of it's ABCD parameters as follows

$$S_{11} = S_{22} = (B/Z_0 - CZ_0) / (2A + B/Z_0 + CZ_0) \qquad (5\ 2a)$$

$$S_{21} = S_{12} = 2 / (2A + B/Z_0 + CZ_0) \qquad (5\ 2b)$$

where, Z_0 is the wave impedance of the dominant mode of the fin line

if we take $Z_1 = Z_2 = X_{se}$ and $Z_3 = X_{sh}$ (for loss less network), X_{se} and X_{sh} are the series and shunt reactances of the equivalent circuit, we can write (5 2b) as below

$$S_{21} = 2 / \{2(1 + X_{se}/X_{sh}) + X_{se}/Z_0(X_{se}/X_{sh} + 2) + Z_0/X_{sh}\}$$

Simplifying, we get

$$S_{21} = 2\bar{X}_{se} / (1 + \bar{X}_{se}) (1 + \bar{X}_{se} + 2\bar{X}_{sh}) \quad (5\ 3)$$

$\bar{X}_{se}$ and $\bar{X}_{sh}$ are the normalized series and shunt reactances with respect to Z_0 As we can see in (5 3) that Z_0 does not appear in the expression any more, which means that we do not need any information of characteristic impedance (or wave impedance of the dominant mode in case of fin line), for determining S-parameters of the discontinuity The normalized values of series and shunt reactances have been presented in sec 6 2 of chapter 6

5 2 1 2 Experimental method [37]

Equivalent transmission line representation of a uniform fin line section is shown in in Fig 5 1(a) An idealized model of a fin line section containing the discontinuity, which assumes the strip width to be zero, is shown in Fig 5 1(b) and Fig 5 1(c) shows the practical model of the fin line section with discontinuity As we can see Fig 5 1(c) takes the width of the discontinuity strip into account Transmission coefficients S_{21} in the above three cases are given below

$$S_{21} = e^{-j\beta\ell}, \quad \text{for uniform fin line section} \quad (5\ 4a)$$

$$S^d_{21} = |S^d_{21}|\ e^{j(\theta^d - \beta\ell)}, \quad \text{for ideal model} \quad (5\ 4b)$$

$$S^d_{21} = |S^d_{21}|\ e^{j(\theta^d - \beta\ell - \beta c)}, \quad \text{for practical model} \quad (5\ 4c)$$

where, β is the dominant mode propagation constant of the fin line, $|S^d_{21}|$ and θ^d are the magnitude and phase of transmission coefficient of the discontinuity

Now, in practice we can make measurements for case (a) and case (c)only, therefore we can extract the magnitude(in dB) and phase(in degrees) information for S_{21} from these measurement as follow

$$|S^d_{21}| \text{ in dB} = |S^d_{21}| \text{ in dB}|_{\text{practical model}} - |S^d_{21}| \text{ in dB}|_{\text{uniform fin line}} \quad (5\ 5a)$$

Z_0 , β

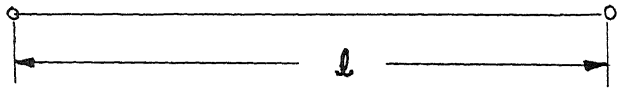

(a) Uniform fin line

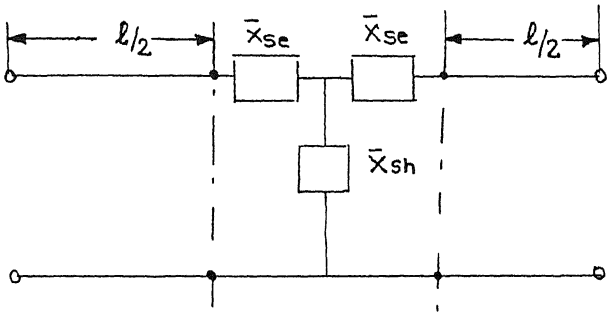

(b) Ideal equivalent circuit of fin line section containing the discontinuity

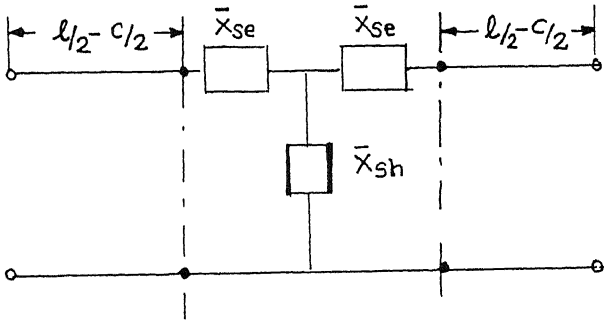

(c) Practical equivalent circuit of fin line section containing the discontinuity

Fig 5 1 Transmission line representation of a uniform fin line section and, ideal and practical equivalent circuit of fin line section containing the discontinuity

$$\theta^{d} \text{ in deg} = \angle S_{21} \text{ in deg}\,|_{\text{practical model}} - \angle S_{21} \text{ in deg}\,|_{\text{uniform fin line}} - \beta c \qquad (5\ 5b)$$

The results are given in section 6 2 of chapter 6

5 2 2 *Cascaded Discontinuities A Low Pass Filter*

Fig 5 2 shows the cascaded discontinuities and equivalent circuit representation of the cascaded network Overall ABCD matrix for the cascaded network can be found by multiplying the individual ABCD matrix of each of the discontinuity and the line section joining them The ABCD matrix of the circuit shown in Fig 5 2 can be written as

$$[ABCD]^{T} = [ABCD]^{a}[ABCD]^{LS_{ab}}[ABCD]^{b}[ABCD]^{LS_{bc}}[ABCD]^{c} \qquad (5\ 6a)$$

where, superscript

T refers to overall cascaded network

a, b and c refer to discontinuities of strip widths c_1, c_2 and c_3 respectively

LS_{ab} refers to line section joining strip 'a' with strip 'b'

LS_{bc} refers to line section joining strip 'b' with strip 'c'

Matrices in (5 6) can be given as

$$[ABCD]^{\Lambda} = \begin{bmatrix} 1 + Z_{1\Lambda}/Z_{3\Lambda} & D_{\Lambda}/Z_{3\Lambda} \\ 1/Z_{3\Lambda} & 1 + Z_{2\Lambda}/Z_{3\Lambda} \end{bmatrix}$$

$$\text{where, } D_{\Lambda} = Z_{1\Lambda}Z_{2\Lambda} + Z_{2\Lambda}Z_{3\Lambda} + Z_{3\Lambda}Z_{1\Lambda}, \text{ for } \Lambda = a, b, c, T \qquad (5\ 6b)$$

$$[ABCD]^{\Theta} = \begin{bmatrix} \cos(\beta\tau) & j\sin(\beta\tau) \\ j\sin(\beta\tau) & \cos(\beta\tau) \end{bmatrix}, \ \Theta = LS_{ab}, LS_{bc} \text{ and } \tau = \ell_{ab}, \ell_{bc} \qquad (5\ 6c)$$

Using (5 6) and (5 5), we can find the overall ABCD parameters of the cascaded network These parameters are thus transformed to equivalent impedence parameters with the help of transformation given in (5 6b) Knowing T-equivalent circuit parameters of the overall circuit, S-parameters are

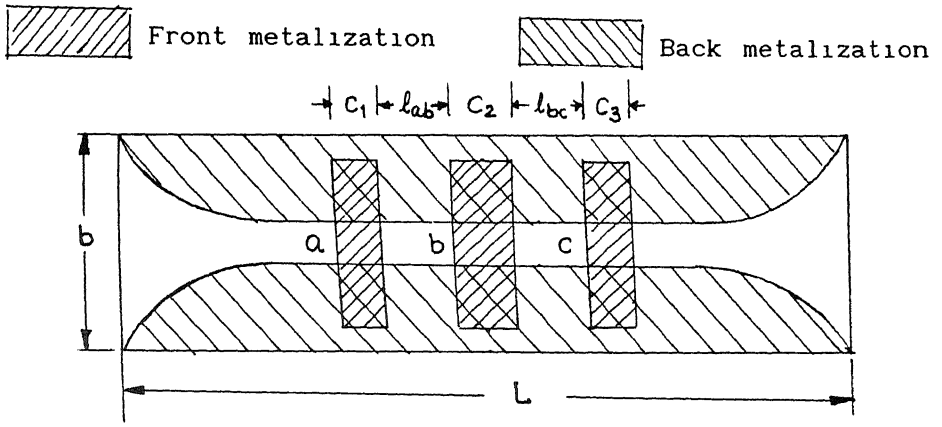

(a) Cascaded off slot discontinuities

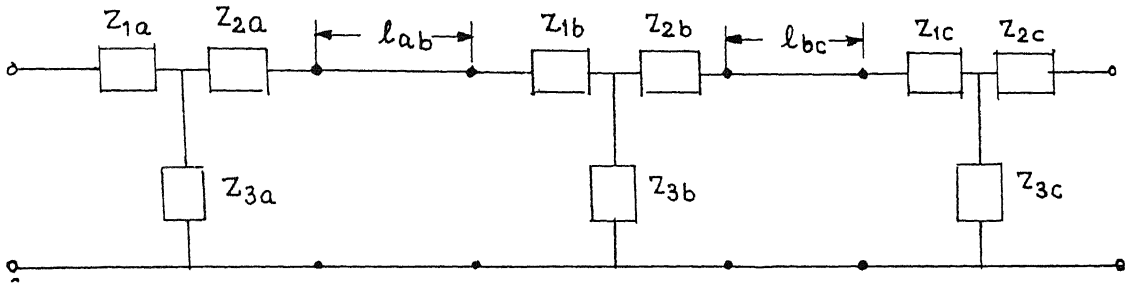

(b) Equivalent circuit of (a)

Fig 5 2 Cascaded off slot discontinuities in unilateral fin line and their equivalent circuit

derived using the following relations [38]

$$S_{11} = (-Z_0^2 + PZ_0 + D)/ D_s, \qquad S_{12} = 2 Z_0 Z_3 / D_s$$
$$S_{21} = S_{12}, \qquad S_{22} = (-Z_0^2 - PZ_0 + D)/ D_s \qquad (5\ 7)$$

where,

$$D_s = Z_0^2 + QZ_0 + D, \qquad D = Z_{1T} Z_{2T} + Z_{2T} Z_{3T} + Z_{3T} Z_{1T}$$
$$P = Z_{1T} - Z_{2T}, \qquad Q = Z_{1T} + Z_{2T} + 2 Z_{3T} \qquad (5\ 8)$$

The theoretical results of insertion loss (S_{21}), for a three section low pass filter based on above theory has been calculated and presented in sec 6 3 of chapter 6 along with the measured results.

5 3 FIN LINE CONSTRUCTION [1]

Construction of fin line involves mounting of a planar circuit in the E-plane of a rectangular wave guide housing The planar circuit consisting of a printed conducting pattern on a thin dielectric substrate are fabricated using the conventional thin film photo lithographic technique The most commonly used substrate, which has also been used for experiment in this thesis, is copper clad RT-duroid (ε_r=2 22) with standard thickness of 794mm (for X-band) and 254mm(for Ka-band) Being a soft material it can be securely clamped between the two halves of metal housing Semiconductor devices with soft gold beam lead can be soldered onto the circuit pattern

There is a provision for inserting thin insulator to prevent contact between the printed pattern and the housing The thickness of the broad walls of the guide is chosen equal to one quarter wavelength in the dielectric to present an effective short at the inner walls of the guide in the dielectrically loaded region This quarter wave choke prevents any TEM mode propagation out through the broad wall

Two types of housing are adopted in practice one that is suitable for all passive circuitry (Fig 5 3(a)) and another that has provisions for

d c biasing of semiconductor devices (Fig 5 3(b))

5.4 TRANSITION FROM FIN LINE TO RECTANGULAR WAVE GUIDE

Broad band transitions between rectangular wave guide and fin lines generally employ tapered fin line sections, in which the slot width of the fin line is gradually increased to the full wave guide height The discontinuity effect, which is due to the finite thickness of the dielectric substrate at the tapered end, facing the empty wave guide, is minimized by introducing one or two quarter wave transformer sections [44] Such quarter wave transformers take the form of stepped protrusions or notches cut in the substrate or quarter wave printed step in continuation of the fin line taper Fig 5 4 shows the schematic of a fin line taper followed by a stepped protrusion

The design of a fin line taper involves choosing a smooth impedance variation along the taper so that reflection loss is below a tolerable limit over a prescribed bandwidth, while keeping the physical length of the taper as small as possible so that transmission loss will be negligible Furthermore, when the impedance variation is translated into the slot width variation, it should result in a smooth taper contour, which can be easily implemented in practice Some of the empirical slot profiles reported in literature are exponential, parabolic, cos-square and circular arc tapers Empirical relations for three tapers are given by[37]

exponential $w \exp [z/\ell \ln(b/w)$

parabolic $[(\sqrt{b} - \sqrt{w})\, z/\ell + \sqrt{w}]$

cos-square $w \cos^2 [\, z/\ell \cos^{-1}\sqrt{b/w}\,]$

where W is the slot width, b is the height of the fin line housing and ℓ is the length of the taper.

Exponential taper is generally used as a transition from fin line with centrally located slot to rectangular wave guide because it gives moderate

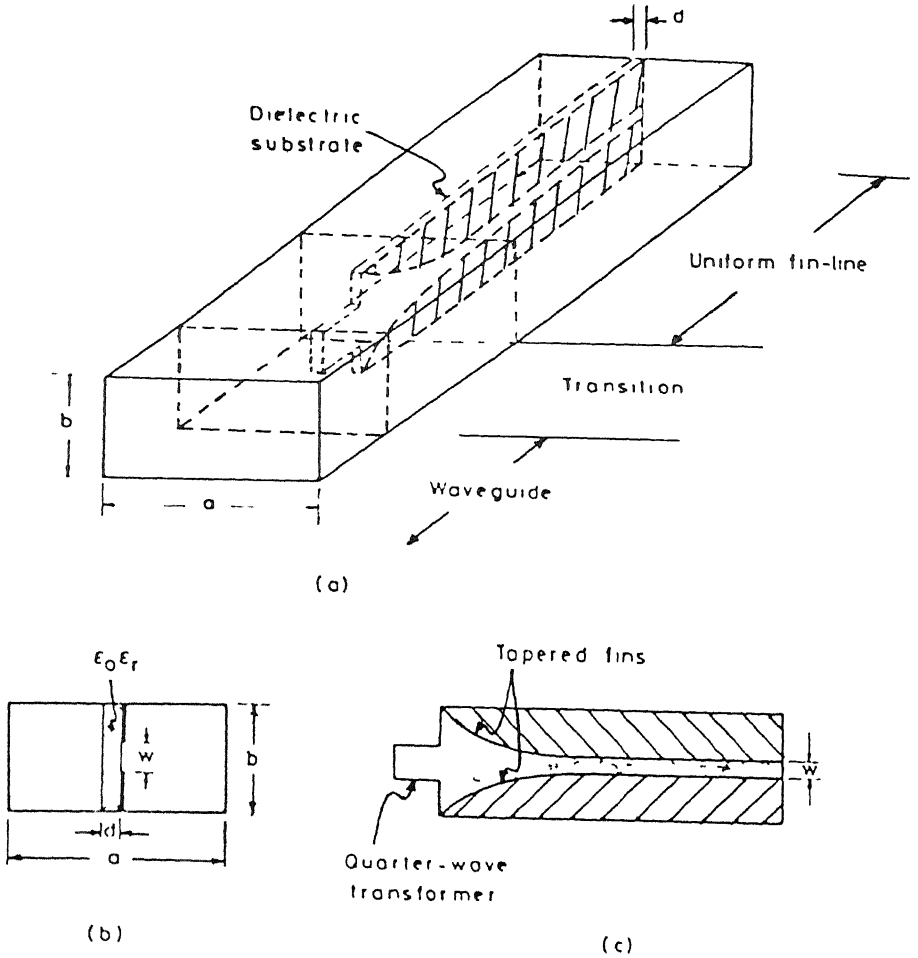

Fig 5 4 A typical fin line to wave guide transition [1]

return loss

For the experiment purpose we have used the exponential taper while designing the fin line fixture, without introducing any quarter wave transformer The taper length has been chosen 67λo at 10 GHz, where λo is the free space wave length Fig 5 5 shows the transmission and reflection losses of a uniform fin line section with exponential taper It can be seen that slot profile with exponential taper results in transmission loss less than 5 dB over the X-band

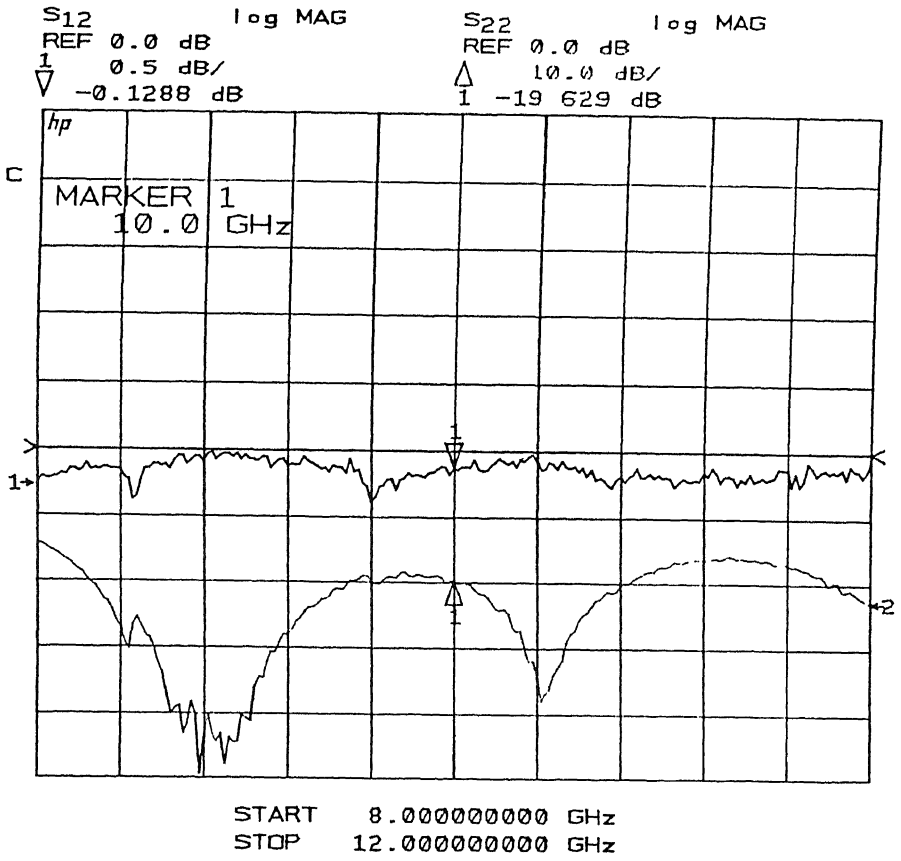

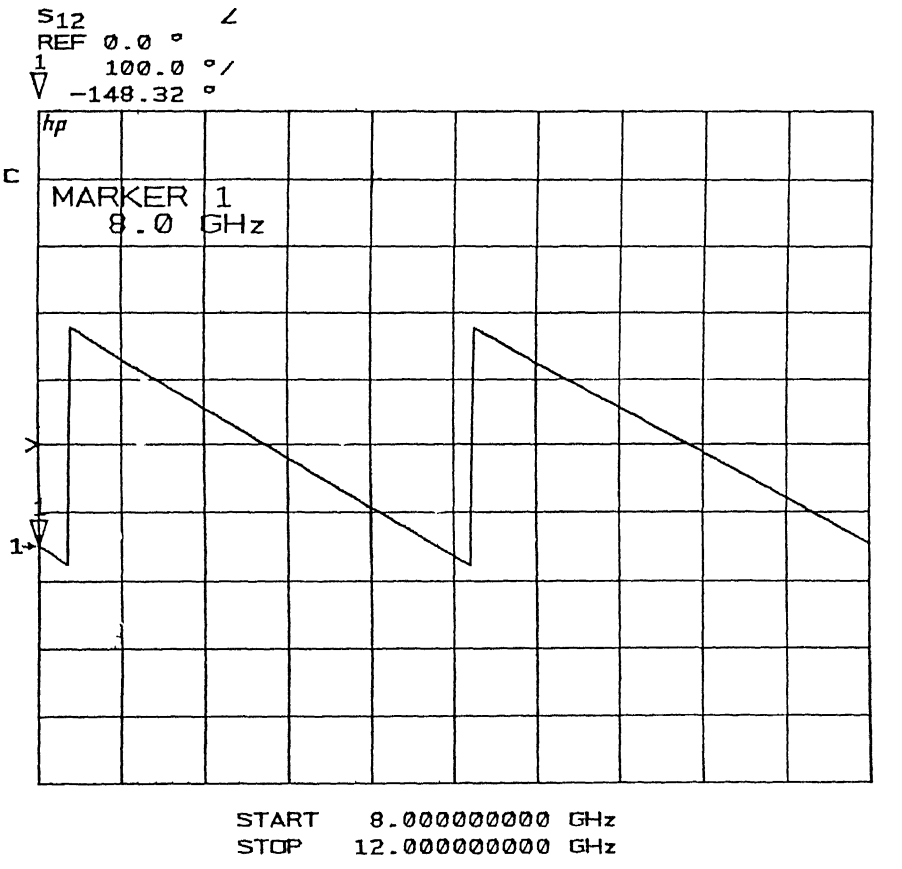

Fig 5 5 Experimental results of an exponential taper in unilateral fin line

CHAPTER 6

NUMERICAL RESULTS

6.1 INTRODUCTION

This chapter contains the theoretical as well as experimental results for equivalent circuit parameters and transmission coefficient(magnitude and phase) of a discontinuity in unilateral fin line Insertion loss characteristics(experiment and theory) of a unilateral fin line low pass filter, realized using the off slot discontinuities in cascade is also given in this chapter Theoretical results of equivalent circuit parameters for off slot discontinuity in insulated fin line are given for a specific case of overlapping strips (see Fig 4 1)

6.2 DISCONTINUITY IN UNILATERAL FIN LINE

6.2 1 *Description of the Program*

A FORTRAN program UNIRESLEN is written to compute the resonant length of the cavity containing the discontinuity The program uses NAG library subroutine C05ADF to find the root of a function In our case the function is the determinant of coefficient matrix as in equations(3 28) NAG library routine F03ADF is called in the program to find out the determinant of the coefficient matrix The value of the determinant is supplied to C05ADF, which approximately after 10 calls, gives the root of the function (determinant of the coefficient matrix)in the range specified to the routine For a fixed value of frequency, with all the dimensions specified,if we choose certain values for ℓ_1 and c (see Fig 3 1), and substitute in (3 28), then it will be left as a function ℓ_2 The program UNIRESLEN, hence will give the resonant length ℓ_2(we

will take the first root of the function for dominant mode resonance), for specified values of ℓ_1 and c , such that the cavity containing the discontinuity with overall length $(\ell_1 + \ell_2 + c)$ will resonate at the frequency used Also as given in (3 28), we can not take m = n = ∞ , we assign some finite values to m and n, such that we may get sufficient accuracy in the result

Now before we actually begin with computation, we have to apply certain tests to the program to check its accuracy These tests are as follows

(i) if strip width c→0, the ℓ_2 as given in program output, should be such that the total length $(\ell_1+\ell_2+c)\rightarrow\lambda_g/2$, where λ_g is the dominant mode guide wavelength of the fin line for a specified slot width and frequency

(ii) if the no of iterations increases the result should converge to a finite value In fact we can make out the value m and n this way i e we will assign m and n those numbers for which results almost converge

(iii) increase in the no of basis functions should also result in convergence Similar to the no of iteration we also fix the no basis functions for which the results seem to converge

Out of the above three the first one is the most important one If this test fails, we must conclude that something is wrong either with the formulation or with the source code of the program

6 2 2 *Numerical Results*

We have taken m = n = 100 for getting an accuracy up to third decimal place in the results Fig 6 1 shows the variation of $\bar{X}_{se}$ and $\bar{X}_{sh}$ with the no of z-depedent basis functions for the slot field Fig 6 2 and Fig 6 3 shows the variation of $\bar{X}_{se}$ and $\bar{X}_{sh}$ with frequency for c = 2 0mm and c = 1 5mm respectively, in X-band Fig 6 4 shows the variations of $\bar{X}_{se}$ and $\bar{X}_{sh}$ with the width of the strip in X-band Fig 6 5 shows the variation of $\bar{X}_{se}$ and $\bar{X}_{sh}$ with the height of the strip Fig 6 6 shows the variations of $\bar{X}_{se}$ and $\bar{X}_{sh}$ with it's

distance from the bottom wall of the housing Fig 6 7 shows the variations of $\bar{X}_{se}$ and $\bar{X}_{sh}$ with frequency in Ka-band for c = 7112mm Fig 6 8 shows the variations of $\bar{X}_{se}$ and $\bar{X}_{sh}$ with strip width c for a frequency of 34 GHz As it is evident from all the above Figures, $|\bar{X}_{se}|$, which is the inductive reactance, increases with frequency and strip width both Also $|\bar{X}_{sh}|$, which is the capacitive reactance, decreases with frequency and strip width both This could be explained in this way since λ_g decreases with increase in the frequency, the thickness of the dielectric substrate width and height of the discontinuity strip increase with respect to λ_g, if we increase the frequency Also if we keep the frequency fixed and increase the strip width, we are again increasing one of the dimensions (longitudinal) of the strip with respect to λ_g Thus c/λ_g increases in both the cases, causing series inductance and shunt capacitance both to increase

Measurements have been made in X-band for a sample discontinuity of width c = 2 0mm and height h = 8 16mm Fig 6 9 shows the experimental results of transmission coefficient(magnitude and phase) of the sample discontinuity Comparison of theoretical and experimental results of S_{21}(mag in dB and phase in deg) for the sample discontinuity are shown in Fig 6 10

6 3 *Discontinuities in Cascade Low Pass Filter*

A program INLOSS is written which uses the results Fig 6 2 and Fig 6 3 to compute the insertion loss of the filter The program is in fact a FORmula TRANslation of equations 5 5 to 5 9 It accepts the line length between the strips, equivalent circuit parameters and propagation constant of the fin line as the input data and produces insertion loss as the output Fig 6 11 shows the variation of insertion loss of one such filter with frequency in X-band, for various interstrip spacings Fig 6 12 shows the experimental results of insertion loss of a sample low pass filter Specifications are given with the

figure Fig 6 13 shows the comparison of theoretical and experimental results of insertion loss of a sample three section low pass filter which uses the off slot discontinuity as prototype

6 4 *Discontinuity in insulated fin line*

Another FORTRAN program similar to UNIRESLEN is written which finds the resonant length of insulated fin line cavity housing the discontinuity Similar tests,as were performed in UNIRESLEN, are performed for this also Since the program takes 5 hours of C P U time on a HP 9000 supermini computer for generalized discontinuity due to increased matrix size (Fig 4 1(b)), we have considered only a special case of the discontinuity for characterization purpose, in which the strips are exactly overlapping each other and symmetrically placed across the slot Also for the same reason we have cut down the no. of iterations, though it results in some amount of inaccuracy Taking m = n = -25 to +25, we have calculated $\bar{X}_{se}$ and $\bar{X}_{sh}$ and plotted as a function of frequency Fig 6 14 and 6 15 shows these variations in X-band and Ka-band, respectively

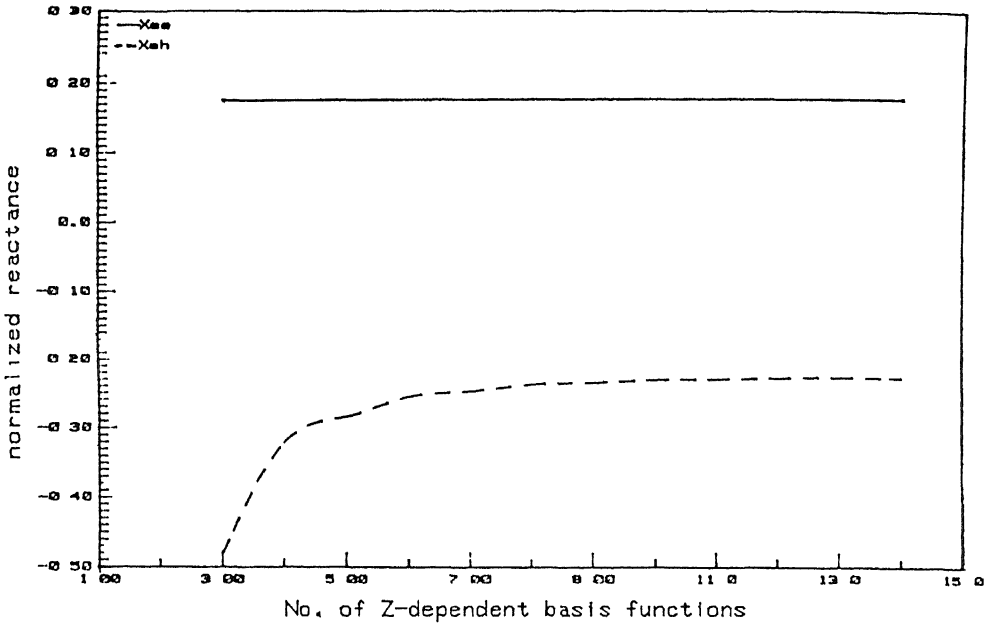

Fig 6 1 Variation of equivalent circuit parameters ($\bar{X}_{se}$ and $\bar{X}_{sh}$) of the off slot discontinuity in unilateral fin line with the No of z-dependent basis functions for the slot field(strip width C = 2 0mm, strip height h = 8 16mm, frequency = 10 GHz)

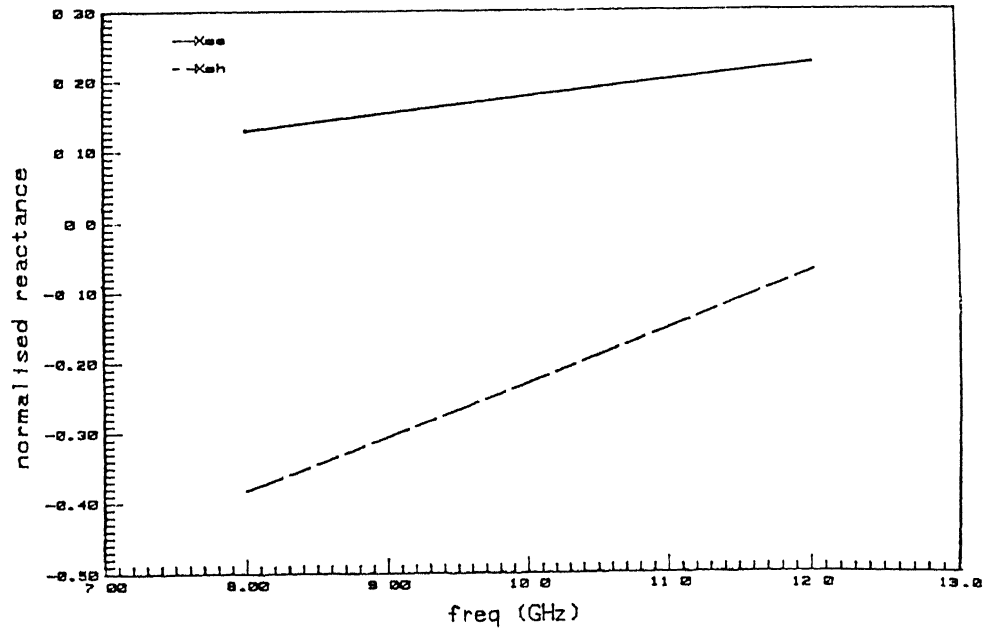

Fig 6 2 Variation of equivalent circuit parameters ($\bar{X}_{se}$ and $\bar{X}_{sh}$) of the off slot discontinuity in unilateral fin line with frequency in X-band for strip width C = 2 0mm and strip height h = 8 16mm

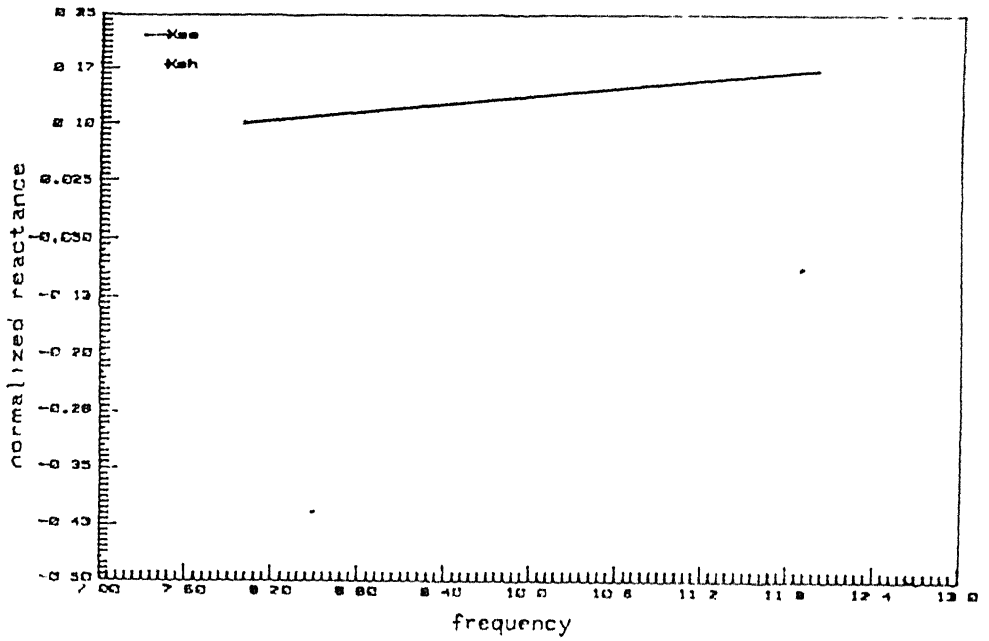

Fig 6 3 Variation of equivalent circuit parameters ($\bar{X}_{se}$ and $\bar{X}_{sh}$) of the off slot discontinuity in unilateral fin line with frequency in X-band for strip width C = 1 5mm and strip height h = 8 16mm

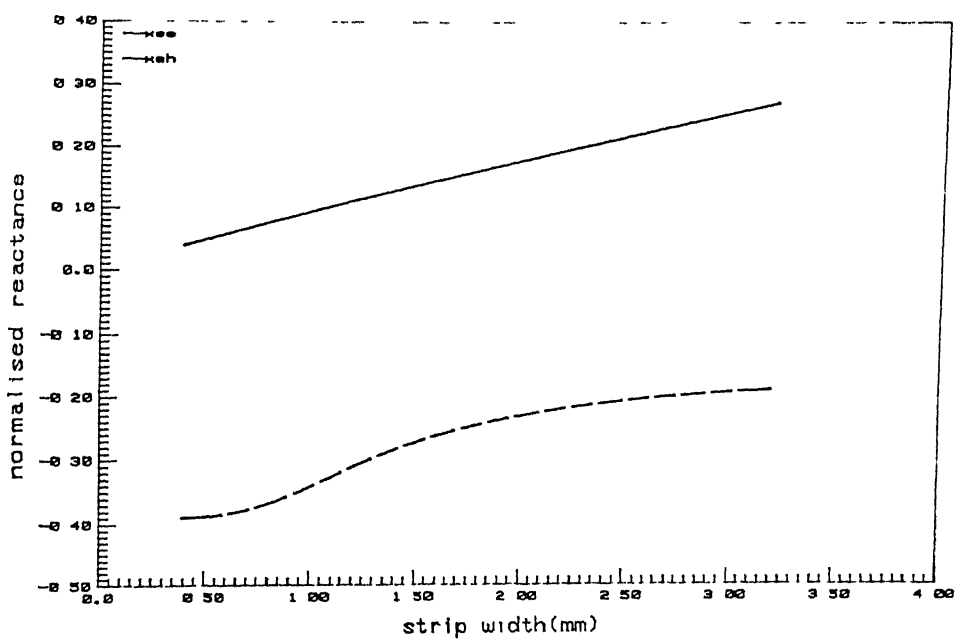

Fig 6 4 Variation of equivalent circuit parameters ($\bar{X}_{se}$ and $\bar{X}_{sh}$) of the off slot discontinuity in unilateral fin line with the width of the strip for strip height = 8 16mm and frequency = 10 GHz

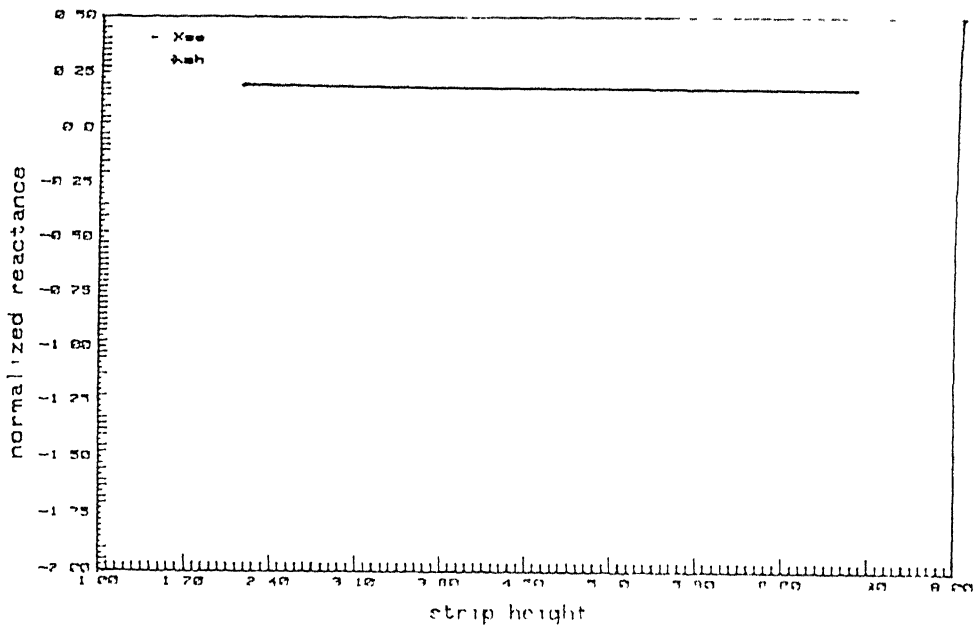

Fig 6 5 Variation of equivalent circuit parameters ($\bar{X}_{se}$ and $\bar{X}_{sh}$) of the off slot discontinuity in unilateral fin line with the height of the strip for strip width = 2 0mm and frequency 10 GHz

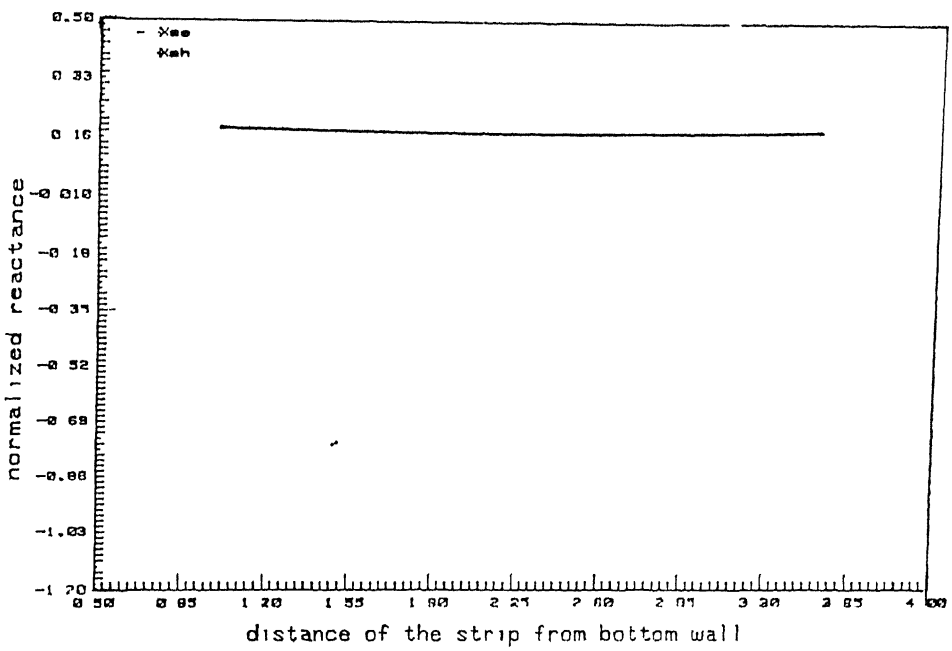

Fig 6 6 Variation of equivalent circuit parameters ($\bar{X}_{se}$ and $\bar{X}_{sh}$) of the off slot discontinuity in unilateral fin line with the distance of the strip from the bottom wall of the fin line housing for strip width C = 2 0mm, strip height h = 5 16mm and frequency = 10 GHz

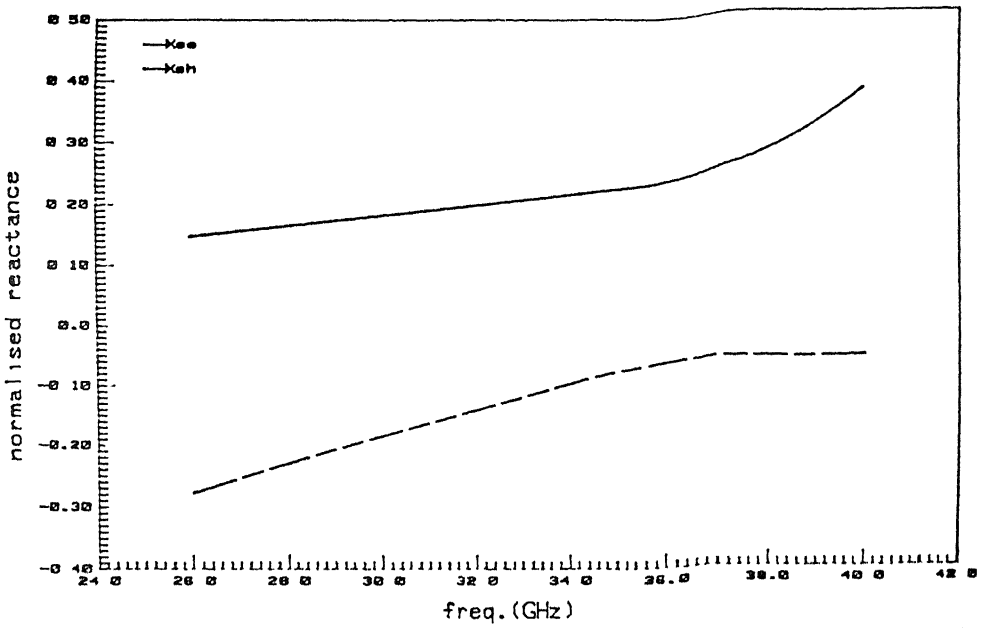

Fig 6 7 Variation of equivalent circuit parameters ($\bar{X}_{se}$ and $\bar{X}_{sh}$) of the off slot discontinuity in unilateral fin line with frequency in Ka-band for strip width C = .7112mm and strip height h = 2 85mm

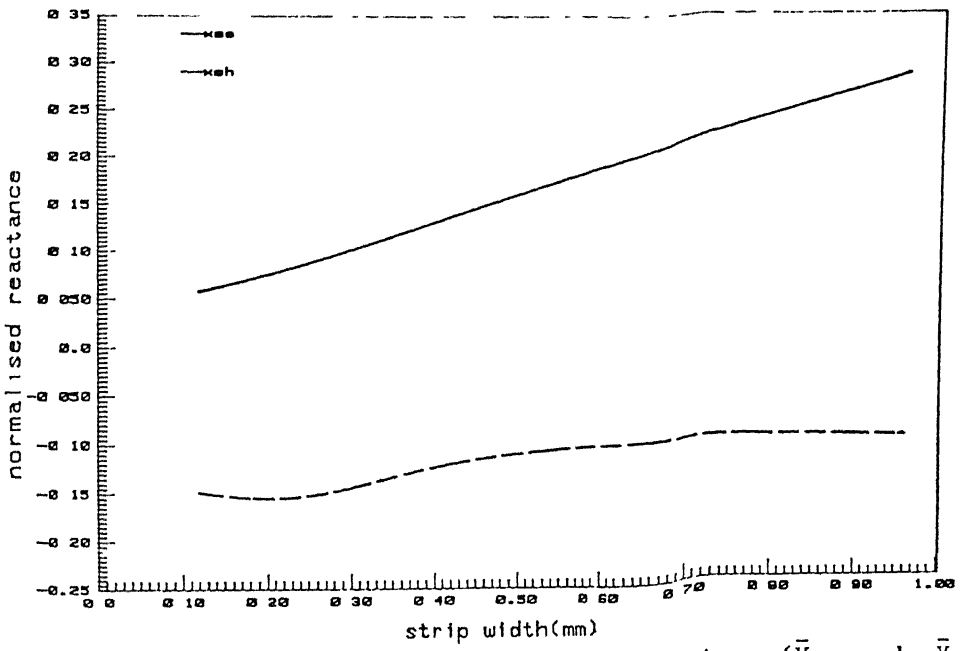

Fig 6 8 Variation of equivalent circuit parameters ($\bar{X}_{se}$ and $\bar{X}_{sh}$) of the off slot discontinuity in unilateral fin line with the width of the strip for strip height h = 2 85mm and frequency = 34 GHz

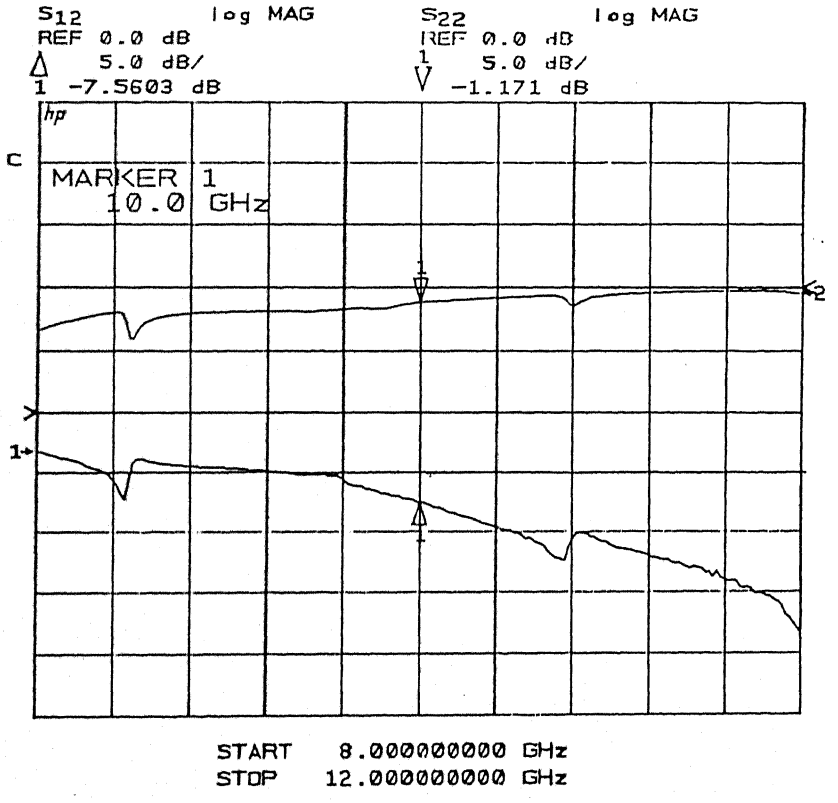

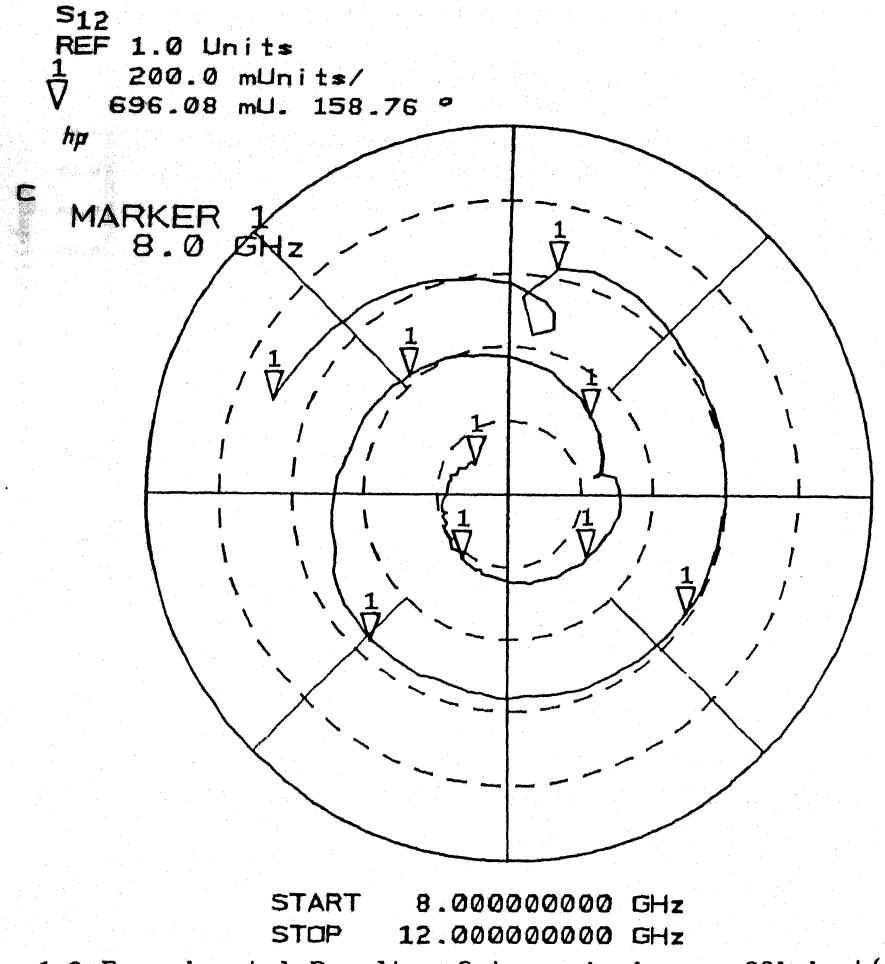

Fig.6.9 Experimental Results of transmission coefficient(magnitude and phase) of a sample discontinuity(strip width C = 2.0mm and Strip height = 8.16mm) in unilateral fin line

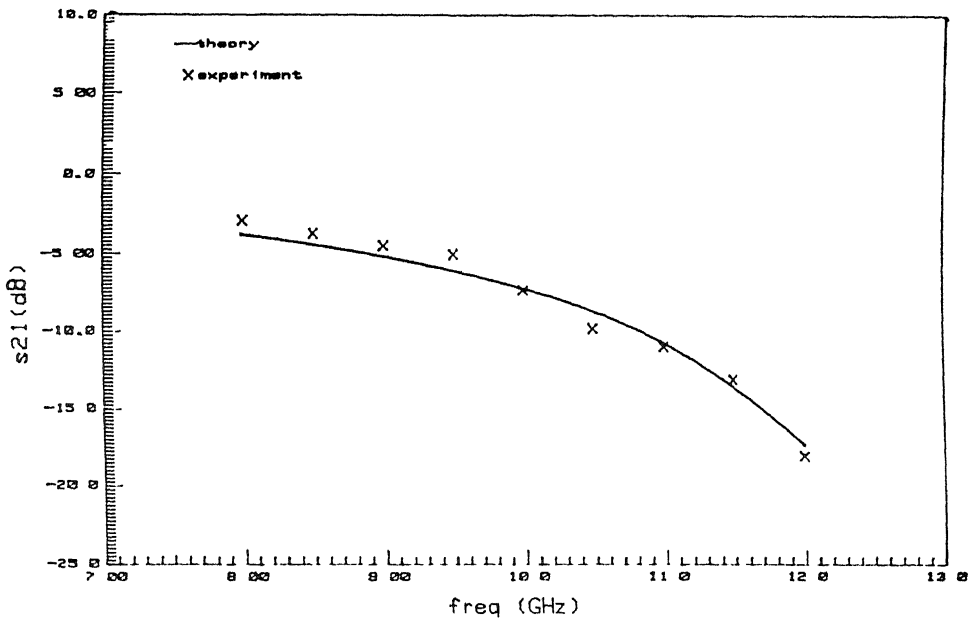

(a)Magnitude of the transmission coefficient(dB)

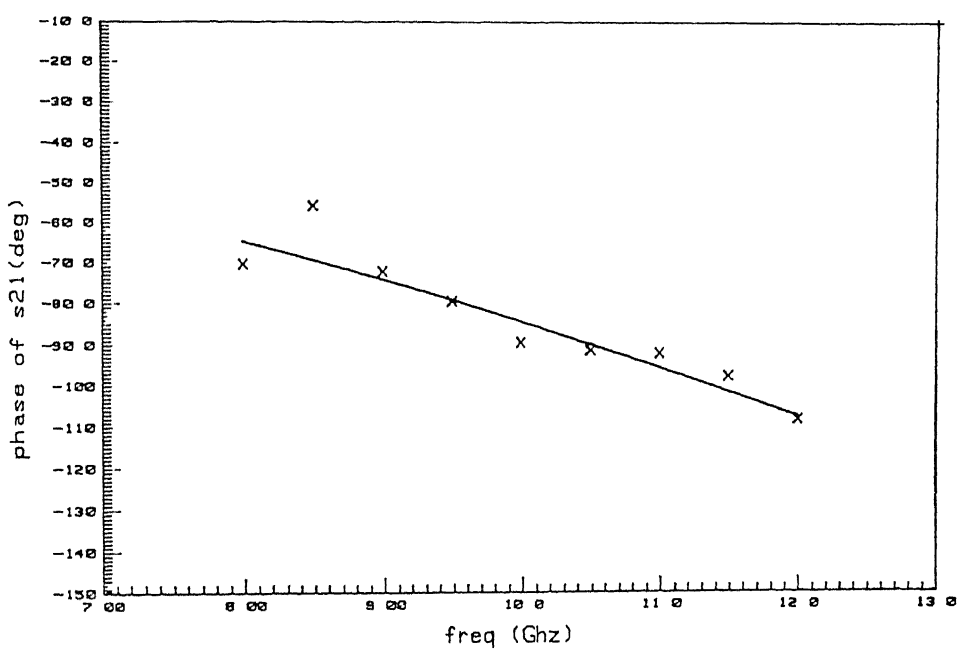

(b)Phase of the transmission coefficient(deg)

Fig 6 10 Comparison of theoretical and experimental results of transmission coefficient of the sample discontinuity

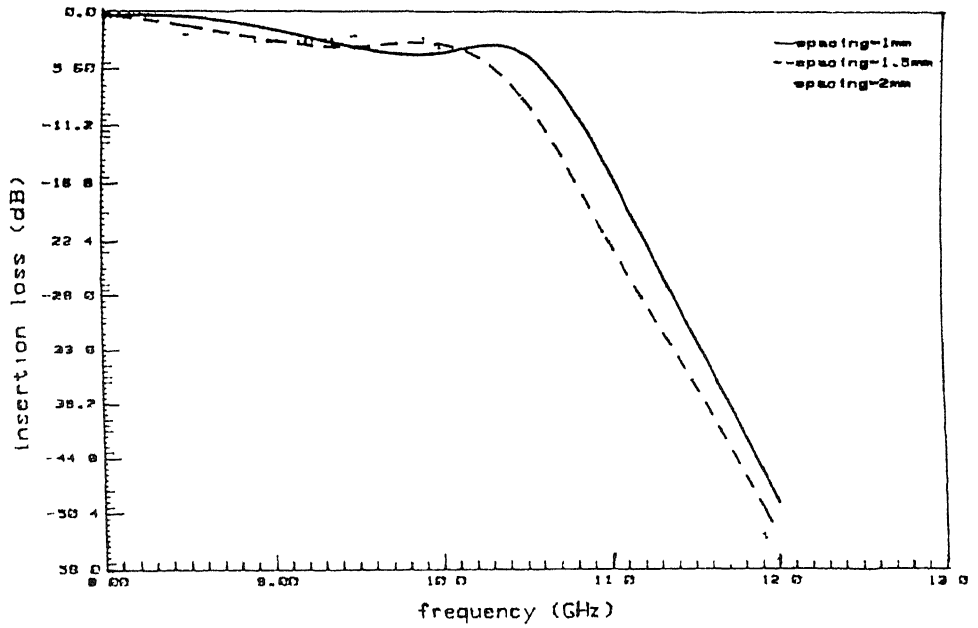

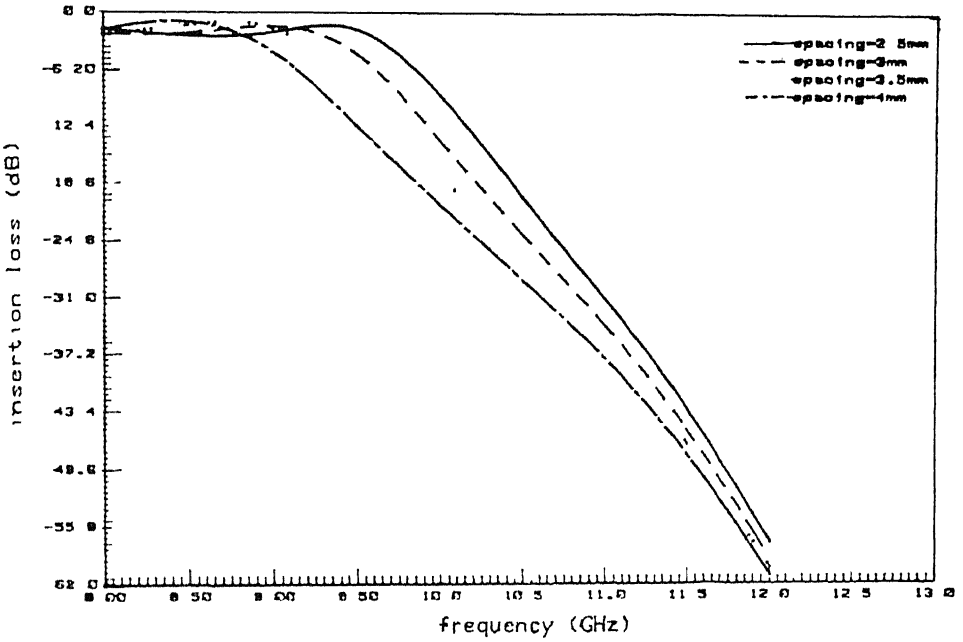

Fig 6 11 Variation of insertion loss of the filter with frequency in X-band for various lengths of fin line sections connecting the discontinuity strips ($C_1 = C_3 = 15$mm, $C_2 =$ 20mm and $\ell_{ab} = \ell_{bc}$ in Fig 5.2(a))

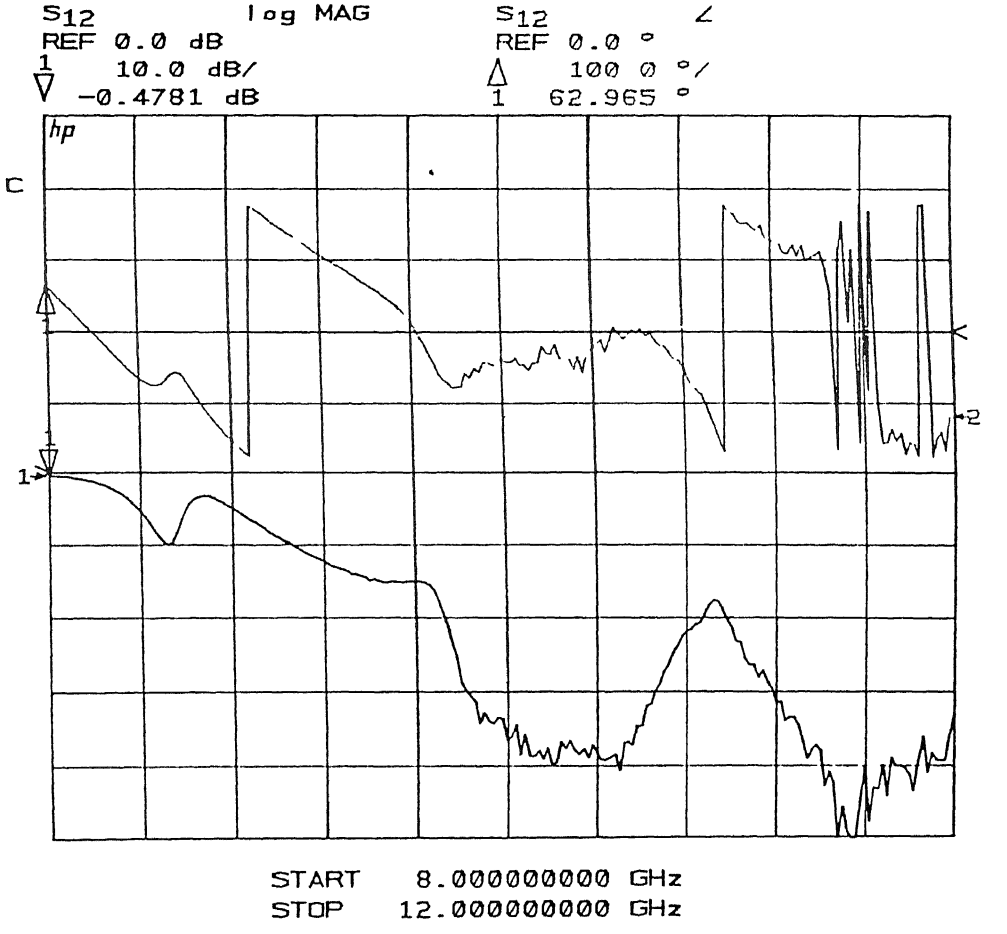

Fig 6 12 Experimental results of insertion loss of a sample three section unilateral fin line low pass filter ($C_1 = C_3 = 1.5$mm , $C_2 = 2.0$mm , $\ell_{ab} = \ell_{bc} = 5.32$mm in Fig 5.2(a))

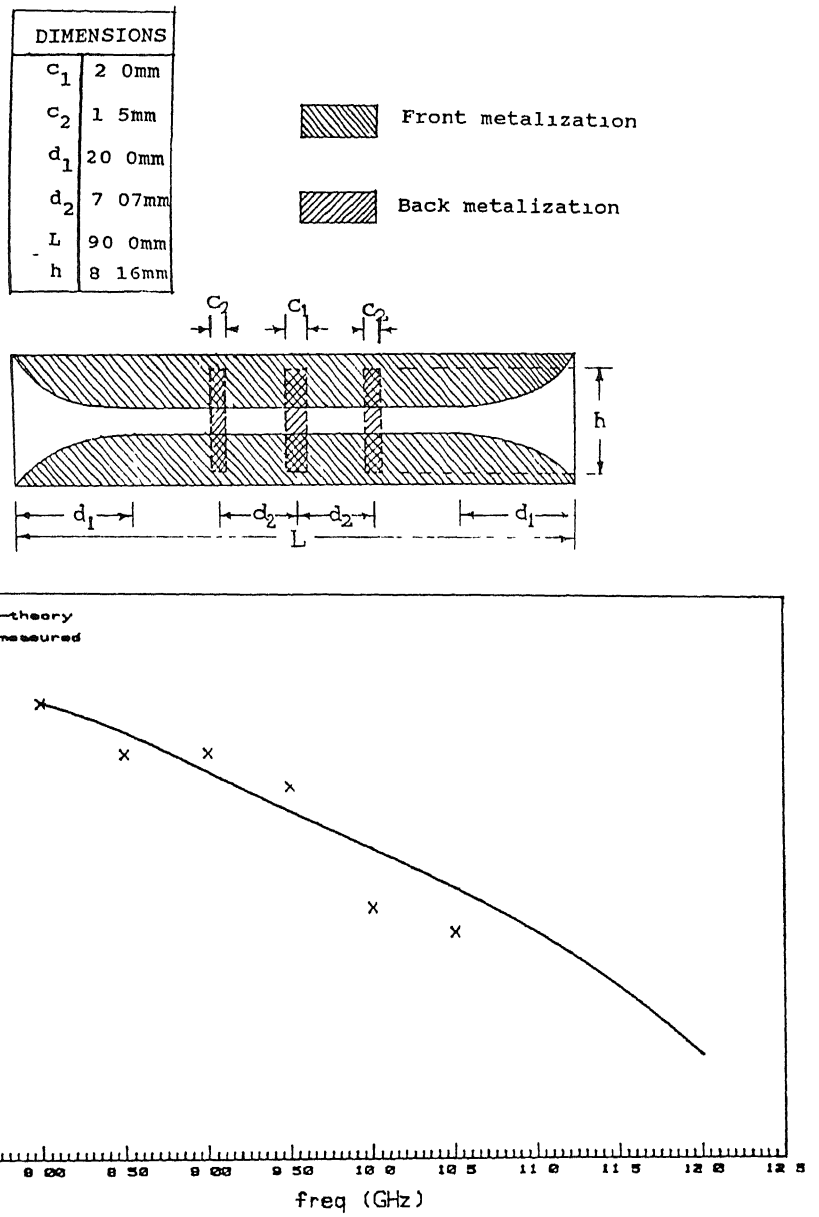

Fig 6 13 Comparison of theoretical and experimental results of insertion loss of the unilateral fin line low pass filter

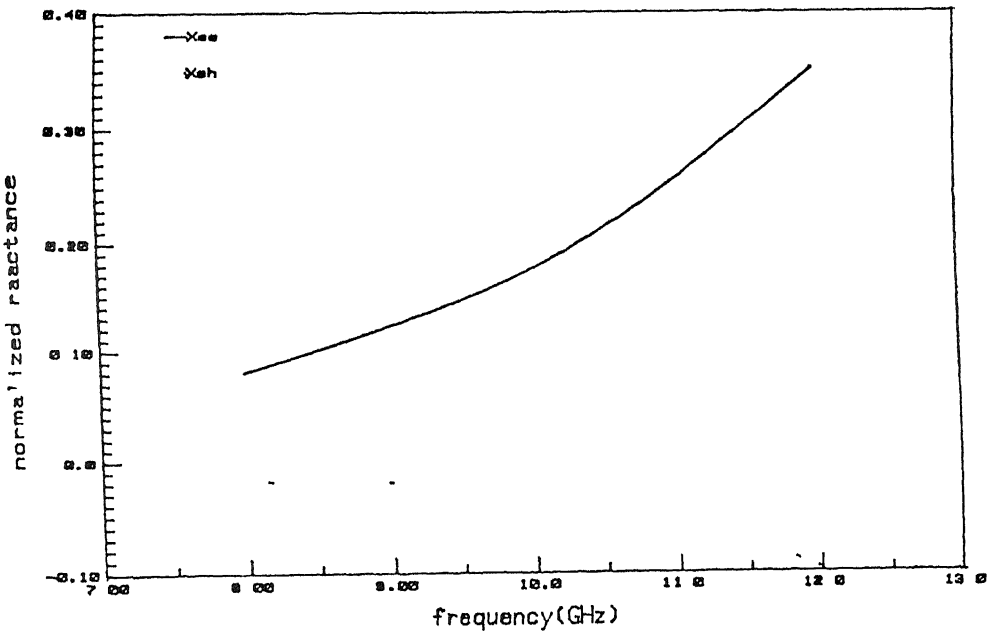

Fig 6 14 Variation of equivalent circuit parameters ($\bar{X}_{se}$ and $\bar{X}_{sh}$) of the off slot discontinuity in insulated fin line with frequency in X-band for width of each of the two strips = 2 0 mm and height of each of the two strips = 8 16mm

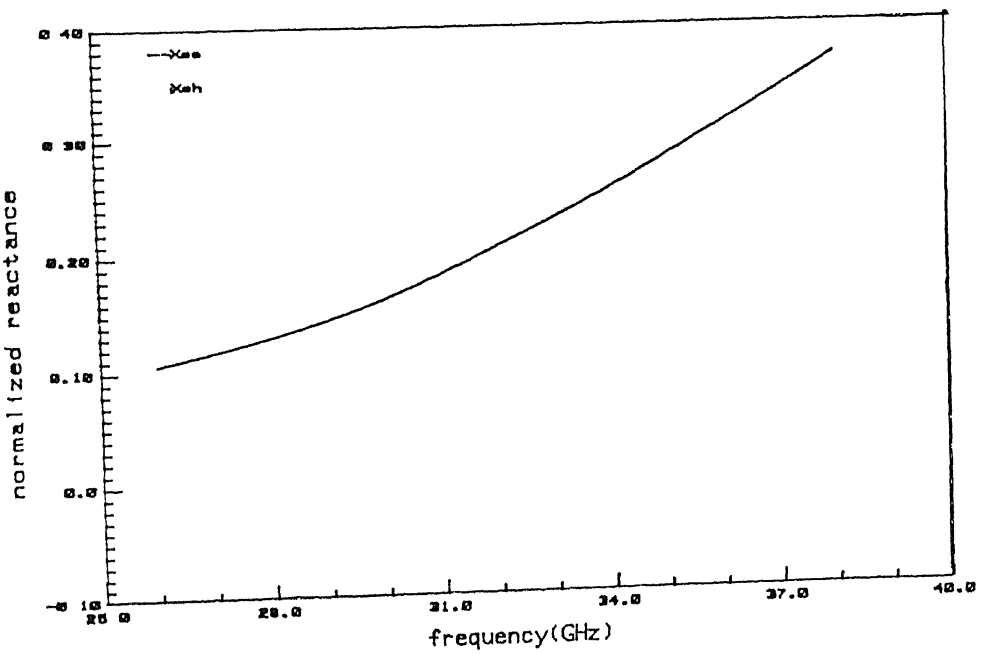

Fig 6 15 Variation of equivalent circuit parameters ($\bar{X}_{se}$ and $\bar{X}_{sh}$) of the off slot discontinuity in insulated fin line with frequency in Ka-band for width of each of the two strips = 7112mm and height of each of the two strips = 2 85mm

CONCLUSIONS AND DISCUSSION

This chapter discusses in brief about the problem solved and techniques used in this thesis In most part of the thesis we have been concerned about characterizing the discontinuities in unilateral and insulated fin line structures Later,using the discontinuity equivalent circuit parameters, we have shown its use in the realization low pass filter The characteristics of the discontinuity in unilateral fin line has also been verified experimentally

For formulation of eigenvalue problem for resonant length in unilateral fin line, we have used modal analysis But in the insulated fin line we used spectral domain immitance approach for formulation of eigen value problem to avoid unnecessary analytical labor Due to its simplicity, Transverse Resonance Technique is then used to extract the discontinuity equivalent circuit parameters of both fin line discontinuities Simpler and suitable basis functions,which take into account the edge conditions have been used to accurately modal the fields and the currents on the strips During the computation, it has been observed that the accuracy of the theoretical results depends very much on the choice of basis functions chosen Experimental results along with the theoretical results proves the choice of basis functions to be appropriate

As we can see from Fig 6.13, experimental and theoretical results of insertion loss of a three section low pass filter does not seem to match well, the discrepancy can be attributed mostly to neglecting the higher order mode interaction between the strips Since strips have been placed only $\lambda_g/4$ apart,where λ_g is the guide wavelength of the fin line , the coupling through higher order modes is very likely A better design could be achieved , if we

include the effect of complex modes [36] in the analysis or analyze the cascaded discontinuity 'as a whole' Among other factors which might cause the error are fabricational inaccuracies, substrate bending, effect of mounting grooves [39] [40] and the assumption that the thickness of the conductor is zero

APPENDIX A

Final Expessions for G_{11}, G_{12} G_{44} as referred to equations (3 26) are given as under

$$F_1(\rho,\phi) = 4\rho\phi [N_{11} + N_{12}] / D_1$$

$$F_2(\rho,\phi) = -4 [N_{21} + N_{22}] / D_1$$

$$F_3(\rho,\phi) = 4\rho\phi N_3 / D_2$$

$$F_4(\rho,\phi) = -4 [N_{41} + N_{42}] / D_2$$

$$F_5(\rho,\phi) = 4\rho\phi N_5 / D_3$$

$$F_6(\rho,\phi) = 4 [N_{61} - N_{62}] / D_3$$

$$F_7(\rho,\phi) = 4j\omega\mu_o\rho\phi [N_{71} + N_{72}] / D_4$$

$$F_8(\rho,\phi) = -4j\omega\mu_o [N_{81} + N_{82}] / D_4$$

where

$$N_{11} = \gamma_{mn2} (\gamma_{mn1}^2 - k_o^2) \cot(\gamma_{mn1} h_2)$$

$$N_{12} = \gamma_{mn1} (\gamma_{mn2}^2 F_{mn2} - k_o^2 \varepsilon_r F_{mn1})$$

$$N_{21} = \gamma_{mn2} (k_o^2 \rho^2 + \gamma_{mn1}^2 \phi^2) \cot(\gamma_{mn1} h_2)$$

$$N_{22} = \gamma_{mn1} (k_o^2 \varepsilon_r \rho^2 F_{mn1} + \gamma_{mn2}^2 \phi^2 F_{mn2})$$

$$N_3 = (\gamma_{mn2}^2 - \gamma_{mn1}^2 \varepsilon_r) \cot(\gamma_{mn1} h_1) \cot(\gamma_{mn2} d)$$

$$N_{41} = (\varepsilon_r \gamma_{mn1}^2 \rho^2 + \gamma_{mn2}^2 \phi^2) \cot(\gamma_{mn1} h_1) \cot(\gamma_{mn2} d)$$

$$N_{42} = \varepsilon_r \gamma_{mn1} \gamma_{mn2} (\rho^2 + \phi^2) \cot^2(\gamma_{mn2} d)$$

$$N_5 = (F_{mn2} - F_{mn1}) \sin(\gamma_{mn2} d)$$

$$N_{61} = (\rho^2 + \phi^2) \cos(\gamma_{mn2} d)$$

$$N_{62} = (\rho^2 F_{mn1} + \phi^2 F_{mn2}) \sin(\gamma_{mn2} d)$$

$$N_{71} = \gamma_{mn2} (k_0^2 - \gamma_{mn1}^2) \cot(\gamma_{mn1} h_1)$$

$$N_{72} = \gamma_{mn1} (k_0^2 \varepsilon_r - \gamma_{mn2}^2) \cot(\gamma_{mn2} d)$$

$$N_{81} = \gamma_{mn2}(k_o^2\ \phi^2 + \gamma_{mn1}^2\ \rho^2)\ \cot(\gamma_{mn1}\ h_1)$$

$$N_{82} = \gamma_{mn1}(k_o^2\ \varepsilon_r\ \phi^2 + \gamma_{mn2}^2\ \rho^2\ )\ \cot\ (\gamma_{mn2}\ d)$$

and

$$D_1 = j\omega\ \mu_o\ \gamma_{mn1}\ \gamma_{mn2}\ D_3$$

$$D_2 = D_3\ \cos(\gamma_{mn2}\ d)\ [\gamma_{mn2}\ \cot(\gamma_{mn1}\ h_1) + \varepsilon_r\ \gamma_{mn1}\cot(\gamma_{mn2}\ d)\ ]$$
$$[\gamma_{mn1}\ \cot(\gamma_{mn1}\ h_1) + \gamma_{mn2}\ \cot(\gamma_{mn2}\ d)\ ]$$

$$D_3 = \ell b(\rho^2 + \phi^2)$$

$$D_4 = D_2\ k_o^2\ /\cos(\gamma_{mn2}\ d)$$

$$F_{mn1} = \frac{[\ \gamma_{mn2}\ \cot(\gamma_{mn1}\ h_1)\ \cot(\gamma_{mn2}\ d) - \varepsilon_r \gamma_{mn1}\ ]}{[\ \gamma_{mn2}\ \cot(\gamma_{mn1}\ h_1) + \varepsilon_r\ \gamma_{mn1}\ \cot\ (\gamma_{mn2}\ d)\ ]}$$

$$F_{mn2} = \frac{[\ \gamma_{mn1}\ \cot(\gamma_{mn1}\ h_1)\ \cot(\gamma_{mn2}\ d) - \gamma_{mn2}\ ]}{[\ \gamma_{mn1}\ \cot(\gamma_{mn1}\ h_1) + \gamma_{mn2}\ \cot(\gamma_{mn2}\ d)\ ]}$$

$$\gamma_{mn1} = \sqrt{\rho^2 + \phi^2 - k_0^2}$$

$$\gamma_{mn2} = \sqrt{\rho^2 + \phi^2 - k_0^2 \varepsilon_r}$$

we can write Green'n functions as

$$G_{11} = \delta mn\ F_1(\alpha_n, \beta_m)\ , \qquad G_{12} = \delta' mn\ F_2(\alpha_n, \beta_m)$$

$$G_{13} = \delta mn\ F_3(\alpha_n, \beta_m)\ , \qquad G_{14} = \delta' mn\ F_4(\alpha_n, \beta_m)$$

$$G_{21} = \delta mn\ F_2(\beta_m, \alpha_n)\ , \qquad G_{22} = \delta' mn\ F_1(\alpha_n, \beta_m)$$

$$G_{23} = \delta mn\ F_4(\beta_m, \alpha_n)\ , \qquad G_{24} = \delta' mn\ F_3(\alpha_n, \beta_m)$$

$$G_{31} = \delta mn\ F_5(\alpha_n, \beta_m)\ , \qquad G_{32} = \delta' mn\ F_6(\alpha_n, \beta_m)$$

$$G_{33} = \delta mn\ F_7(\alpha_n, \beta_m)\ , \qquad G_{34} = \delta' mn\ F_8(\alpha_n, \beta_m)$$

$$G_{41} = \delta mn\ F_6(\beta_m, \alpha_n)\ , \qquad G_{42} = \delta' mn\ F_5(\alpha_n, \beta_m)$$

$$G_{43} = \delta mn\ F_8(\beta_m, \alpha_n)\ , \qquad G_{44} = \delta' mn\ F_7(\alpha_n, \beta_m)$$

where

$\alpha_n = 2n\pi/b$, n = 0, 1, 2,

$\beta_m = m\pi/\ell$ where $\ell = \ell_1 + \ell_2 + c$, m = 0, 1, 2,

δ_{mn} = 0 , when n =0

= 1/2 , when n ≠ 0 and m = 0

= 1 , when n ≠ 0 and m ≠ 0

δ'_{mn} = 0 , when m =0

= 1/2 , when m ≠ 0 and n = 0

= 1 , when m ≠ 0 and n ≠ 0

APPENDIX B

Transforms of the basis functions for field in the slot and current on the strip

B.1 *For symmetrically located strip across the centrally located slot case (refer to equations (3 30))*

$$\tilde{f}^{(1)}_{yy}(\alpha_n) = \pi\, J_0(\alpha_n\, w/\,2)\, \cos(\alpha_n\, b/\,2)$$

$$\tilde{f}^{(2)}_{yy}(\alpha_n) = \frac{w^2}{2}\cos(\alpha_n\, b/\,2)\,\left[\frac{\pi}{2}\, J_0(\alpha_n w/\,2) - \frac{\pi}{\alpha_n w}\, J_1(\alpha_n\, w/\,2)\right]$$

$$\tilde{f}^{(q)}_{yz}(\beta_m) = \ell/\,2 \qquad \text{if } m = q, \qquad q = 1,\ 2,\ \ldots\ 12$$

$$= 0 \qquad \text{otherwise}$$

$$\tilde{f}^{(1)}_{zy}(\alpha_n) = \frac{\pi\, w^2}{4\,\alpha}\, J_2(\alpha_n\, w/\,2)\cos(\alpha_n\, b/\,2) \qquad \text{if } n \neq 0$$

$$= 0 \qquad \text{if } n = 0$$

$$\tilde{f}^{(2)}_{zy}(\alpha_n) = \frac{w^5}{16}\cos(\alpha_n\, b/\,2)\,\left[\frac{\pi}{\alpha_n w}\, J_0(\alpha_n\, w/\,2) - \frac{6\,\pi}{(\alpha_n w)^2}\, J_1(\alpha_n\, w/\,2)\right]$$

$$\text{if } n \neq 0$$

$$= 0 \qquad \text{if } n = 0$$

$$\tilde{f}^{(q')}_{zz}(\beta_m) = \ell/\,2 \qquad \text{if } m = q', \qquad q' = 1,\ 2,\ \ldots\ 12$$

$$= \qquad \text{otherwise}$$

$$\tilde{g}^{(r)}_{yy}(\alpha_n) = (-1)^{(r-1)}\frac{\pi\, h}{4}\cos(\alpha_n\, b/\,2)\,\left[\, J_0\{\,(2r-1)\pi/\,2 - \alpha_n\, h/\,2\right.$$

$$\left. + J_0\{(2r-1)\pi/\,2 + \alpha_n\, h/\,2\}\right]$$

$$r = 1,\ 2$$

$$\tilde{g}^{(1)}_{yz}(\beta_m) = \pi\, J_0(\beta_m\, c/\,2)\, \sin\{\beta_m(\ell_1 + c/\,2)\}$$

$$\tilde{g}^{(2)}_{yz}(\beta_m) = \frac{\pi\, c}{2}\, J_1(\beta_m\, c/\,2)\, \cos\{\beta_m(\ell_1 + c/\,2)\}$$

$$\tilde{g}_{zy}^{(r')}(\alpha_n) = (-1)^{r'}\frac{\pi\, h}{4}\cos(\alpha_n\, b/2)\,[\,J_0\{(2r'-1)\pi/2 - \alpha_n\, h/2 - J_0\{(2r'-1)\pi/2 + \alpha_n\, h/2\}]$$

$$r' = 1,\ 2$$

$$\tilde{g}_{zz}^{(1)}(\beta_m) = \frac{\pi\, c}{2\,\beta_m}\, J_1(\beta_m\, c/2)\cos\{\beta_m(\ell_1 + c/2)\} \qquad \text{if } m \neq 0$$

$$= \frac{\pi\, c^2}{8} \qquad \text{if } m = 0$$

$$\tilde{g}_{zz}^{(2)}(\beta_m) = -\frac{\pi\, c^2}{4\,\beta_m} J_2(\beta_m\, c/2)\sin\{\beta_m(\ell_1 + c/2) \qquad \text{if } m \neq 0$$

$$= 0 \qquad \text{if } m = 0$$

B.2 *For asymmetrically located strip across the centrally located slot case (refer to equations (3 32))*

$$\tilde{f}_{yy}^{(1)}(\alpha_n) = \frac{\pi\, w}{4}\sin(\alpha_n\, w/2)\,[J_0(\pi/2 - \alpha_n\, w/2) - J_0(\pi/2 + \alpha_n\, w/2)]$$

$$\tilde{f}_{yy}^{(2)}(\alpha_n) = \frac{-\pi\, w}{4}\cos(\alpha_n\, w/2)\,[J_0(\pi - \alpha_n\, w/2) + J_0(\pi + \alpha_n\, w/2)]$$

$$\tilde{f}_{zy}^{(1)}(\alpha_n) = \frac{\pi\, w}{4}\sin(\alpha_n\, w/2)\,[J_0(\pi/2 - \alpha_n\, w/2) + J_0(\pi/2 + \alpha_n\, w/2)]$$

$$\tilde{f}_{zy}^{(2)}(\alpha_n) = \frac{-\pi\, w}{4}\cos(\alpha_n\, w/2)\,[J_0(\pi - \alpha_n\, w/2) - J_0(\pi + \alpha_n\, w/2)]$$

$$\tilde{g}_{yy}^{(1)}(\alpha_n) = \frac{\pi\, h}{4}\cos\{\alpha_n(h' + h/2)\}\,[J_0(\pi/2 - \alpha_n\, h/2) + J_0(\pi/2 + \alpha_n\, h/2)]$$

$$\tilde{g}_{yy}^{(2)}(\alpha_n) = \frac{\pi\, h}{4}\sin\{\alpha_n(h' + h/2)\}\,[J_0(\pi - \alpha_n\, h/2) - J_0(\pi + \alpha_n\, h/2)]$$

$$\tilde{g}_{yy}^{(1)}(\alpha_n) = -\frac{\pi\, h}{4}\cos\{\alpha_n(h' + h/2)\}\,[J_0(\pi/2 - \alpha_n\, h/2) - J_0(\pi/2 + \alpha_n\, h/2)]$$

$$\tilde{g}_{yy}^{(1)}(\alpha_n) = -\frac{\pi\, h}{4}\sin\{\alpha_n(h' + h/2)\}\,[J_0(\pi - \alpha_n\, h/2) + J_0(\pi + \alpha_n\, w/2)]$$

$J_n(x)$ in the above expressions is the Bessel function of order 'n' and we have used following recurrence relation which relates higher order

Bessel function to lower order one

$$\frac{2\,n}{x}\; J_n(x) = J_{n-1}(x) + J_{n+1}(x)$$

Also in the evaluation of integrals,we have made use of the following expression [46]

$$J_\nu(z) = \frac{2\left(\frac{1}{2}z\right)^\nu}{\pi^{1/2}\;\Gamma\left(\nu + \frac{1}{2}\right)} \int_0^1 \left(1 - t^2\right)^{\nu - 1/2} \cos(z\,t)\; dt$$

where $\mathrm{Re}(\nu) > -\frac{1}{2}$

Here 'Γ' represents the Gamma function It satisfies following functional relation

$$\Gamma(n + 1) = n\,\Gamma\,n$$

Also we have

$$\Gamma_{1/2} = \sqrt{\pi}$$

APPENDIX C

Referring to equation (4 11) in chapter 4, various matrices involved in the equation are written as

$$[\ EJE\ ]_{uv} = \begin{bmatrix} \hat{E}_u\ (\alpha_n, y_1) \\ \hat{E}_v\ (\alpha_n, y_1) \\ \hat{J}_u\ (\alpha_n, y_2) \\ \hat{J}_v\ (\alpha_n, y_2) \\ \hat{E}_u\ (\alpha_n, y_3) \\ \hat{E}_v\ (\alpha_n, y_3) \end{bmatrix}, \qquad [\ JEJ\ ]_{uv} = \begin{bmatrix} \hat{J}_u\ (\alpha_n, y_1) \\ \hat{J}_v\ (\alpha_n, y_1) \\ \hat{E}_u\ (\alpha_n, y_2) \\ \hat{E}_v\ (\alpha_n, y_2) \\ \hat{J}_u\ (\alpha_n, y_3) \\ \hat{J}_v\ (\alpha_n, y_3) \end{bmatrix}$$

where

$$y_1 = h_1 + d_1 + d_2, \qquad y_2 = h_1 + d_1, \qquad y_3 = h_1$$

$$[\ G'\ ] = \begin{bmatrix} Z^e_{11} & 0 & FR^e_{12} & 0 & Z^e_{13} & 0 \\ 0 & Z^h_{11} & 0 & FR^h_{12} & 0 & Z^h_{13} \\ CR^e_{21} & 0 & Y^e_{22} & 0 & CR^e_{23} & 0 \\ 0 & CR^h_{21} & 0 & Y^h_{22} & 0 & CR^h_{23} \\ Z^e_{31} & 0 & FR^e_{32} & 0 & Z^e_{33} & 0 \\ 0 & Z^h_{31} & 0 & FR^e_{32} & 0 & Z^h_{33} \end{bmatrix}$$

$$[\ L\ ] = \begin{bmatrix} \sin\theta & \cos\theta & 0 & 0 & 0 & 0 \\ -\cos\theta & \sin\theta & 0 & 0 & 0 & 0 \\ 0 & 0 & \sin\theta & \cos\theta & 0 & 0 \\ 0 & 0 & \cos\theta & \sin\theta & 0 & 0 \\ 0 & 0 & 0 & 0 & \sin\theta & \cos\theta \\ 0 & 0 & 0 & 0 & -\cos\theta & \sin\theta \end{bmatrix}$$

REFERENCES

[1] Bharthi Bhat and S K Kaul, Analysis Design and Applications of Fin Lines, Artech House, M A , 1987

[2] F A Bension, Millimeter and Sub Millimeter Waves, Iliffe Books, London, 1969

[3] P Bhartia and I J Bahl, Millimeter Wave Engineering and Applications, John Wiley and Sons, New York, 1984

[4] J C Wiltse, " History of Millimeter and Sub Millimeter Waves," IEEE Trans Microwave Theory Tech , Vol MTT-32, pp 1118-1127, Sept 1984

[5] L Young and H Sobol, Advances in Microwaves, Vol 8, Acedemic Press, New York, 1974

[6] R A Pucel, " D J Masse and C P Hartwigs," Losses in Microstrip," IEEE Trans Microwave Theory Tech , Vol MTT-16, 342-350, June 1968

[7] F A Bension and F J Tischer, " Some Guiding Structures For Millimeter Waves," IEE Proc , Vol 131, Pt A, No 7, pp 429-449, Sept 1984

[8] P J Meier, " Integrated Fin Line Millimeter Components," IEEE Trans Microwave Theory Tech , Vol MTT-22, pp 1209-1216 Dec 1974

[9] P J Meier, " Integrated Fin Line A Versatile and Proven Millimeter Transmission Line," Microwave Journal, pp 24-25, Nov 1976

[10] K Solbach, " The Status of Printed Millimeter Wave E-plane Circuits," IEEE Trans Microwave Theory Tech , Vol MTT-31 pp 107-121, Feb 1983

[11] K J Button, Topics in MillimeterWave Technology, Academic Press, Inc , London, 1987

[12] L P Schmidt, T Itoh, and H Hofmann, " Characteristics of Unilateral Fin Line Structure with Arbitrary Located Slots," IEEE Trans Microwave Theory Tech , Vol MTT-29, pp 352-355, April 1981

[13] R N Simon, " Analysis of Millimeter Wave Integrated Fin Line," IEE Proc

Vol 130, Pt H, No 2, pp 166-169, March 1983

[14] J B Knorr and P M Shayda, " Millimeter Wave Fin Line Characteristics," IEEE Trans Microwave Theory Tech , Vol MTT-28, pp 737-743, July 1980

[15] D M Syahkal and J B Davis, " An Accurate Unified Solution to Various Fin Line Structures, of Phase Constant, Characteristic Impedance, and Attenuation, " IEEE Trans Microwave Theory Tech , Vol MTT-30 pp 1854-1861, Nov 1982

[16] L P Schmidt and T Itoh, " Spectral Domain Analysis of Dominant and Higher Order Modes In Fin Line," IEEE Trans Microwave Theory Tech , Vol MTT-28, pp 981-985, Sept 1980

[17] T Itoh and R Mittra, " A Technique for Computing Dipersion Characteristics of Shielded Microstrip Lines, IEEE Trans Microwave Theory Tech , Vol MTT-22, pp 896-898, Oct 1974

[18] J B Davis and D Mirshekar Syahkal, " Spectral Domain Analysis of Arbitrary Co planar Transmission Lines with Multilayer Substrate, " IEEE Trans Microwave Theory Tech , Vol MTT-25, pp 143-146, Feb 1977

[19] T Itoh , " Spectral Domain Immittance approach for Dispersion characteristics of Generalized Printed Transmission Lines," IEEE Trans Microwave Theory Tech , Vol MTT-28, No 7, pp 733-736, July 1980

[20] A Beyer, " Analysis of Characteristic of an Earthed Fin Line," IEEE Trans Microwave Theory Tech , Vol MTT-29, pp 676-680, July 1981

[21] Y Konishi and K Uenakada, " The Design of a Band Pass Filter with Inductive Strip Planer Circuit Mounted in Wave Guide," IEEE Trans Microwave Theory Tech , Vol MTT-22, pp 869-873, Oct 1974

[22] A M K Saad and K Schunemann, " A Simplified Method for AnalyzingFin Line Structure," IEEE Trans Microwave Theory Tech , Vol MTT-26, pp 1002-1007, Dec 1978

[23] R H Jansen, "Hybrid Mode Analysis Of End Effects Of Planar Microwave And

Millimeter Wave Transmission Lines," IEE Proc Vol 128, Pt H, pp 77-86, April 1981

[24] A Wexler, " Solution of Wave Guide Discontinuities by Modal Analysis," IEEE Trans Microwave Theory Tech , Vol MTT-22, pp 508-517, Sept 1967

[25] H El Hennaway and K Schunemann, "Impedance Transformation in Fin Lines," IEE Proc Vol 129 Pt H, pp 342-350, Dec 1982

[26] R Sorrentino and T Itoh, " Transverse Resonance Analysis of Fin Line Discontinuity, "IEEE Trans Microwave Theory Tech Vol MTT-32, pp 1633-1638, Dec 1984

[27] H Helard, J Citerne, O Picon, and V F Hanna, " Theoretical and Experimental Investigation of Fin Line Discontinuities," IEEE Trans Microwave Theory Tech , Vol MTT-33, pp 994-1003, Oct 1985

[28] J B Knorr and J C Deal, " Scattering Coefficients of an Inductive Strip in Fin Line," IEEE Trans Microwave Theory Tech , Vol MTT-33, pp 1011-1017, Oct 1985

[29] A Biswas and Bharthi Bhat, " Accurate Characterization of an Inductive Strip Discontinuity," IEEE Trans Microwave Theory Tech , Vol MTT-36, pp 1233-1238, Aug 1988

[30] Giovani Schiavon, Piero Tognolatti and Roberto Sorrentino, " Full Wave Analysis of Coupled Fin Line Discontinuities," IEEE Trans Microwave Theory Tech , Vol MTT-36, pp 1889-1894, Dec 1988

[31] Ruediger Vahldieck, " Quasi Planar Filter For Millimeter Wave Applications," IEEE Trans Microwave Theory Tech , Vol MTT-37, pp 324-334, Feb 1989

[32] C Nguyen and K Chang, " Millimeter Wave Low Loss Low Pass Filter," Electronic Lett , Vol 20, pp 1010-1011, Nov 1984

[33] R Safavi- Naini and R H Macphie," On Solving Wave Guide Junction Scattering Problem By Conservation Of Complex Power Technique," IEEE

Trans Microwave Theory Tech , Vol MTT-29, pp 337-343, April 1981

[34] Abbas Sayed Omar and K Schunemann, " Transmission Matrix Representation Of Fin Line Discontinuities, " IEEE Trans Microwave Theory Tech , Vol MTT-32, pp 756-770, Sept 1985

[35] R R Mansour and R H Macphie, " An Improved Transmission Matrix Formulation of Cascaded Discontinuity and It's Application to E-plane Circuits," IEEE Trans Microwave Theory Tech , Vol MTT-34, pp 1490-1498,Dec 1986

[36] A S Omar and K F Schunemann, "The Effect of Complex Modes at Fin Line Discontinuities," IEEE Trans Microwave Theory Tech , Vol MTT-34, pp 1508-1514, Dec 1986

[37] A Biswas, " Studies of Fin Line Discontinuities and Their Applications in Periodic Structures and Filters," Ph D Thesis, C A R E , I I T , Delhi, 1988

[38] K C Gupta, Ramesh Garg and Rakesh Chandha, Computer Aided Design of Microwave Circuits, Halsted Press, New York,1975

[39] G Eshwarappa, G I Costacheand W J R Hoefer, " Fin Lines in Rectangular and Circular Wave Guide Housing Including Substrate Mounting and Bending Effects Finite Element Analysis,"IEEE Trans Microwave Theory and Tech Vol MTT-37, pp 299-305, Feb 1989

[40] S L Foo and P P Silvester, " Finite Element Analysis of Inductive Strip in Unilateral Fin Lines," IEEE Trans Microwave Theory Tech , Vol MTT-41, pp 298-304, Feb 1993

[41] R E Collin, Foudation For Microwave Engineering, Mc Graw-Hill, New York, 1966

[42] R E Collin, Field Theory of Guided Waves, 2nd Ed , IEEE Press, New York, 1991

[43] C Schieblich, J K Piotrowski and J H Hinken, " Synthesis of Optimum

Fin Line Tapers Using Dispersion Formulas for Arbitrary Slot Width and Location," IEEE Trans Microwave Theory Tech , Vol MTT-32, pp 1638-1645, Dec 1984

[44] C J Verner and W J R Hoefer, " Quarter Wave Matching of Wave Guide to Fin Line Transitions," IEEE Trans Microwave Theory Tech , Vol MTT-32, pp 1645-1648, Dec 1984

[45] E C Jordan and G Balmin, Electromagnetic Waves and Radiating Systems, 2nd Ed Prientice Hall, Inc , N J , USA

[46] Milton Abramowitz and Irene A Stegun, Handbook of Mathematical Functions, Dover Publications, Inc , New York, 1965